AUTOMATED DAM DISPLACEMENT MONITORING USING A ROBOTIC TOTAL STATION

JAMES A. LUTES

February 2002

TECHNICAL REPORT
NO. 214

AUTOMATED DAM DISPLACEMENT MONITORING USING A ROBOTIC TOTAL STATION

James A. Lutes

Department of Geodesy and Geomatics Engineering
University of New Brunswick
P.O. Box 4400
Fredericton, N.B.
Canada
E3B 5A3

February 2002

© James A. Lutes 2002

PREFACE

This technical report is a reproduction of a thesis submitted in partial fulfillment of the requirements for the degree of Master of Science in Engineering in the Department of Geodesy and Geomatics Engineering, February 2002. The research was supervised by Dr. Adam Chrzanowski, and it was financially supported by the Natural Sciences and Engineering Research Council of Canada.

As with any copyrighted material, permission to reprint or quote extensively from this report must be received from the author. The citation to this work should appear as follows:

Lutes, James, A (2002). *Automated Dam Displacement Monitoring Using A Robotic Total Station*. M.Sc.E. thesis, Department of Geodesy and Geomatics Engineering Technical Report No. 214, University of New Brunswick, Fredericton, New Brunswick, Canada, 138 pp.

ABSTRACT

An automated data collection and processing system has been created for geodetic monitoring of point displacements at a large earthfill dam project in southern California. Because of the size of this facility, currently the largest earthfill dam project in the United States, the geodetic monitoring program could not be affordably implemented using traditional survey techniques. Therefore, a system was designed that uses a network of permanently installed robotic total stations (RTS) to carry out the measurements and data processing in a fully automatic fashion, with updated point coordinates delivered to the system operator after each measurement cycle.

Implementation of this automated monitoring system required the development of specialized software to carry out data collection and processing. Because the robotic total stations were to be housed in observation shelters with glass windows, it was necessary to employ data processing algorithms that would not be unduly affected by the resulting refraction effects. This was achieved by treating each observing station as a standalone monitoring system, eliminating the need to combine the biased RTS measurements with external data sources while still recognizing that refraction effects will cancel out in the computation of point displacements.

The automated monitoring system was first activated in October 2000, and has successfully collected displacement measurements for more than a year. A preliminary evaluation of data collected by the system shows that atmospheric refraction has a significant effect on the accuracy achievable during individual measurement cycles. However, averaging measurements collected at different times of day allows the system to meet its design goal of detecting displacements larger than 10 mm at the 95% level of confidence.

ACKNOWLEDGEMENTS

First and foremost, I would like to thank my supervisor, Dr. Adam Chrzanowski, for the many years of friendship, encouragement and financial assistance he has given me during my studies at the University of New Brunswick. I would especially like to thank Dr. Chrzanowski for his continual success in finding challenging projects for his students; the work outlined in this thesis represents but one of many interesting projects I have had the pleasure of working on under his leadership.

I would also like to thank Cecilia Whitaker and Mike Duffy of the Metropolitan Water District of Southern California for choosing Dr. Chrzanowski and his Engineering Surveys Research Group for involvement in this project. We thoroughly enjoyed the opportunity to contribute and to share in their success in creating a truly world-class dam monitoring system.

Finally, I would like to thank Geoffrey Bastin for taking part in software development and site visits during the course of this work. His contribution was invaluable in ensuring that the project was completed on schedule.

Financial support for the studies undertaken in this thesis has been provided in part by the Natural Sciences and Engineering Research Council of Canada. Additional financial support has been provided through a contract agreement between the Metropolitan Water District of Southern California and the University of New Brunswick.

TABLE OF CONTENTS

ABSTRACT ..... **ii**

ACKNOWLEDGEMENTS ..... **iii**

TABLE OF CONTENTS ..... **iv**

LIST OF FIGURES ..... **vi**

LIST OF TABLES ..... **vii**

LIST OF SYMBOLS ..... **viii**

CHAPTER 1 INTRODUCTION **1**

CHAPTER 2 THE DIAMOND VALLEY LAKE MONITORING PROJECT **5**

2.1 History and Overview of Diamond Valley Lake 5
2.2 The Diamond Valley Lake Monitoring System 8
2.2.1 Regional and On-Site Area Monitoring Networks 10
2.2.2 Local Dam Displacement Monitoring (DDM) Network 12

CHAPTER 3 DEVELOPMENT OF THE DIMONS SOFTWARE FOR AUTOMATED DISPLACEMENT MONITORING **17**

3.1 Software Design Considerations 18
3.2 DIMONS Architecture 20
3.2.1 Program Structure 21
3.2.2 Data Storage 35
3.3 Data Processing Methodology 40
3.3.1 Field Data Reduction 41
3.3.2 Preliminary Coordinate Calculation 52
3.3.3 Reference Point Check 53
3.3.4 Final Coordinate Calculation 54

CHAPTER 4 MONITORING SYSTEM IMPLEMENTATION **63**

4.1 Instrument Selection and Calibration 63
4.1.1 Meteorological Sensors 64
4.1.2 Robotic Total Stations 66
4.2 Power Supplies 68
4.3 Communication System 69
4.4 Monumentation 70
4.5 Instrument Shelters 72
4.6 Software Configuration 77

CHAPTER 5 PRELIMINARY EVALUATION OF SYSTEM PERFORMANCE **81**

5.1 Internal Precision of Individual Measurement Cycles 82
5.2 Comparison of Different Cycles 85
5.2.1 Cycles at Same Time of Day 85

5.2.2 Cycles at Different Times of Day 92
5.3 Cycles Averaged Over Time..... 96
5.4 Comparison of Displacements at Double Prisms..... 99
5.5 Summary of System Evaluation..... 102

CHAPTER 6 CONCLUSIONS AND RECOMMENDATIONS 103

REFERENCES..... 107

Appendix I. DIMONS Database Tables..... 110

Appendix II. Refraction Effects on Displacement Accuracy 124

Appendix III. Displacement Differences Observed At Double Prisms 132

LIST OF FIGURES

Figure 2-1. Diamond Valley Lake 7
Figure 2-2. Regional and on-site GPS monitoring stations 11
Figure 2-3. RTS observing station layout at DVL 15
Figure 2-4. RTS observing scheme, West Dam 16
Figure 3-1. DIMONS program modules 23
Figure 3-2. DIMONS Project Manager window 29
Figure 3-3. Defining a data collection task 30
Figure 3-4. Real-time display of data collection activities 31
Figure 3-5. DIMONS Processing Manager window 32
Figure 3-6. Defining a data processing task 32
Figure 3-7. DIMONS Data Browser window 33
Figure 3-8. Annotated plot of horizontal displacements 34
Figure 3-9. Effect of target or RTS replacement on measured distances 43
Figure 3-10. Minimum constraints datum bias caused by random pointing errors 56
Figure 3-11. Pattern of confidence regions for reference points 59
Figure 3-12. Precision improvement in weighted constraints solution 61
Figure 4-1. SensorMetrics ENV-50-HUM meteorological sensor module 65
Figure 4-2. Solar panels at observing station TS4 68
Figure 4-3. Batteries and computer at observing station TS4 69
Figure 4-4. (a) monument for dam face and (b) monument for bedrock 71
Figure 4-5. West Dam observing station TS4 73
Figure 4-6. RTS mounted on observing pillar 73
Figure 4-7. GPS antenna attachment on shelter roof 74
Figure 4-8. Ray path refraction caused by change in atmospheric conditions 76
Figure 4-9. Ray path deflection as a function of temperature differential 77
Figure 4-10. Relationships among DIMONS hosts at DVL 79
Figure 5-1. Coordinate system used to show variation in target positions 86
Figure 5-2. Point 1088 coordinate changes derived from 12 p.m. measurement cycles 88
Figure 5-3. Temperature increase inside observing shelter, station 1740 91
Figure 5-4. Point 1088 coordinate changes derived from all measurement cycles 93
Figure 5-5. Time-of-day height bias, point 1079 94
Figure 5-6. Point 1088 coordinate changes derived from weekly averages 98
Figure 5-7. Computation of check point accuracy 101
Figure II-1. Quantities involved in determining refraction effects on RTS displacement measurements 126

LIST OF TABLES

Table 3-1. Major items stored in the DIMONS database 36
Table 3-2. RTS-survey point setup records 39
Table 5-1. Empirical standard deviations of RTS measurements 83
Table 5-2. Standard deviations of coordinates derived from 12 p.m. measurements ... 89
Table 5-3. Standard deviations of coordinates derived from 4 a.m. measurements 90
Table 5-4. Standard deviations of coordinates derived from weekly averages 99
Table 5-5. Computed standard deviations of displacement components 101

LIST OF SYMBOLS

α, ν	Azimuth and elevation angle from robotic total station to target
δ, d, z	Local coordinate system used in accuracy analysis
$\delta_{i,j}, z_{i,j}, d_{i,j}$	Direction, zenith angle and distance measured to target i in set j of measurement cycle
Δ_i, Z_i, D_i	Direction, zenith angle and distance to target i as estimated in least squares set reduction
ω_j	Orientation unknown of set j as estimated in least squares set reduction
θ_i, θ_o	Angle between RTS beam and glass on inside and outside of RTS shelter
$s, \omega, \phi, \kappa, dX, dY, dZ$	Helmert similarity transformation parameters: scale, rotations around the X, Y and Z axes, and translation components
$\sigma_\delta^2, \sigma_z^2, \sigma_d^2$	Variances of directions, zenith angles, and distances
a_{EDM}	Additive constant of EDM portion of robotic total station
a_{prism}	Additive constant of survey prism
b	Scale factor of robotic total station
d_{obs}	Distance measured by robotic total station, no corrections applied
d'	Distance corrected for additive constant/scale factor
d''	d' corrected for atmospheric conditions
n_{REF}	Reference refractive index of robotic total station
n_L	Group refractive index at time of measurement
n_i, n_o	Refractive index of air on inside and outside of RTS shelter
n_{obs}	Total number of measurements used in least squares set reduction
n_s	Number of sets observed in a measuring cycle
n_T	Number of different targets observed in a measuring cycle
$r_\bullet$	Observation residual
$\hat{r}_\bullet$	Estimated observation residual from least squares adjustment
$\hat{\mathbf{x}}_1, \hat{\mathbf{x}}_2$	Preliminary coordinates of points in cycles 1 and 2
$\tilde{\mathbf{x}}_2$	Corrected coordinates of points in cycle 2

CHAPTER 1
INTRODUCTION

Geodetic displacement measurements have long played an important role in the analysis of structural deformation. The accuracy, versatility and capacity for self-checking and accuracy analysis make survey measurements from equipment such as total stations a popular choice in deformation monitoring [Chen, 1983]. While photogrammetric and, particularly, Global Positioning System (GPS) equipment is enjoying increasing acceptance and use in deformation surveys, there are many situations in which accuracy, cost and equipment maintenance considerations are best answered by the use of traditional angle and distance measurements. Geodetic displacement measurements using total stations will be an important source of monitoring data for many years to come.

Historically, one of the major limitations of geodetic monitoring techniques has been the difficulty of performing measurements in an automated fashion. While many geotechnical and other non-geodetic devices for deformation measurement are readily adapted for automated measurements [Chrzanowski, 1986], geodetic surveying has traditionally been a labour-intensive task, highly dependent upon the skill of the operator. Over time, total stations were developed that perform electronic distance measurement and automatic reading of the horizontal and vertical circles, but the biggest obstacle to automation remained the precise telescope pointing required to collect high-quality measurements.

Fortunately, recent developments have solved the problem of instrument pointing. Precise servomotors, combined with automatic target recognition capabilities, have enabled the new generation of robotic total stations (RTS) to achieve angular measurement accuracies better than one arc-second [Leica AG, 1996]. While some robotic total stations require special targets to operate [Trimble Navigation Limited, 2001], other models use standard corner-cube reflectors commonly utilized for distance measurement. The combination of these robotic instruments with data collection and processing software has yielded great advances in productivity for many surveying applications.

When it comes to geodetic displacement measurements, robotic total stations exhibit great potential. Because displacement monitoring is frequently carried out by performing repeated surveys of the same set of survey points, a computer-controlled RTS could be configured to carry out the measurements at a predetermined schedule. Furthermore, automated data processing software could perform field reductions and all other necessary calculations, requiring the user to merely examine the final results. Commercial software has been developed for these purposes; Leica's APSWin [Leica Geosystems, 2001], for example, offers automated data collection and processing for Leica robotic total stations.

This thesis describes the design and implementation of an RTS-based geodetic displacement monitoring system for the recently completed Diamond Valley Lake water reservoir in southern California. The size of the project (currently the largest earthfill dam project in the United States [Duffy and Whitaker, 1998]) and required monitoring

frequency made it necessary to incorporate as much automation as possible; the accuracy requirements, on the other hand, required a geodetic rigour not available using commercial software. Therefore, a new software package for data collection and processing was developed to meet the requirements of this project. The data collected and processed by this software package has also been evaluated to ensure that the completed monitoring system achieves the accuracy goals set forth in the initial system design. Preliminary results indicate that the automated system is a success, although steps were required to reduce the effect of atmospheric refraction.

Chapter 2 of this thesis discusses the Diamond Valley Lake monitoring project in general, and describes the geodetic monitoring program designed by the Metropolitan Water District of Southern California's Geometronics Division and Dr. Adam Chrzanowski of the University of New Brunswick. Part of the geodetic monitoring program is a local Dam Displacement Monitoring (DDM) system whose purpose is to measure the movement of the dams with respect to the underlying bedrock. This system uses permanently installed robotic total stations, for which data collection and processing is controlled by software developed as part of the work described in this thesis. Chapter 3 describes the architecture of this software, with a thorough discussion of the algorithms employed for data processing. In Chapter 4, implementation of the monitoring system is discussed; all of the hardware components required to build the system are presented, as well as a description of the monitoring system software configuration. Chapter 5 gives a preliminary evaluation of the performance of the monitoring system, using data collected in the first few months of system operation. Finally, Chapter 6 lists some major

conclusions arising from the author's experience in implementing this system and recommendations for further work in this area.

CHAPTER 2
THE DIAMOND VALLEY LAKE MONITORING PROJECT

The Metropolitan Water District of Southern California (hereinafter referred to as Metropolitan) is a public agency incorporated in 1928 for the purpose of providing water for the Southern California coastal plain. Metropolitan's infrastructure includes the Colorado River Aqueduct, five pumping plants, and a number of reservoirs for surface storage of drinking water. Metropolitan provides water to 26 member agencies, serving a population of approximately 17 million [Marks, 2001].

With such a large number of people in its service area, ensuring water quality and avoiding shortages is a major challenge for Metropolitan. Its reservoirs are instrumental in maintaining Southern California's water supply during the peak summer months and in times of drought. As the population grows, this task becomes more difficult, and from time to time it is necessary to construct new facilities to deal with increased demand. With this in mind, Metropolitan began in the late 1980s to plan a major expansion of its water storage capacity.

2.1 History and Overview of Diamond Valley Lake

This major expansion came in the form of Diamond Valley Lake (DVL), formerly known as the Eastside Reservoir Project. Located near the city of Hemet, about 160 kilometres southeast of Los Angeles, Diamond Valley Lake will be the largest reservoir in Southern California when it is filled. Containing 986.8 million cubic metres of water [Duffy and Whitaker, 1998], this $2 billion facility will nearly double Southern

California's surface water storage capacity, holding enough water to supply Metropolitan's service population for six months [Duffy and Whitaker, 1998].

Diamond Valley Lake was formed by enclosing the Domenigoni and Diamond valleys by three earth/rock fill type dams [Duffy et al., 2001]. These dams include:

1. The West Dam, which is 87 metres high and 2.9 kilometres long.
2. The East Dam, which is 56 metres high and 3.2 kilometres long.
3. The Saddle Dam, which is 40 metres high and 0.8 kilometres long.

These three dams constitute the largest earth/rock fill dam project ever constructed in the United States [Metropolitan Public Affairs Division, 1997]. The dams enclose an area which is 7.2 kilometres long and approximately 3.2 kilometres wide, covering 1821 hectares. The crest elevations are 539 metres above mean sea level, resulting in a final water depth ranging from 49 to 79 metres. The layout of the three dams with respect to the surrounding topography is shown in Figure 2-1.

Construction of the dams began in September 1995, and proceeded on a very fast pace due to the quarrying of almost all of the construction materials from within the valley. All three dams were completed by December 1999. At this time, filling operations began and they are expected to take 2-5 years, depending upon weather conditions and the availability of water. As of October 2001, the reservoir is 60% full [Chrzanowski, 2001].

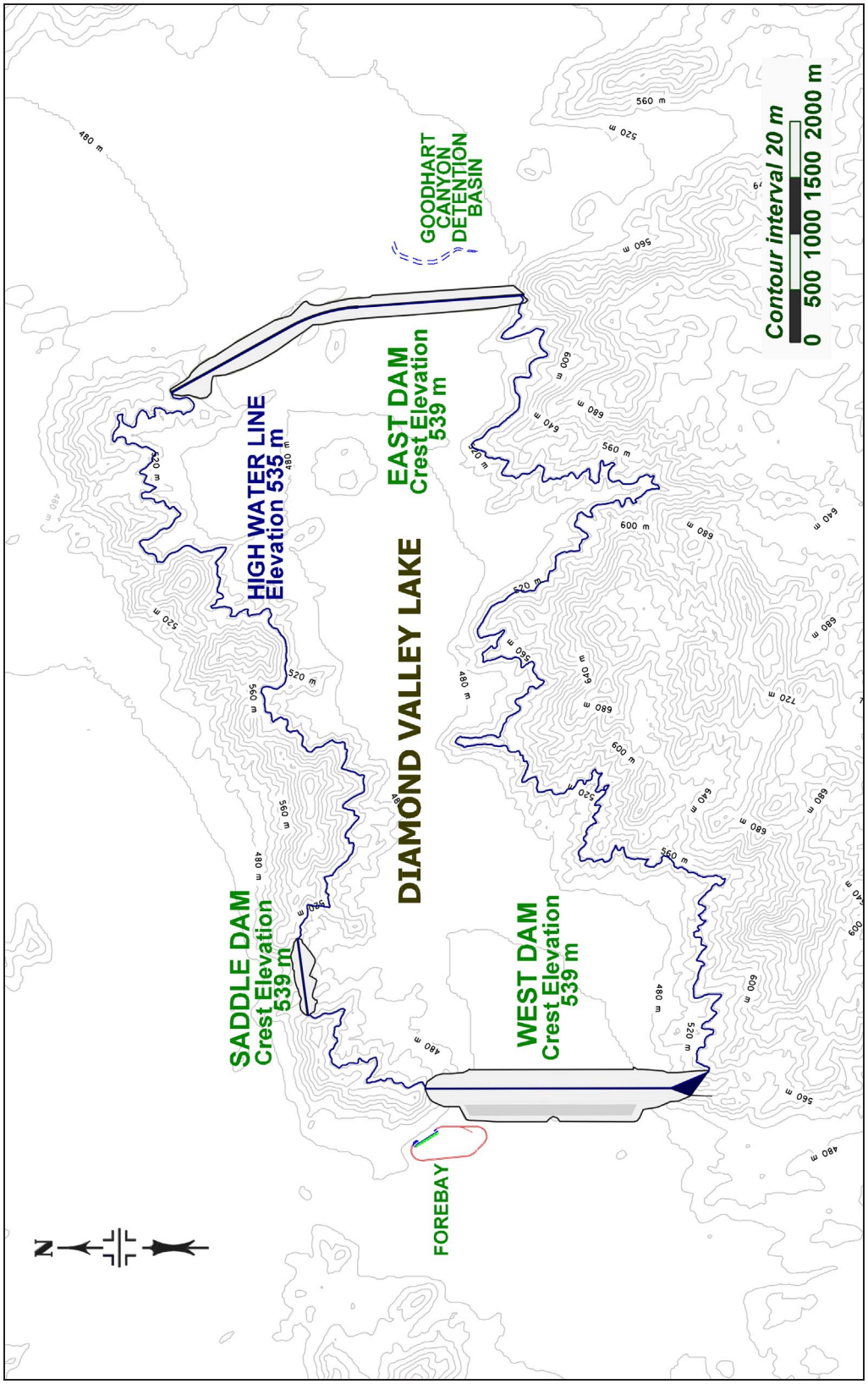

Figure 2-1. Diamond Valley Lake

2.2 The Diamond Valley Lake Monitoring System

All dams constructed in California, subject to height and storage capacity restrictions, fall under the jurisdiction of the California Department of Water Resources [Burkhard, 2001]. Within this department, the Division of Safety of Dams (DSOD) is responsible for monitoring dam safety. The DSOD determines minimum monitoring requirements, as well as supervising and performing periodic reviews of California dam owners' surveillance programs [Smith, 1989]. The dam owners are responsible for instrumenting their structures, performing surveillance measurements and submitting the monitoring results to the DSOD.

At the time of construction of DVL, Metropolitan was performing regular monitoring at nineteen of its facilities [Whitaker, 1996], so they had some experience in the design and implementation of dam monitoring schemes. Due to its size and location, however, the DVL monitoring system would pose some new challenges.

First, DVL is located near the San Jacinto fault, a tributary of the San Andreas fault. The DVL monitoring system would have to be designed with due consideration to the effect of seismic activity, allowing Metropolitan to discriminate between regional movements and local displacement of the dam structures with respect to their immediate surroundings.

Second, the Diamond Valley Lake dams are huge when compared to other facilities operated by Metropolitan. This caused some concern over the amount of labour that would be required to carry out monitoring. While each facility operated by Metropolitan

has unique characteristics, a typical monitoring scheme includes survey monuments on the crest of the dam, on each embankment of the dam, and several lines of points on the upstream side of the reservoir [Whitaker, 1996]. The spacing of survey monuments is normally in the range of 76 to 152 metres (250 to 500 feet). Using a monument spacing of 152 metres on each berm of the dams and 76 metres on the dam crests, approximately 360 survey points are required, with weekly monitoring during the entire filling period [Duffy et al., 2001]. Metropolitan wished to determine displacements of these survey monuments with an accuracy of 10 mm at the 95% confidence level [Duffy and Whitaker, 1998].

Finally, DVL is located approximately 100 kilometres from Metropolitan's survey offices in Glendora, California. Normally, this distance would not pose a problem; many of Metropolitan's other facilities are located even farther from the survey office. However, the amount of survey effort required at DVL would be much greater than at the other facilities, particularly during the filling period. This would result in a lot of time spent travelling to and from the site by field survey personnel.

Because of these considerations, Metropolitan decided to take a new approach in designing a geodetic monitoring system for DVL. An external consultant [Chrzanowski, 1996] was employed to help design a robust scheme that would meet Metropolitan's requirements while minimizing labour costs. The resulting monitoring system design comprises three main components:

1. A local Dam Deformation Monitoring (DDM) system to monitor the behaviour of the dams and surrounding structures with respect to the underlying bedrock.
2. An on-site GPS area control network to monitor the stability of the immediate area surrounding the reservoir and to check and periodically update the positions of DDM reference stations.
3. A regional GPS control network connecting the DDM and on-site GPS network with the permanent observing stations of the Southern California Integrated GPS Network (SCIGN) [Hudnut, 2001].

A general discussion of the system design is presented in the remainder of this chapter, followed in subsequent chapters by a more detailed description of the DDM system implementation.

2.2.1 Regional and On-Site Area Monitoring Networks

The overall stability of the Diamond Valley Lake area with respect to regional crustal behaviour is monitored by two continuously operating GPS reference stations (otherwise known as CORS) connected to SCIGN. These stations, denoted as ESRE and ESRW in Figure 2-2, are located at the northwest and southeast corners of DVL. The two stations, part of a network of 250 such stations operating in southern California, automatically upload data to the SCIGN processing facility in La Jolla, California [Duffy et al., 2001]. Positions of all the SCIGN CORS stations are posted daily on the Internet by the Scripps Orbit and Permanent Array Center (SOPAC) [SOPAC, 2001] and are free for all users.

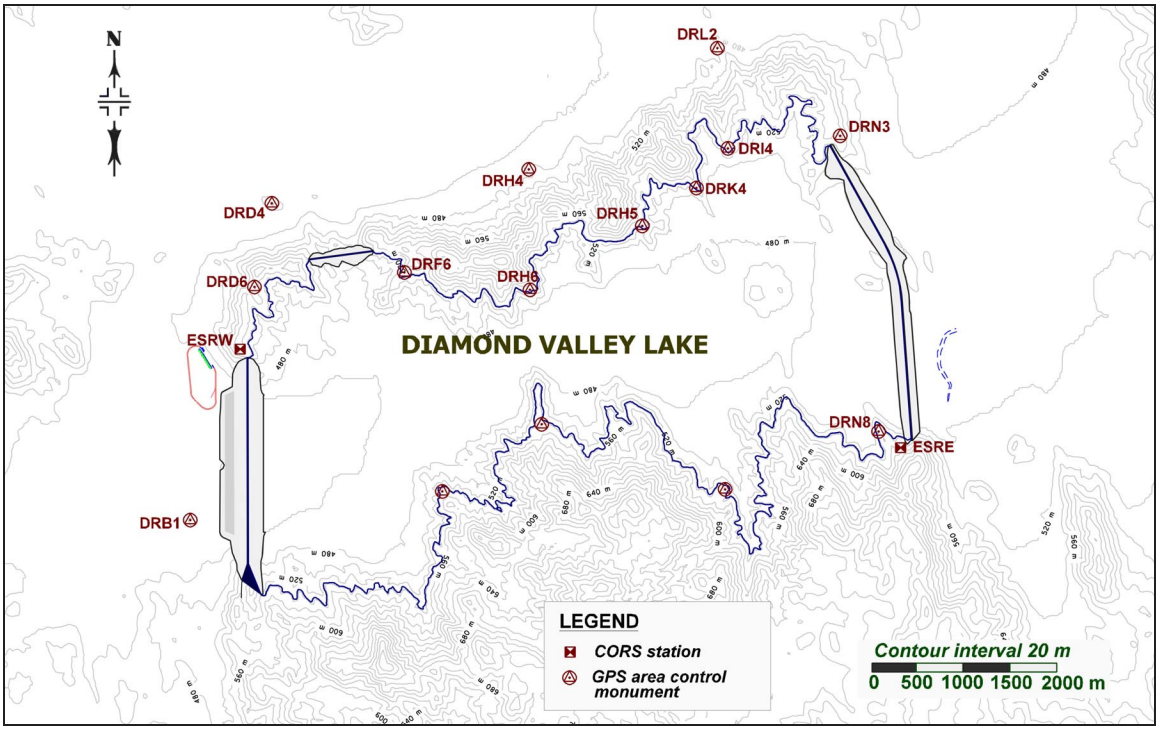

Figure 2-2. Regional and on-site GPS monitoring stations

For monitoring the stability of the area immediately surrounding the reservoir, a network of sixteen survey monuments was designed. These monuments, located on the ridgelines surrounding the reservoir, will be used to monitor the behaviour of the surrounding hills as they are subjected to the increasing load of the rising water level in the valley. They will also be used to monitor the stability of observing stations used in the local dam displacement monitoring network, which will be discussed in the next section. GPS observations will be used to measure the sixteen area monitoring stations annually, or after any major seismic event [Duffy et al., 2001].

2.2.2 Local Dam Displacement Monitoring (DDM) Network

Design of the regional and area control networks was a straightforward task, and the designs could easily be implemented by Metropolitan's survey personnel. Monitoring of local structural movements, however, posed a much greater challenge due to the size of the facility.

The structural monitoring surveys at other facilities operated by Metropolitan involve using either GPS or a total station to monitor horizontal movement and using an electronic level or a total station to measure vertical movement. These techniques, while quite suitable for small projects, are labour-intensive and do not scale well to larger projects. Whitaker [1996] estimated that use of Metropolitan's standard monitoring techniques at DVL would require seven full-time employees and 1168 person-hours per survey (this estimate is based on a monthly survey schedule). Metropolitan at this time was using only five regular employees to monitor nineteen of its other sites [Whitaker, 1996], so this would constitute a major expansion of their monitoring activities.

In order to reduce the cost of monitoring surveys, Metropolitan sought a method for automating the observing procedure. GPS measurements were one possibility, but they were found to be uneconomical in this situation because of the sheer number of points involved: a Real-Time Kinematic (RTK) survey with a mobile receiver would require 17 miles of walking [Duffy and Whitaker, 1998], and permanent installations would be prohibitively expensive and difficult to maintain.

Measurements with a robotic total station (RTS), on the other hand, could be done much more economically. The monitoring points could be equipped with inexpensive, permanently mounted prisms, and many points could be observed from a single location. Furthermore, with appropriate control software, the sequence and timing of measurements could be programmed to take place without operator intervention.

The robotic total station scheme, therefore, was chosen as the preferred scheme for the DDM system. Metropolitan had two choices for its implementation: (1) as a semi-automated system, whereby an operator sets up the total station at each observing point and uses data collection software to carry out the measurements, or (2) as a fully automated system, where a number of total stations are permanently installed and carry out measurements according to a predetermined schedule. For security, and to protect the equipment against environmental conditions, permanent installations would require the instruments to be housed in shelters with glass walls.

Of the two choices, the fully automated scheme was determined to be more attractive. A fully automated monitoring system could be activated remotely, greatly improving response time in emergency situations while not placing survey personnel in danger. The system could also be scheduled to collect measurements as often as desired, day or night, with virtually no increase in cost. This represents a major advantage over the semi-automated scheme; if it is found that the required accuracy is not being met, the system operator can schedule more frequent measurements, choose a different time of day for data collection, or both. The labour cost in this scenario would be reduced to in-office data processing and equipment inspection and maintenance.

The overall cost of implementing this fully automated system would be dominated by the initial cost of construction and equipment purchases. These costs, in turn, would be dictated by the total number of observing locations required, which depends upon the required accuracy of the system. For DVL, Metropolitan wished to detect displacements larger than 10 mm at the 95% confidence level. Realizing that displacements are calculated from two separate position determinations, the maximum allowable major semi-axis lengths of the standard point confidence regions will be $\frac{10\,\text{mm}}{2.45 \cdot \sqrt{2}} = 2.9\,\text{mm}$ in the horizontal plane, and $\frac{10\,\text{mm}}{1.96 \cdot \sqrt{2}} = 3.6\,\text{mm}$ for heights. Given a total station capable of achieving a standard deviation of 1" for horizontal and vertical angles and 1 mm for distances, the maximum sight length is thus restricted to approximately 600 metres. Other error sources, such as atmospheric refraction, will also reduce the achievable precision; it was decided, therefore, to keep all sight lengths shorter than 500 metres if possible [Duffy and Whitaker, 1998]. After several possible configurations were considered, the observing station layout shown in Figure 2-3 was chosen.

A total of eight observing stations are required in this scheme. Each survey monument on the downstream faces of the three dams, around the forebay, and at the west end of the detention basin is measured from one of the observing stations. Only the downstream monuments are visible from the observing stations: the upstream monuments will be observed using conventional GPS, total station, and levelling measurements until they are covered by the rising water.

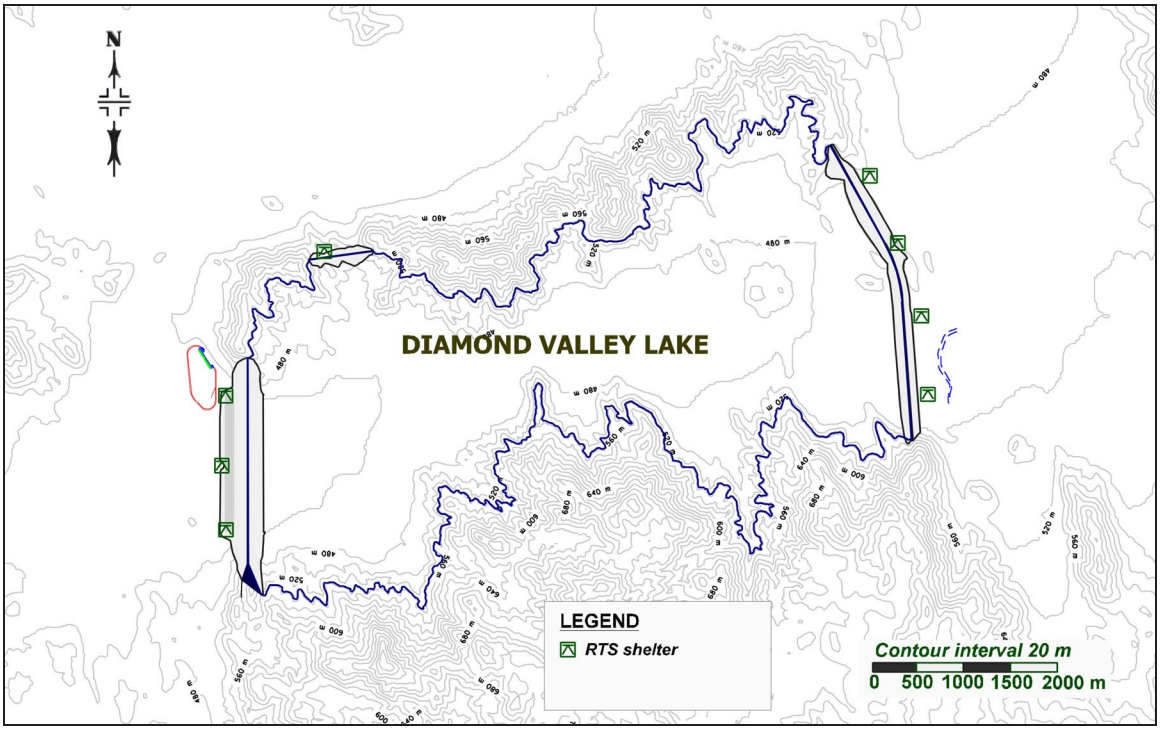

Figure 2-3. RTS observing station layout at DVL

The stability of each automated observing station will be monitored by including observations to at least three reference pillars anchored in sound bedrock. To provide an additional check on the integrity of the survey measurements, some of the survey monuments located between two observing stations are to be equipped with dual prisms, one mounted directly over the other. Displacements measured from adjacent observing points can then be compared to check the overall accuracy of the monitoring system. Figure 2-4 shows the observing scheme design for the three West Dam observing stations.

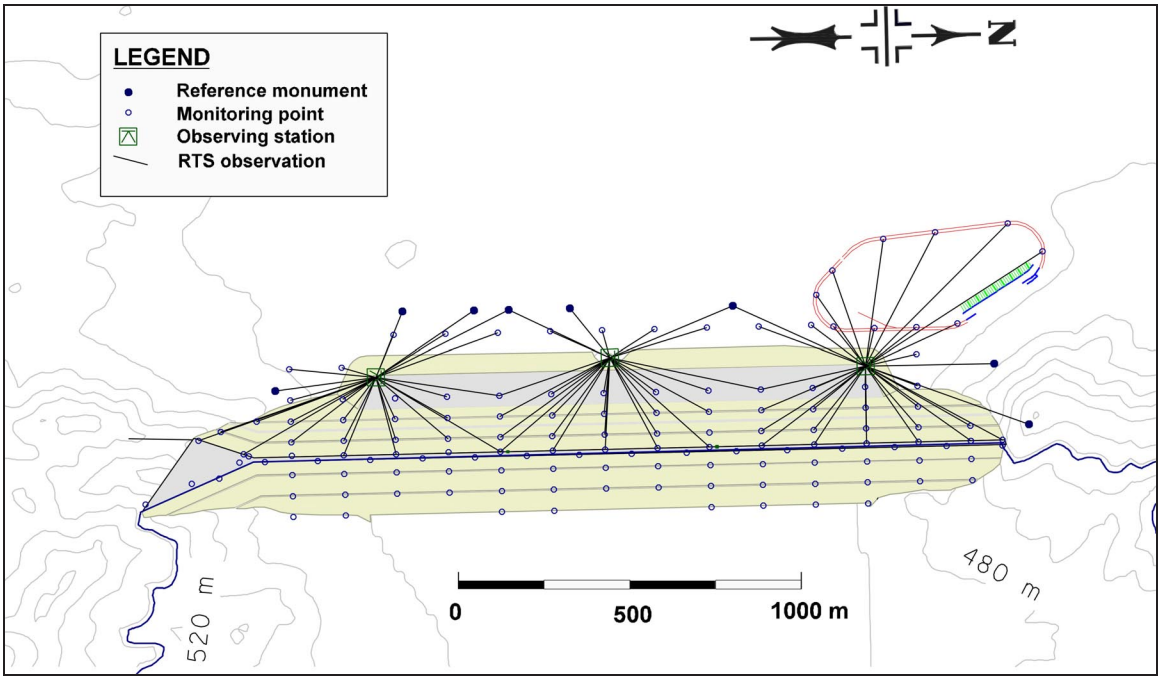

Figure 2-4. RTS observing scheme, West Dam

Whitaker [1996] calculated that an estimated $1.1 million would be needed for initial equipment purchases, software development, and installation of this automated monitoring system. This initial cost would be easily recovered by labour savings during the estimated 5-year filling period. Based on the originally planned monthly observing schedule, the conventional monitoring of upstream monuments would cost a total of $570,000. Conventional monitoring of all monuments, on the other hand, would cost $3.4 million. Therefore, the use of an automated system would result in a total savings of $1.7 million over five years. The later change in required monitoring frequency to a weekly rather than monthly schedule further highlights the savings to be realized using the automated system.

CHAPTER 3
DEVELOPMENT OF THE DIMONS SOFTWARE FOR AUTOMATED DISPLACEMENT MONITORING

As illustrated in the previous chapter, an automated system utilizing robotic total stations was found to be the most practical and cost-efficient method of monitoring the large number of points at Diamond Valley Lake. Creation of such a system, however, could not be accomplished by simply purchasing off-the-shelf hardware and software components. In addition to designing and building structures to house the robotic total stations, it would be necessary to develop a software system to collect and process the observation data. Therefore, in September 1999 Metropolitan released a Request for Proposals (RFP) inviting contractors to design and implement a software package for the proposed DDM system at Diamond Valley Lake [Metropolitan, 1999]. This RFP was answered by several bidders, including the Engineering Surveys Research Group at UNB who were eventually awarded the contract.

This chapter describes the DIMONS (DIsplacement MONitoring System) software that was developed at UNB for use at Diamond Valley Lake. In section 3.1, basic requirements for the monitoring software are outlined. Section 3.2 describes the resulting software architecture and data storage strategy that were developed to meet these requirements. Finally, section 3.3 presents the major algorithms used in the software.

3.1 Software Design Considerations

As with any software package, the design of DIMONS had to be carried out with careful consideration of the needs of its users. DIMONS was to be developed for use by Metropolitan at its Diamond Valley Lake facility. Therefore, it was crucial that the UNB development team gain a clear understanding of Metropolitan's goals in this project.

Because UNB had been involved in development of the monitoring scheme, we were already familiar with some aspects of the project. It was known, for instance, that the site was located over 100 kilometres from the survey office, and that the monitoring surveys would be conducted for several years. This highlighted the need for a reliable system that could operate in a highly automated fashion for long periods of time, and that would be flexible enough to accommodate future changes in the system configuration. These necessary characteristics were reflected in the RFP for the software development contract, which stated a number of explicit requirements for the monitoring system software. The stated requirements included the following:

1. The software must operate under the most recent version of the Microsoft Windows NT operating system.
2. It must store its data in a relational database.
3. It must support operation in fully automatic, semi-automatic, or interactive measurement modes.
4. It must be compatible with the Leica TCA1800S robotic total station.
5. It must support flexible, user-configurable scheduling of data collection activities.

6. It must interface with digital temperature and pressure sensors for meteorological data storage and correction of measured distances.
7. It must support remote access through the area communications network.
8. It must have the ability to transfer observation data between different computers.
9. It must perform an automatic restart of measurements following a power loss.
10. It must perform automatic data processing, including a stability analysis of the reference points observed by each RTS.
11. It must be possible to incorporate data from a roving total station, which would be moved from observing point to observing point.

Discussions with Metropolitan were also helpful in determining their expectations and intended use of the software. Their general concept of operations was that once the software was appropriately configured, it would run automatically and would send data from all observing stations to be combined in one database in the survey office in Glendora. Only routine maintenance, such as relevelling and recalibrating the total stations or cleaning the glass walls of the observation shelters, would require a site visit.

In spite of frequent communication with Metropolitan, a number of important details were not known at the time the software design was begun. First, the software was required to store its data in a relational database; the RFP did not state what database management software would be used to access this database. Second, the software was required to interface with digital temperature and pressure sensors; the make and model of sensor were not stated either. UNB would be required to choose a supplier and implement device drivers for them in DIMONS. Finally, the software was required to

support remote access through the communications network. At the time the RFP for software development was released, Metropolitan had not yet released an RFP for supplying the communications network, and they had not decided what communications technology to employ.

Successfully delivering a working software product with so many factors still to be decided would require careful design of a suitable software architecture. This design took place over the course of approximately one month following the awarding of the development contract. The following section describes the DIMONS software architecture and discusses how this design meets Metropolitan's requirements.

3.2 DIMONS Architecture

Before any implementation details were considered, an overall system design was created outlining in broad terms how the requirements could most effectively be met. This was done by examining some of the key requirements and their implications from a software development standpoint.

First, the system was required to be usable in both fully automatic and interactive modes. To avoid duplication of functionality, this would be accomplished most easily by utilizing a client/server model. Most of the software functionality would be contained in server programs, which would provide an Application Programming Interface, or API as it is commonly known. Different client programs could then be used to access the system; one client could work by reading its commands from a file, for example, while another could present the user with a graphical interface.

Second, the system was required to be accessible across the communications network. This is another good reason to use a client/server model. The amount of effort required to achieve remote access, however, would be highly dependent on the nature of the communications network; our goal was to minimize development time by using facilities offered by the operating system rather then creating specialized communication protocols.

Third, the system was required to support a particular make and model of robotic total station. To ease future hardware upgrades, the instrument controllers should be implemented as plugin modules that could be replaced without affecting the rest of the software.

Finally, the system was required to support data storage in a relational database. To ease future software upgrades, the system should be highly flexible in supporting different database formats, enabling Metropolitan to choose from a wide variety of vendors while minimizing the development effort involved. This could be accomplished by encapsulating all database access routines within a single module, thus minimizing the impact of a particular choice of database vendor on the overall system design.

3.2.1 Program Structure

The design considerations outlined in the previous sections suggested strongly that the monitoring system software should be implemented as a system of discrete modules, each responsible for a particular task. Core functionality of the system would be

contained in server modules, while different client programs would offer different levels of user interaction with the system.

The base technology chosen for development of these program modules was Microsoft's Distributed Component Object Model (DCOM). COM itself is an object-based programming model designed by Microsoft to promote software interoperability [Microsoft, 1995]. DCOM extends this interoperability to include networking support. The principles and usage of COM and DCOM are described in detail by many authors; the reader is referred to Microsoft [1995] and Grimes [1997] for further information. DCOM offered several key features that made it a desirable choice for development of DIMONS:

1. It is fully supported by Microsoft, and runs on all versions of Windows (starting with Windows 95), the Macintosh operating system, and various UNIX platforms [Grimes, 1997].
2. It enables programmers to easily mix software components written in different programming languages. This enables the programmer to choose the programming language best suited to a particular task.
3. It enables programmers to easily support remote procedure calls across the network. To a large extent, the COM subsystem of the operating system takes care of network communication, so that the programmer does not have to be concerned with developing protocols to transfer data across the network.

4. The security mechanisms offered by the Windows operating system are fully supported. This means that no one could use the RTS computers to break into Metropolitan's enterprise network.

These features greatly reduced the difficulty in designing a software architecture to meet Metropolitan's needs.

Using DCOM, the DIMONS software was designed as a collection of server and client components. Each component is responsible for a specific task; for instance, the meteorological sensor controller is responsible for reading temperature, pressure, and relative humidity when instructed to do so. A schematic overview of the different software components in DIMONS is presented in Figure 3-1.

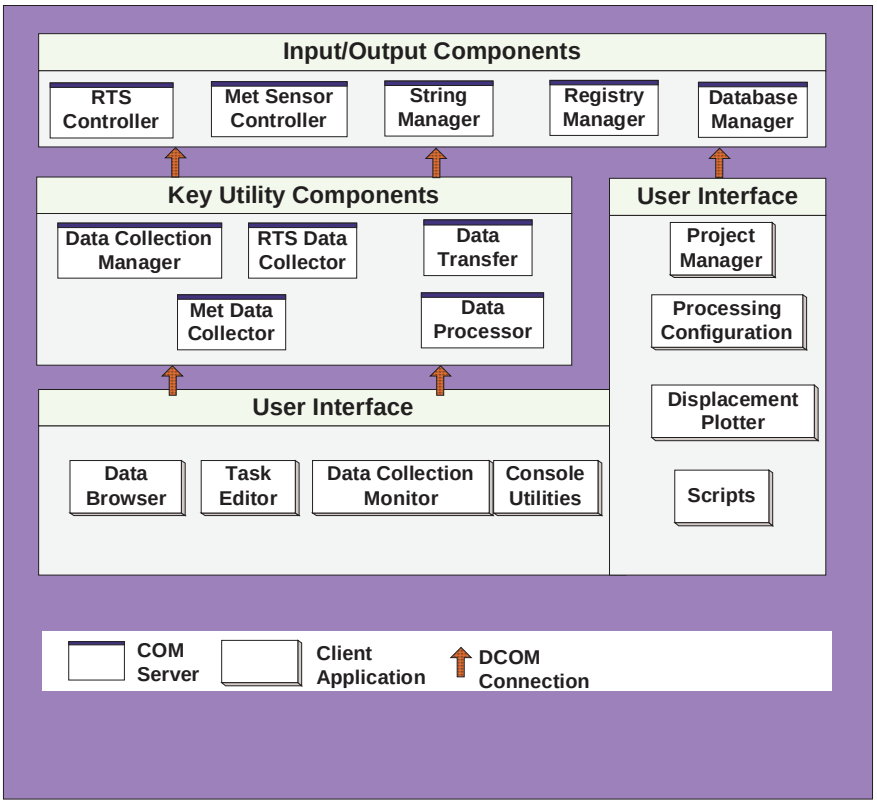

Figure 3-1. DIMONS program modules

The DIMONS modules can be divided into three main layers of functionality: an input/output layer, responsible for accessing external devices, the program database, and the Windows registry; a layer of key utilities, where most of the system functionality is contained; and a user interface layer, containing client applications that utilize the system to perform various configuration and data manipulation tasks. Most of the input/output components, key utility components, and console (command-line) utilities are written in C++, while the interactive client applications are written in Visual Basic. The different program modules and their responsibilities are outlined in the following sections, grouped by functionality layer.

3.2.1.1 Input/Output

Several different program modules encapsulate the different methods of getting data into and out of the DIMONS software. These modules are described below.

The *RTS Controller* is a module responsible for basic control of a robotic total station. It turns the instrument on and off, guides it to different targets, and prompts it to collect observations. The RTS Controller interface (its properties and the functions it supports) was defined when developing the RTS Data Collector, described in the following section; all different RTS controller components must support the same interface. This means that multiple controller components (for different makes and models of RTS) can be introduced without modifying any other part of DIMONS. The RTS Data Collector already knows what functions it can call, and what properties it can set or query, on any RTS controller installed on the system. From a client standpoint, they are all the same.

For the DVL monitoring project, only one RTS controller (for the Leica TCA1800S total station) would need to be developed, but this approach allows new controllers to be created and added at any time without modification.

The *Met Sensor Controller* is responsible for basic control of a meteorological (atmospheric temperature, pressure, and relative humidity) sensor module. When prompted, it queries the sensor and returns the readings. The controller interface was developed using the same philosophy as for the RTS controllers; a plug-in concept is employed, whereby a common interface is supported by controllers for different instruments. For the DVL project, a sensor controller would be developed for one make and model of sensor, to be chosen by the development team.

The *String Manager* handles all text strings used by all DIMONS program modules. The String Manager uses a message table to store the strings; client applications provide the String Manager with the numeric ID of the desired string, and the string is returned. Because the storage of application strings takes place in a single location, different languages can easily be supported by adding new message tables with the same numeric identifiers for corresponding strings. Furthermore, centralized storage improves consistency among applications (by sharing the same strings) and makes it easier to fix typographical errors.

The *Registry Manager* handles DIMONS configuration management by interacting with the Windows Registry. User interface clients use the Registry Manager to store session parameters (last project opened, window location and size, etc.), while the RTS

and Met Sensor controllers use it to register themselves as plugin modules available to DIMONS.

The *Database Manager* hides the database implementation from the rest of the DIMONS software. Any program module that wishes to retrieve data from, or add data to, the database must do so by calling the functions of the Database Manager; for instance, to add a new RTS observation record to the database, the client calls the `AddRtsObs()` function. Because of the data abstraction offered by this component, changes in the DIMONS database structure affect only the Database Manager and no other component of DIMONS.

3.2.1.2 Key Utilities

The key utility components contain most of the functionality required to collect observation cycles, transfer data from the field to the office, and process the data to yield point coordinates. There are five main utility components that offer this functionality.

The *RTS Data Collector* is the component responsible for carrying out a cycle of RTS observations. Given a set of parameters describing what points to measure, what tolerances to meet, and the name of the observing point, this component first looks up the database record corresponding to this observing point. From this record, it finds out what make and model of instrument are installed on the observing point. It then loads the appropriate RTS controller and instructs the controller to measure each point in turn. Quality checks are performed on the collected data, and the RTS Data Collector stops measurements when the required tolerances have been met.

The *Met Data Collector* carries out the meteorological measurements. Like the RTS Data Collector, it determines the type of instrument installed at the observing point and loads the appropriate sensor controller. It then queries the sensor controller at user-defined intervals, storing the collected measurements in the DIMONS database via the Database Manager.

The *Data Collection Manager* coordinates the data collection activities of the RTS Data Collector and the Met Data Collector. When instructed to begin a measurement cycle, it launches the Met Data Collector and then the RTS Data Collector. When the RTS Data Collector finishes its measurement cycle, the Data Collection Manager stops the Met Data Collector as well. The Data Collection Manager is a multithreaded application that allows multiple clients to connect simultaneously. As the data collection progresses, the Data Collection Manager sends event messages to its clients reflecting the data collection status.

The *Data Transfer* component is responsible for transferring observation data from one computer to another. Given a set of parameters describing what data is to be transferred and where it is to be sent, the Data Transfer component transfers data from one DIMONS database to another. All relevant system configuration parameters, including instrument and target heights, are transferred along with the observation data so that the data can be processed at the destination computer. In DIMONS, the Data Transfer component is used to transfer observation data from the field to the office for processing. Configuration changes made in the field are automatically transferred to the office when new data is collected.

The *Data Processor* carries out the actual data processing, reducing the raw observation data to yield a final set of point coordinates for each cycle of measured data. Given the name of the observing point and the date of the cycle to process, the Data Processor gathers the observation data and configuration parameters from the database. The data is subjected to several stages of reduction and processing (described in section 3.3), finally obtaining a set of point coordinates and adding them to the DIMONS database.

3.2.1.3 User Interface

The user interface layer consists of a number of client applications that are used to interact with the DIMONS server components. Graphical utilities are provided to allow the user interactive access to the system, and a number of command-line utilities are also provided for scheduling and batch processing. The DIMONS user interface utilities are described below.

The *Project Manager* is a graphical utility enabling the user to configure the data collection portion of a DIMONS project. Before it is possible to collect observations, the user must enter parameters describing the survey points, total stations, meteorological sensors, targets, and pointsets, among other things. This information must be entered at each site that will be used for data collection. The DIMONS Project Manager groups the necessary parameters into a number of categories, as shown in Figure 3-2.

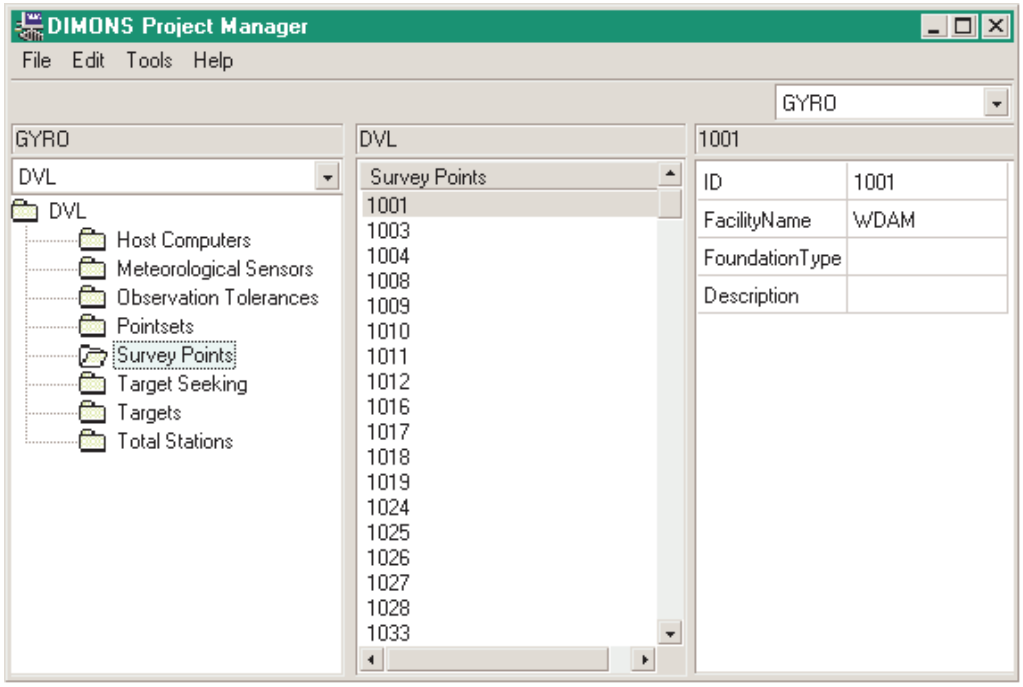

Figure 3-2. DIMONS Project Manager window

The listbox in the upper-right corner shows the word 'GYRO'. This is the name of the computer being configured. Different DIMONS host computers can be accessed from a central location by specifying the IP address and a username and password valid on each remote host. Once this has been done, changing the DIMONS configuration on a remote computer is as simple as selecting its name from this list.

When the project has been configured on each DIMONS host, the system is nearly ready for data collection. To perform data collection, it is first necessary to define a *task* (a collection of parameters describing an activity to be carried out) indicating which observing point to used, what targets to observe, what tolerances to meet, and how often to log meteorological readings. This is performed using the *Task Editor*, as shown in Figure 3-3.

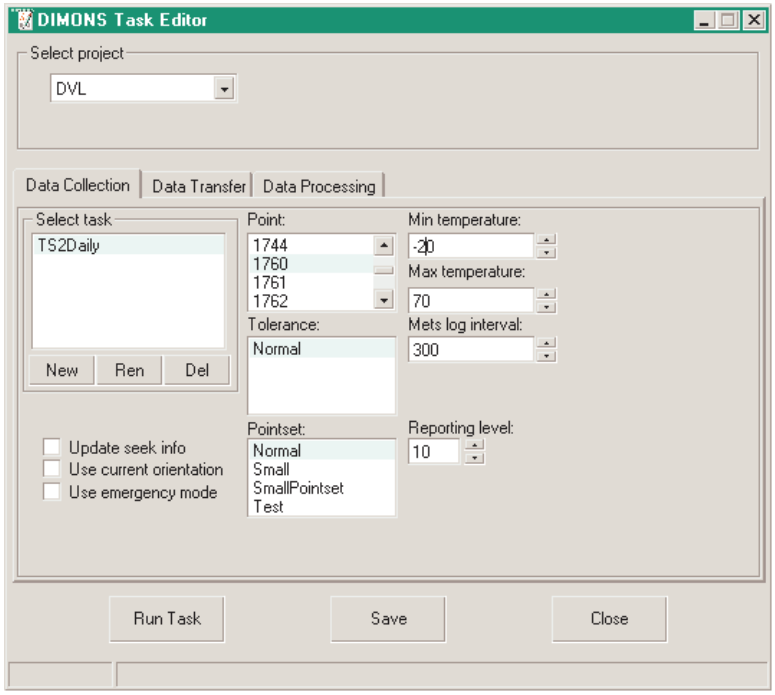

Figure 3-3. Defining a data collection task

Once a data collection task has been defined, the *Data Collection Monitor* can be used to start data collection. The Data Collection Monitor can be launched from any DIMONS host computer, and can be used to stop, start, and monitor the progress of data collection tasks on any other host computer. A sample Data Collection Monitor display is shown in Figure 3-4.

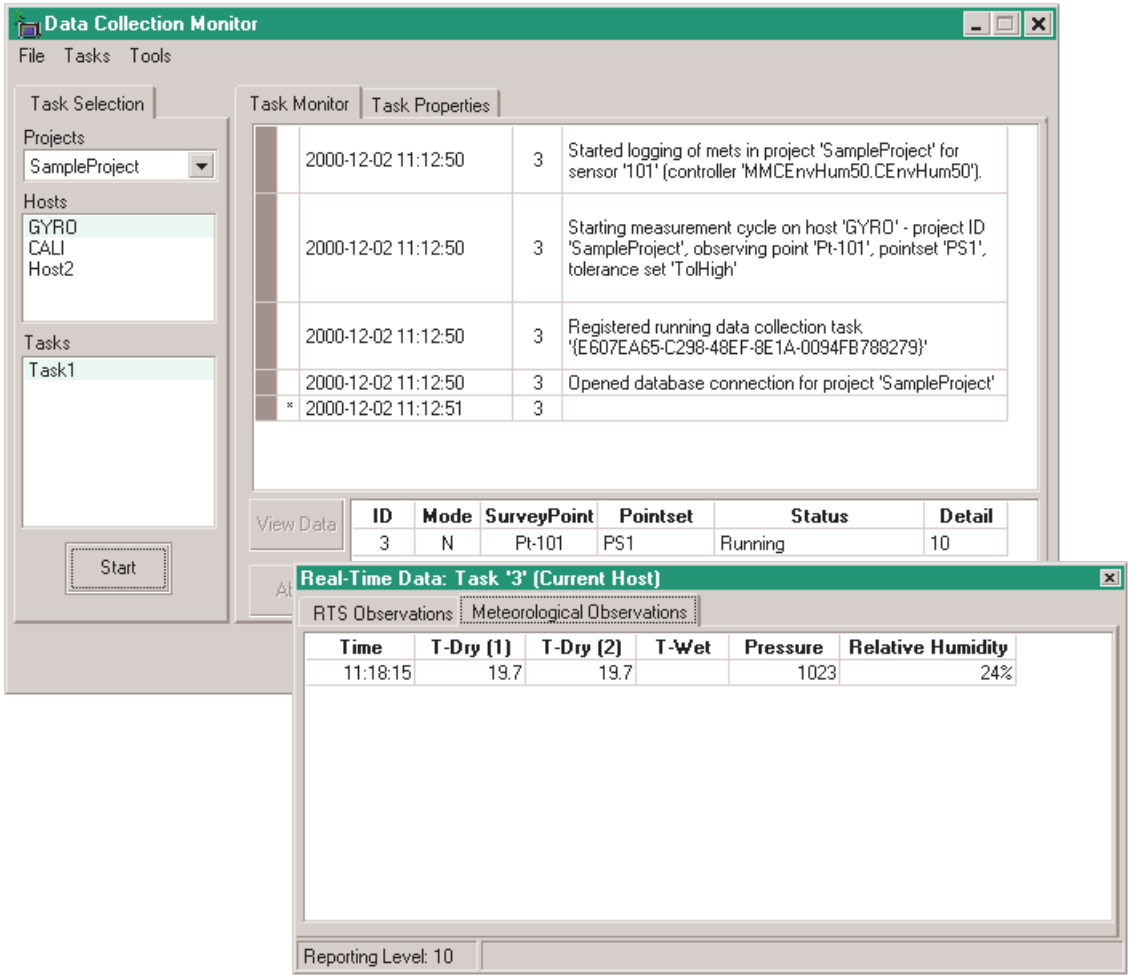

Figure 3-4. Real-time display of data collection activities

After the data has been collected, it must be processed to yield point coordinates. The processing parameters are defined using the *Processing Manager*, shown in Figure 3-5. Tolerance criteria, listings of reference points, and other settings are required by the data processor. The stages of data processing are described in section 3.3.

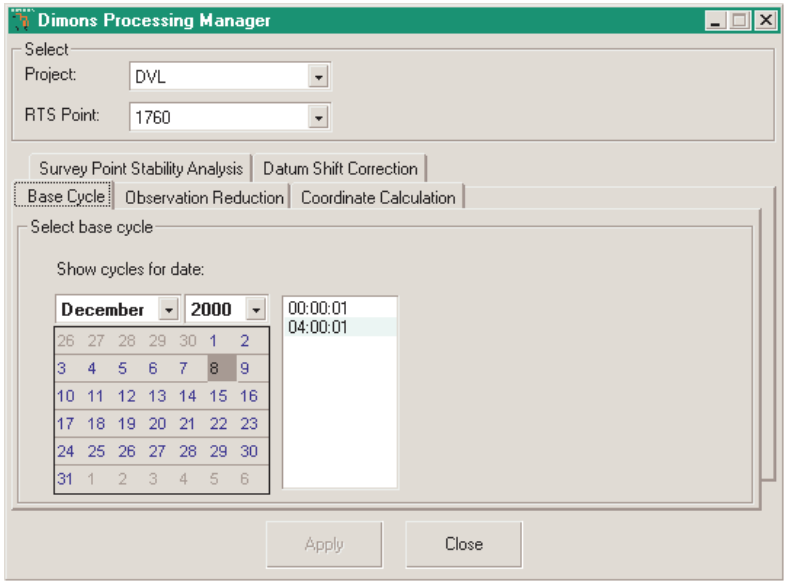

Figure 3-5. DIMONS Processing Manager window

As with data collection, data processing tasks can be defined using the Task Editor, and can be scheduled for automatic execution. The Task Editor interface for defining data processing tasks is shown in Figure 3-6. As can be seen in the figure, data processing tasks are defined using many parameters, which will not be discussed here.

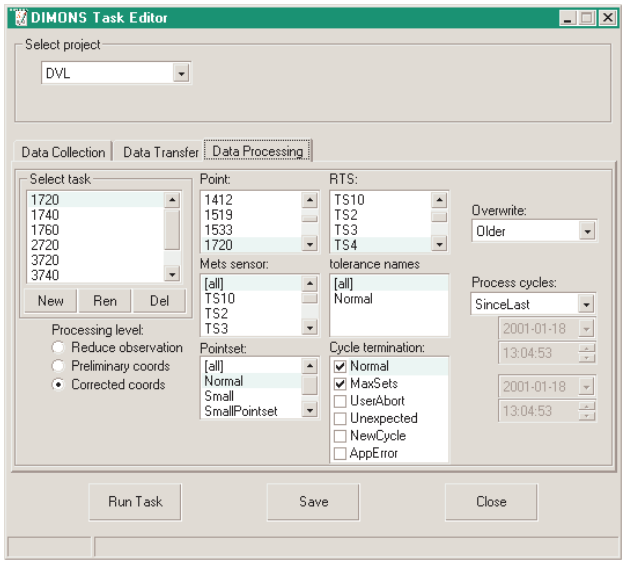

Figure 3-6. Defining a data processing task

The user can browse through the raw observations, as well as the final point coordinates, by using the *Data Browser*. The data can be sorted using a number of different criteria, enabling the user to easily make comparisons between different observation cycles. The Data Browser interface is shown in Figure 3-7.

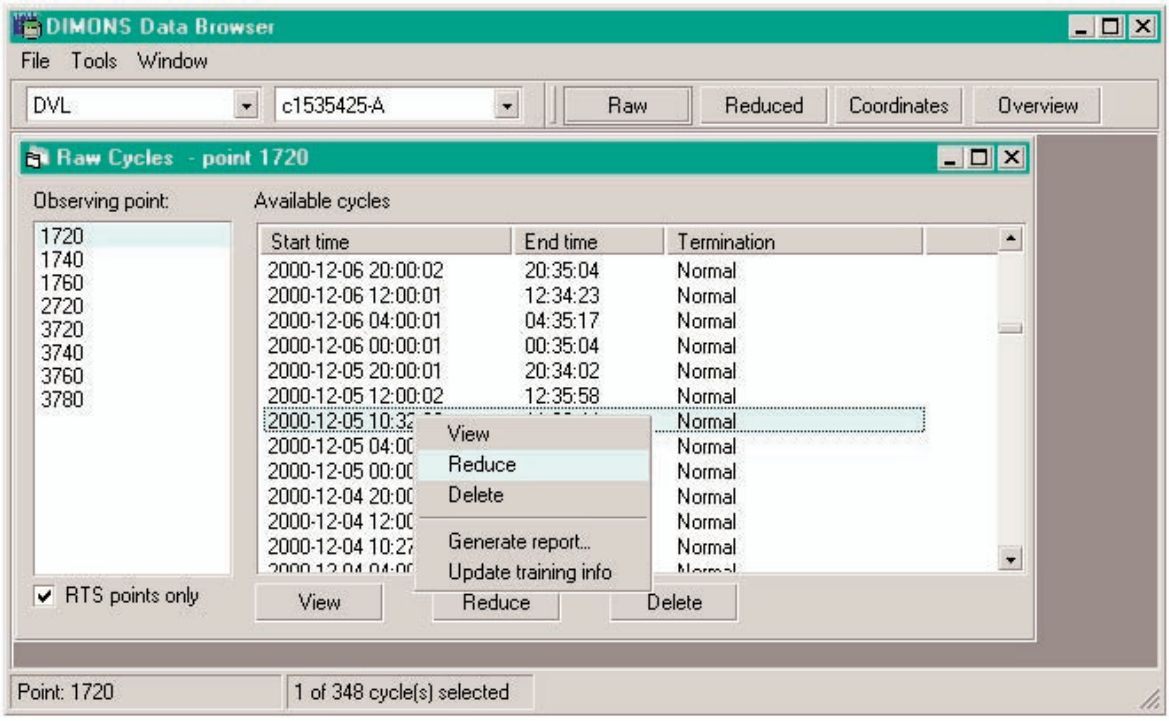

Figure 3-7. DIMONS Data Browser window

For visualization of the monitoring results, a decision was made to use COTS (Commercial Off-The Shelf) software instead of developing new software. This was done to reduce the development effort, as well as to give Metropolitan much more flexibility in generating figures for their reports. Because Metropolitan already used a popular CAD (Computer-Aided Drafting) package called MicroStation, the DIMONS *Displacement Plotter* is restricted to generating plots of displacements and their error

ellipses in the MicroStation file format. This allows Metropolitan to use the displacement plot as merely one layer in a much more complex figure, as shown in Figure 3-8.

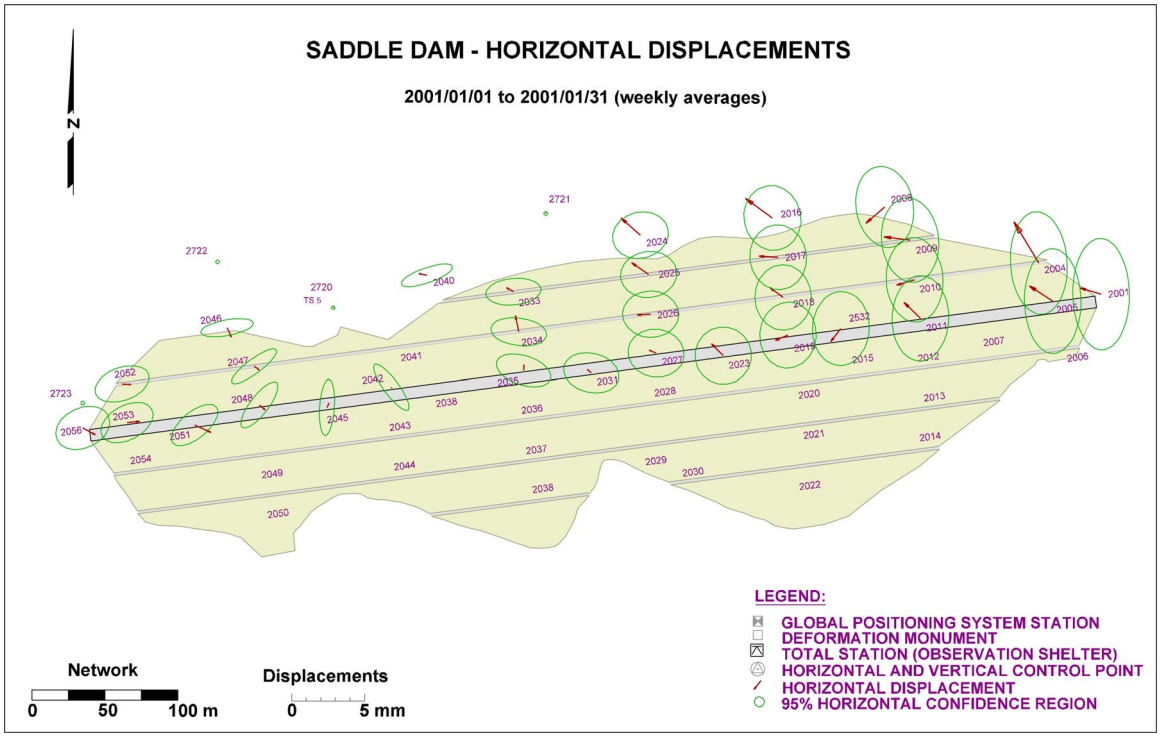

Figure 3-8. Annotated plot of horizontal displacements

In addition to the graphical utilities, the DIMONS user interface layer also contains a number of command-line utilities and scripts that run in a completely automated fashion. There are utilities to collect data, transfer data, process data, and automatically restart data collection after a power loss. When used with a scheduling utility such as the Windows Scheduler, these non-interactive utilities can be used to automate the entire monitoring process; data collection in the field, transfer to a central computer located in Metropolitan's office, and processing of the data to yield final coordinate values.

3.2.2 Data Storage

The previous section outlined the numerous software components making up the DDM system that was designed for Diamond Valley Lake. The component-based approach simplified sharing the development load among different programmers, and provided an easy upgrade path to support the future addition of different instrument controllers. In addition, the system takes full advantage of the scheduling and remote access capabilities offered by the underlying operating system.

One important part of the monitoring system design that has not yet been discussed in detail is the strategy that would be employed for storing the measurements and system configuration parameters. As mentioned in §3.1, one of the requirements for the DIMONS software was storage of its data in a relational database; however, no specific database vendor was specified. This proved not to be a problem, as the Windows operating system provides uniform access to a wide variety of database management services via its OLE DB (Object Linking and Embedding Database) technology. No vendor-specific code is required to handle the relatively simple database management functions (adding and deleting records) that are used in DIMONS.

More important than the physical database format is the way in which the data is logically organized. To store data in a relational database, it is first necessary to identify the different types of data that must stored, and then to divide the data into a number of relational tables. In Table 3-1, the major items that required storage in the DIMONS database are listed.

Table 3-1. Major items stored in the DIMONS database

Category	Stored Items
Object Definitions	Survey Points Robotic Total Stations Mets Modules Targets Host Computers
Network Configuration	RTS-Survey Point Setups RTS-Host Connection Mets Module-Survey Point Setup Mets Module-Host Connection Target-Survey Point Setup Host-Host Connection Observing Pointsets Target Search Parameters Raw Observation Tolerances
Processing Parameters	Base Cycle Definition Minimum Constraints Reference Points Unstable Point Detection settings Datum Shift Correction settings
Data	Raw RTS Observations Raw Mets Observations Reduced RTS Observations Minimum Constraints Coordinates Final Point Coordinates

They are divided into four general categories:

1. *Object Definitions*: The physical objects making up the monitoring network. Each of these objects is associated with a unique identifier and has various attributes (make and model, for instance) which must be described.
2. *Network Configuration*: The parameters describing the relationships between the objects, containing all the information needed to describe how the network

is physically laid out. This includes information such as which targets and instruments are set up on which survey points, initial readings to aid the instrument in finding targets, and connection parameters describing how the instruments are connected to the host computers.

3. *Processing Parameters*: The information needed for computation of point coordinates from the raw collected data. Outlier rejection thresholds, lists of reference points, and the base cycle for coordinate comparisons are included in this category.
4. *Data*: The actual data, in various stages of processing. Intermediate stages, such as mark-to-mark reduced observations, are stored in the database to reduce the time needed for any later reprocessing.

It is important to remember that this database represents a monitoring project that will operate for several years, containing data collected by several different host computers which is to be combined in a central location. This leads to two major considerations affecting the design of the relational tables.

First, there can be no guarantee that the communications network will always be operational. Therefore, the DIMONS database at each observing site must contain enough information to perform any needed data collection or processing tasks on its own. Ultimately, however, this information will be combined in a single database. All data and configuration parameters should be identified so that the user can know exactly what instruments and survey points are involved.

Second, some of the system parameters are expected to change with time. For example, it may be necessary to replace a malfunctioning instrument or to add or remove targets from the observations. Therefore, it is necessary to retain the time history of these parameters, so that the data processing modules can use the settings that were active at the time of measurement.

To ensure that data from different databases could be combined without clashes, unique identifiers are used. Before the DIMONS project is configured, the user must make a list of survey points, RTSs, targets, and meteorological sensors. Each of these objects is then assigned an integer identifier. When DIMONS is configured at each of the observing sites, the appropriate identifiers are specified depending upon the equipment used at this site. Each piece of information recorded by the monitoring system is then tagged with the appropriate identifiers, so there is no possibility of clashes with the data from another observing site.

For time-varying parameters, it was necessary to introduce time tags. Items such as RTS and target setup records, observing pointsets, and observation tolerance criteria are given a start time and end time indicating when they were valid. For example, Table 3-2 shows the records affected when an RTS is relevelled. The first record, which represents the original setting, was first introduced to the database on August 17, 2001. The height was changed on October 02, 2001, and DIMONS closed this record by setting its 'Tend' field to the current time. A new record for this point was then opened, and its 'Tend' field was left at zero to indicate that it is valid for any time after its start time. A 'LastModified' field indicates whether or not the record was later edited. When

observation data is later processed by DIMONS, observations from before October 02, 2001 will be reduced using an instrument height of 0.235 m while observations made after October 02, 2001 will use the value of 0.236 m.

Table 3-2. RTS-survey point setup records

Rtsid	Ptid	Hi	Tstart	Tend	LastModified
10	3780	0.235	2001-08-17 12:46:16	2001-10-02 12:28:17	2001-10-02 12:28:17
10	3780	0.236	2001-10-02 12:28:17	00:00:00	2001-10-02 12:28:17

For this strategy to work, all collected observations must be time-tagged, and the software used to modify the database must contain the logic to close records as new ones are added. This is accomplished by the Database Manager component, used by all DIMONS modules to access the database. In addition to maintaining the time tags, it enforces a number of rules to ensure the consistency of the database as settings change over time. One example of such a rule is the fact that only one RTS can be set up on a given survey point at a given time; another example is that each RTS can be connected to only one host computer at a given time, while a host computer may have any number of RTSs connected to it (on different serial ports, of course). Appendix I gives a more thorough description of the relational tables used in the DIMONS database, and of the rules enforced by the Database Manager.

For the DVL implementation of DIMONS, the Microsoft Jet database driver (which is bundled with Windows NT 4.0) was used. While this driver has the advantage of being readily available, it is somewhat slow. In time, this may become an issue as the database size grows; with the DVL dataset, a significant performance degradation was observed in data processing as the size of the DIMONS database approached 100 Megabytes. As the

DIMONS Database Manager can be used with a wide variety of database formats, a more powerful database management system may be desirable for future DIMONS installations.

3.3 Data Processing Methodology

Once the DIMONS software architecture and database design had been completed, the final phase of software design involved deciding upon how to process the raw data. As with other aspects of the software design, flexibility was a key design goal; however, the planned method of data collection at DVL would impose some restrictions on the choice of processing algorithms.

Because the RTSs at DVL are permanent installations, they must be housed in observation shelters with glass windows. The RTS measurements through this glass will therefore be affected by refraction; the measurement to each target is affected differently, depending on the angle of incidence of the RTS beam with the glass. While this is not important from a displacement monitoring point of view (the refraction error cancels out in the computation of displacements), it means that observations taken from within the shelters cannot be easily combined with external measurements. The data processing techniques used in DIMONS, therefore, were designed with this consideration in mind.

The final output of the DIMONS data processing module is a set of coordinates for all observed points. In order to calculate these coordinates, the raw observations are subjected to several stages of processing. These stages include: (1) field data reduction, (2) preliminary coordinate calculation, (3) reference point stability testing, and (4) final

coordinate calculation. The following sections describe the algorithms used at each stage of data processing.

3.3.1 Field Data Reduction

The data collected by an RTS during a measurement cycle consists of several sets of horizontal directions, zenith angles and slope distances, measured between the RTS and prism and collected in both telescope faces. Atmospheric temperature, pressure, and humidity are also collected at user-defined intervals during the measurement cycle.

The first stage in data processing involves combining the sets, correcting for the instrument and prism offsets from the survey markers, and removing the effect of atmospheric conditions on the measured distances. The output of the field data reduction stage is a set of horizontal directions, zenith angles, and spatial distances from the observing point to each of the targeted survey monuments (rather than from the RTS to the survey prisms), suitable for use in calculation of point coordinates.

Just as the overall data processing algorithm progresses in a series of stages, so does the reduction of field data. The reductions are applied sequentially, as follows:

1. The scale bias and additive constant of the RTS, and the additive constant for each prism, are applied to the measured distances.
2. The measured distances are corrected for the scale bias caused by ambient atmospheric conditions.
3. A station adjustment is performed to combine the multiple observation sets.

4. The adjusted observations are corrected for instrument and target height above the survey monuments.

These reduction steps are detailed in the following subsections.

3.3.1.1 Correction for Additive Constant and Scale Bias

The additive constant of a robotic total station (or any electro-optical distance meter, in fact) is a constant bias in measured distances caused by the electrical origin, or "zero," of the instrument not being located exactly on the instrument's vertical axis [Rüeger, 1990]. There is also a constant offset at the prism, caused by refraction as the signal passes through the prism glass. Generally, these two offsets are determined as part of the same calibration procedure to yield a combined correction for a given instrument/reflector pair, which is then applied to all distances measured with this pair.

The scale error of an RTS can be caused by a number of factors, but is primarily caused by the oscillator and the emitting and receiving diodes [Rüeger, 1990]. This error can be determined either by direct laboratory calibration (by measuring the frequency of the radiation emitted by the instrument) or by comparing measured distances with values determined using a more accurate method.

In DIMONS, the scale and additive constant corrections are applied to the measured distances using equation (3.1):

$$d' = b \cdot d_{obs} + a_{EDM} + a_{prism}, \qquad \textbf{(3-1)}$$

where

d_{obs} is the measured distance,

b is the scale factor to apply to the measured distance,

a_{EDM} is the additive constant of the EDM,

a_{prism} is the additive constant of the prism, and

d' is the corrected distance.

Determining the values of these correction parameters to correct the measured distances at DVL would be quite difficult due to the refractive effect of the shelter glass between the instrument and the prisms. In fact, for monitoring purposes, this correction is usually not necessary because every measurement to the same target will be affected identically; the error will therefore cancel out in the calculation of point displacements.

The scale and additive constant corrections do, however, become necessary when an instrument or prism is replaced. They are used to maintain consistency in the dataset by compensating for differences between different instruments and prisms. As an example, consider the two consecutive configuration changes and the resultant distance measurements depicted in Figure 3-9.

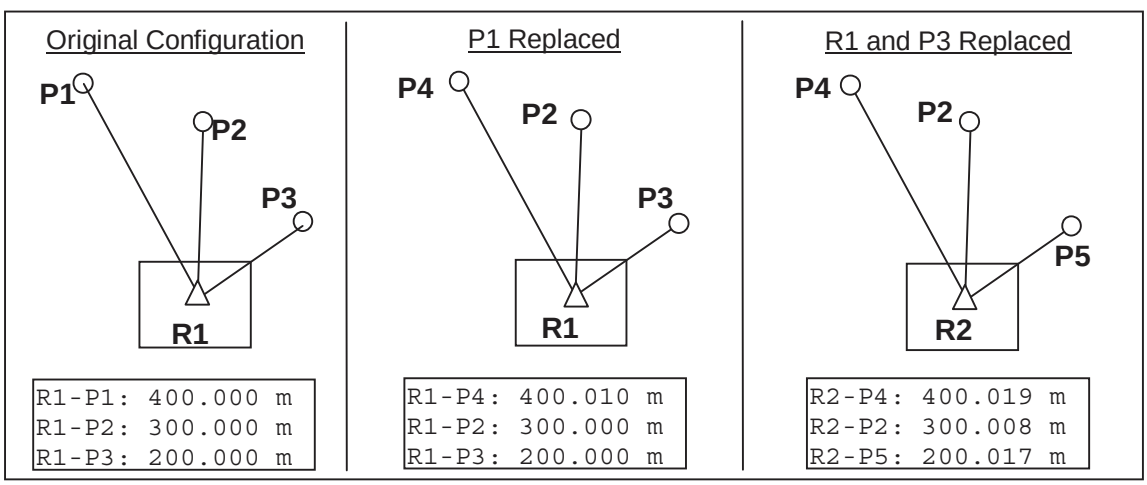

Figure 3-9. Effect of target or RTS replacement on measured distances

In the original instrument and target configuration, the measured distances from R1 were 400.000 m to P1, 300.000 m to P2, and 200.000 m to P3. The system configuration was then changed by replacing prism P1 with prism P4, and the new measured distance was 400.010 m. To maintain consistency with earlier measurements to this point, an additive constant of –0.010 m should be assigned to prism P4.

In the second change to the system, prism P3 was replaced with prism P5, and instrument R1 was replaced with R2. The measured distances to P4 and P2 are used to derive values of –0.005 m and –10 ppm (i.e., b_{R2} = 0.99999) for the additive constant and scale factor of R2; an additive constant of –0.01 m can then be computed for prism P5. When these new values are applied to the measured distances, the correct values of 400.000 m, 300.000 m, and 200.000 m are obtained. This method of modifying calibration values allows the system to undergo numerous instrumentation changes without affecting the consistency of the reduced measurements, making interpretation much simpler.

3.3.1.2 Atmospheric Correction

After the scale and offset corrections, the distances are corrected for the effect of atmospheric conditions. The distance measurement component of an RTS is factory calibrated under a specific set of atmospheric conditions; changes in atmospheric temperature, pressure, and relative humidity result in a change in the refractive index of air and thus the speed of signal propagation. This results in a scale change in the measured distances. By measuring the temperature, pressure, and relative humidity, the

actual refractive index can be computed. The measured distance is then reduced to the reference refractive index by equation (6.5) in Rüeger [1990], repeated as equation (3.2) below:

$$d'' = \frac{n_{REF}}{n_L} d', \qquad \textbf{(3-2)}$$

where

n_{REF} is the reference group refractive index for the instrument,

n_L is the group refractive index at time of measurement,

d' is the observed distance, corrected as in equation (3.1), and

d'' is the distance corrected for atmospheric conditions.

The reference refractive index n_{REF} is a constant value specified by the instrument manufacturer, while the refractive index at the time of measurement is computed from the observed meteorological values. Equations (A.4) to (A.10) of Rüeger [1990] are used to compute the group refractive index.

The correction shown in equation (3.2) accounts for the change in the signal propagation velocity caused by atmospheric conditions, and is known as the first velocity correction. Another correction, known as the second velocity correction, can be applied to account for ray path curvature as it passes through the atmosphere. With a maximum sight length of approximately 500 metres at DVL, however, the second velocity correction is not needed; it would be well below 0.1 mm for such short distances.

As an alternative to direct measurement of atmospheric conditions, some investigators [Rüeger et al., 1989; Rüeger, 1994; Rüeger et al., 1994] have recommended using a technique known as the local scale parameter method. In this method, observations made to a number of stable reference stations are used to derive the scale change, simply by comparing the measured distances with values observed at an earlier date. The derived scale change is then used to correct all other measured distances. Because this technique does not require the purchase, installation, and maintenance of meteorological sensors, it was considered for use in DIMONS. However, it was found to be unsuitable for the DVL monitoring system for three reasons:

1. The technique requires several stable points for computation of the scale parameter. At DVL, the stability of the reference stations and observing points was not guaranteed, as evidenced by the requirement that DIMONS perform a stability analysis on reference points.
2. At DVL, the reference points are all located off the dams, while most of the object points are on the dams. The lines of sight from the instrument to object points are typically much higher above the ground than those to the reference points. The derived scale parameter, therefore, may not be representative of the conditions along the lines of sight to the object points.
3. In addition to their use in distance correction, atmospheric measurements can be very useful for interpretation of the results. For example, a time series of computed displacements can be sorted by temperature, enabling the evaluation of possible temperature-related effects in the measurements.

Therefore, the DVL monitoring system design includes measurement of atmospheric conditions during each set of measurements, and these are used to correct the measured distances. This leaves open the possibility of future evaluation of the local scale parameter method in comparison to meteorological measurements.

3.3.1.3 Set Reduction

The automated nature of the DIMONS data collection module posed some challenges in the choice of a suitable set reduction strategy. Because the data collection process takes place with no input from the user, there can be no guarantee that all of the targets will be observed during each set of observations. Adverse weather conditions, human activity near the observing shelter, or wildlife may cause certain targets to be observed in some sets but not in others. Furthermore, robotic total stations can sometimes lock onto the wrong prism if it happens to fall within the field of view. The algorithm for set reduction in DIMONS, therefore, required automatic blunder detection and removal, as well as the ability to function correctly in the presence of missing data.

A secondary but nonetheless important requirement of the DIMONS set reduction module is that it be usable for field data checks. To obtain a monitoring dataset of uniformly high quality, Metropolitan wished to ensure that each cycle of observations satisfies certain consistency criteria. Therefore, at the end of a prescribed minimum number of sets, a preliminary set reduction would be performed for the purpose of quality checking. If the collected sets did not meet a specified level of consistency, another set

of observations would be collected. This was to continue until either the requirements were met or a user-specified maximum number of sets was reached.

In order to meet these functionality requirements, the classical method of set reduction (as described in Blachut et al. [1979]) was first considered. In the classical method of set reduction, one of the targets is chosen as a reference. In each set, the measured direction to the reference target is subtracted from all the other directions, giving the reference direction a value of zero in all sets. The arithmetic mean of reduced directions is then computed for each target, and these means are the final result of the set reduction [Blachut et al., 1979]. Distances and zenith angle measurements are averaged separately.

The classical set reduction method is very straightforward, and works very well when directions are collected in full sets. However, it becomes quite complicated when missed observations are involved. If the reference target is missed in one of the sets, a different reference must be chosen. If no single target appears in all sets (which could be the case if weather effects cause targets to be missed), the observation sets must be partitioned into groups and processed separately. This, of course, complicates statistical analysis of the observations and requires complex coding to handle the different possible combinations of observed and missed targets.

Ultimately, it was decided that the complexity of implementing the classical approach for all data collection scenarios outweighed any possible advantages of using the method. Instead, a more general approach is used for set reduction in DIMONS. Reduced direction measurements, zenith angles and distances are estimated using a parametric

least squares adjustment that allows all of the observations in a given cycle to be included, regardless of the amount of missing data. The adjustment procedure also performs blunder checking and removal, as described later in this section.

Before the least squares adjustment, the RTS observations undergo a preprocessing stage to simplify the adjustment process. Preprocessing consists of two steps. First, the observations from the two telescope positions in each set are averaged; any observation which is not collected in both telescope positions in a given set is left out of the adjustment. Averaging of the two telescope positions removes the effect of collimation error from the measurements, and is a recommended procedure for any precision survey [Blachut et al., 1979]. The second preprocessing step is an approximate set alignment, which is designed to circumvent difficulties that occur when combining horizontal direction measurements that are near zero. In these situations, it is possible for a given observation to be, for example, 0º 0' 0.5" in one set, and 359º 59' 59.5" in another. Obviously, the average of these two should be 0º 0' 0.0" and not 180º 0' 0.0". To fix this problem, direction observations to the same target in different sets are compared to see if they are within ±180º of one another; if not, they are brought into alignment by adding or subtracting 360º, as necessary. This may make some direction observations have negative values, but this poses no problem in the least squares adjustment.

Once the observations have been preprocessed, the least squares adjustment is a straightforward procedure. The observation equations for directions, zenith angles, and distances are, respectively:

$$\delta_{i,j} + r_{\delta_{i,j}} = \Delta_i - \omega_j \qquad \textbf{(3-3)}$$

$$z_{i,j} + r_{z_{i,j}} = Z_i \tag{3-4}$$

$$d_{i,j} + r_{d_{i,j}} = D_i\,, \tag{3-5}$$

where

$\delta_{i,j}, z_{i,j}, d_{i,j}$ are the observed direction, zenith angle, and distance measured to the ith target in the jth set (corrected for atmosphere and scale/additive constant),

Δ_i, Z_i, D_i are the "true" direction, zenith angle, and distance between the instrument and the ith target,

ω_j is the orientation unknown of the jth set, and

r is an observation residual.

The observations are processed using a linear parametric least squares adjustment. In matrix form, the observations are expressed as a function of the unknown parameters:

$$\ell + \mathbf{r} = \mathbf{Ax}\,, \tag{3-6}$$

where

$$\ell = \begin{bmatrix} \delta_{1,1} \\ z_{1,1} \\ d_{1,1} \\ \delta_{2,1} \\ \vdots \\ z_{m,n} \\ d_{m,n} \end{bmatrix} = \begin{bmatrix} \Delta_1 - \omega_1 - r_{\delta_{1,1}} \\ Z_1 - r_{z_{1,1}} \\ D_1 - r_{d_{1,1}} \\ \Delta_2 - \omega_1 - r_{\delta_{2,1}} \\ \vdots \\ Z_m - r_{z_{m,n}} \\ D_m - r_{d_{m,n}} \end{bmatrix} \tag{3-7}$$

for observations to *m* targets in *n* sets,

$$\mathbf{A} = \frac{\partial \ell}{\partial \mathbf{x}}, \tag{3-8}$$

and

$$\mathbf{x} = [\Delta_1 \quad Z_1 \quad D_1 \quad \Delta_2 \quad \cdots \quad Z_m \quad D_m \quad \omega_1 \quad \cdots \quad \omega_n]^T \tag{3-9}$$

is the vector of unknown parameters. The least squares estimate of $\mathbf{x}$ is then obtained, following Wells and Krakiwsky [1971]:

$$\hat{\mathbf{x}} = (\mathbf{A}^T \mathbf{C}_\ell^{-1} \mathbf{A})^{-1} \mathbf{A}^T \mathbf{C}_\ell^{-1} \ell, \tag{3-10}$$

where $\mathbf{C}_\ell$ is the covariance matrix of the observations.

Once the least squares estimate of the parameters is obtained, the observation residuals $\hat{\mathbf{r}}$ are computed:

$$\hat{\mathbf{r}} = \mathbf{A}\hat{x} - \ell. \tag{3-11}$$

These residuals are compared with user-defined tolerance levels. For zenith angles and distances, the observations to each target are examined in turn. For a given target, the largest zenith angle residual is compared with the tolerance. If it is larger, this observation is flagged as a possible outlier. The same procedure is followed for distance residuals; for directions, the procedure is somewhat different. Because all of the direction observations in a set are associated with the same orientation unknown, a pointing blunder for a single target will affect the estimate of the orientation unknown, and thus all of the other direction observations in the set will be affected. Therefore, the direction residuals are not examined separately for each target. Of all the direction

residuals, the observation with the residual of largest magnitude, if it exceeds the tolerance level, is flagged for rejection.

Leaving out the flagged observations, a new vector of observations and design matrix are formed and the adjustment is repeated. The new solution is then rechecked for outliers; the process of outlier removal and readjustment continues until either no more outliers are detected or until a user-defined minimum number of observations remain for each target. At this point, the least squares set reduction is complete.

3.3.1.4 Mark-To-Mark Correction

The final stage in field data reduction is mark-to-mark correction of the observations. Using the reduced observations from the set reduction stage, the stored instrument and prism heights are used to correct the zenith angles and slope distances so that they refer to the survey monuments and not to the instrument and prism. This ensures that the computed survey monument coordinates will remain consistent even if the instrument and prism heights are changed in the future. Standard reduction formulae listed in Rüeger [1990] (equations (8.14), (8.15), and (8.19), in particular) are used for the reductions.

3.3.2 Preliminary Coordinate Calculation

At the end of the data reduction stage, the horizontal directions, zenith angles, and distances have been reduced mark-to-mark and are suitable for use in computation of

survey point coordinates. This computation is carried out using a minimally constrained least squares adjustment. The datum is defined by holding the position of one point and the azimuth between two points fixed in the calculations; in practice, this is achieved by introducing these values as pseudo-observations with small variances.

At this stage of processing, only the minimum information needed to define the datum is used; coordinate information from all of the observed reference points is not incorporated in the adjustment. This is because the preliminary coordinates will be used to test the reference point stability. The minimum constraints solution is needed for the point stability check because it can exhibit only rigid-body translations or rotation in the presence of an unstable reference point; no distortions are incurred in the solution. Rigid-body movements do not affect the stability check, as described in the following section.

3.3.3 Reference Point Check

To test the stability of reference points, the Iterative Weighted Similarity Transformation (IWST) [Chen et al., 1990] is used. The reference point coordinates from the current cycle are compared with those from a user-specified base cycle. The IWST has been well-described in several publications (for example, Chen [1983] and Chen et al. [1990]), so it will not be described in detail here. In short, the IWST finds and applies the set of Helmert transformation parameters which minimizes the sum of the absolute values of the displacement components. The transformed displacements are then tested for significance by comparing them against their confidence regions.

In DIMONS, displacements referred to minimum constraints are computed for the reference points. These displacements are then transformed using the IWST and tested for significance. If any reference points are found to have moved significantly, they are not included as reference points in the final computation of survey point coordinates, described in the following section.

3.3.4 Final Coordinate Calculation

After the reference points have been checked for stability, they can be used as constraints in the computation of object point coordinates. There are several alternative techniques for using the reference point coordinate information; the method of data collection (each point is measured through glass by a single RTS) was a major factor in deciding which method to use. This section outlines the different algorithms considered for use in final coordinate calculation in DIMONS; the technique ultimately chosen for implementation is then presented.

3.3.4.1 Algorithms Considered

Three main techniques were considered for implementation in DIMONS: (1) readjustment of the reduced observations using stable reference points as minimum constraints, (2) Helmert transformation of the preliminary coordinate estimates, and (3) readjustment of the reduced observations using stable reference points as weighted constraints. Advantages and drawbacks of each method are presented below.

1. Minimum Constraints

The minimum constraints technique requires selecting two points from the list of stable reference stations. The reduced observations are then readjusted, holding fixed (or tightly constrained) the position of one point and the azimuth between the two points. The coordinates and azimuth are obtained from the reference point coordinates that were determined in a user-defined base cycle; this would ensure that the datum definition remains consistent between observation cycles.

Although this technique is computationally simple and easy to understand, it has a couple of drawbacks. First, the algorithm does not make use of all of the stable reference points. This information is available and should be utilized if possible. Second, this method does not work well with the observing configuration used at DVL. By definition, the minimum constraints solution provides no redundancy in the definition of the datum orientation. Even though both of the points used to define the datum are known to be stable, the use of a single azimuth to define the orientation can sometimes cause a noticeable bias in the coordinate solution, as shown in Figure 3-10. This pattern is caused by random pointing errors in observations to the azimuth-defining stations. While statistically insignificant, the pattern is easily noticeable; even though the displacements are all smaller than their 95% confidence regions, they could still be misinterpreted by the end user as representing movement. For this reason, the minimum constraints solution is not a good choice for the final calculation of point coordinates.

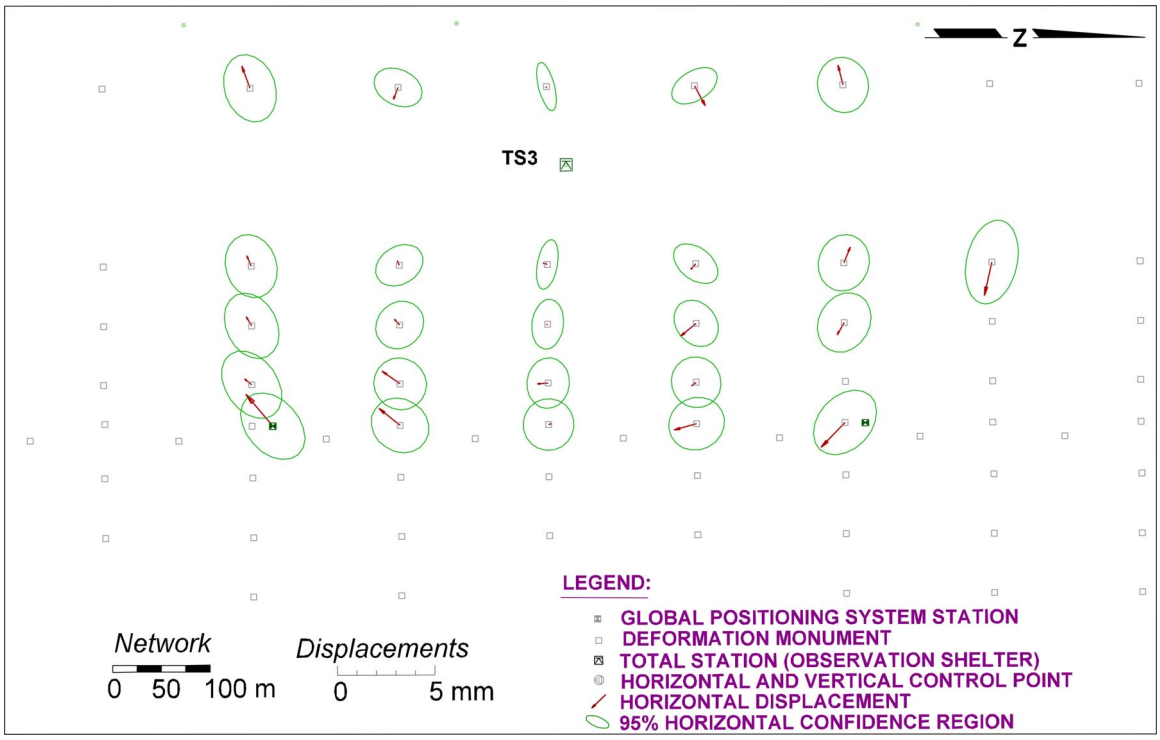

Figure 3-10. Minimum constraints datum bias caused by random pointing errors

2. Helmert Transformation

The datum bias caused by random pointing errors can be removed by applying a similarity transformation to the preliminary coordinates. Reference station coordinates from the base cycle, along with the reference station coordinates from the cycle being processed, are used to estimate the amount of translation and rotation to apply to the network. Once the transformation parameters have been determined, all the station coordinates (reference and object points) are then transformed, along with their covariance matrix.

The estimation of similarity transformation parameters and the application of these parameters to transform the station coordinates can be performed as part of the same procedure. This is done by expressing the 'observed' (i.e., computed in the

preliminary coordinate calculation) coordinates of the points as a function of the 'true' unbiased point coordinates and the transformation parameters. The base cycle coordinates of the stable reference points are introduced as weighted constraints to aid the solution.

In a general case with seven similarity transformation parameters, the problem is expressed as follows:

$$\hat{\mathbf{x}}_2 = s \cdot \begin{bmatrix} 1 & \kappa & -\phi \\ -\kappa & 1 & \omega \\ \phi & -\omega & 1 \end{bmatrix} \cdot \tilde{\mathbf{x}}_2 + \begin{bmatrix} dX \\ dY \\ dZ \end{bmatrix} + \mathbf{r}_1 \qquad \textbf{(3-12)}$$

$$\hat{\mathbf{x}}_{1RS} = \tilde{\mathbf{x}}_{2RS} + \mathbf{r}_2$$

where

$\hat{\mathbf{x}}_2$ is the vector of preliminary coordinates for all observed stations, from the cycle being processed,

$\tilde{\mathbf{x}}_2$ is the (unknown) vector of 'true' unbiased coordinates for all observed stations,

s is the scale factor to apply to the coordinates,

ω, ϕ, κ are the (small) rotation angles around the X, Y, and Z coordinate axes, respectively,

$\begin{bmatrix} dX \\ dY \\ dZ \end{bmatrix}$ is the vector of X,Y, and Z datum translations,

$\hat{\mathbf{x}}_{1RS}$ is the vector of coordinates of the stable reference points from the base cycle,

$\tilde{\mathbf{x}}_{2RS}$ is the vector of true unbiased coordinates of the reference points in the cycle being processed (this vector is a subset of $\tilde{\mathbf{x}}_2$), and

$\mathbf{r}_1, \mathbf{r}_2$ are the vectors of observation residuals.

The unknown parameters in equation (3-12) are the transformation parameters and the corrected coordinates for the survey points: $s, \omega, \phi, \kappa, dX, dY, dZ,$ and $\tilde{\mathbf{x}}_2$. These parameters can be estimated using least squares; for the observation scenario at DVL, only $\kappa, dX, dY, dZ,$ and $\tilde{\mathbf{x}}_2$ would be estimated because s is defined by the measured distances and ω, ϕ by the measured zenith angles.

In general, the Helmert transformation is a perfectly suitable way to evaluate and remove the effect of datum bias from the coordinate solution. It uses all of the reference points to determine the transformation parameters, giving it an advantage over the minimum constraints solution. However, the particular observation scenario envisioned for DVL would cause some problems if this technique were used.

As mentioned earlier, all coordinate information for the survey monuments must be derived from measurements taken by the RTS, due to the disturbing effect of the shelter glass. The base cycle coordinates for the reference stations, therefore, must have been derived from a minimally constrained adjustment with one azimuth and the position of one point introduced as pseudo-observations with small variances. The resultant confidence regions of the points will have a pattern as shown in Figure 3-11.

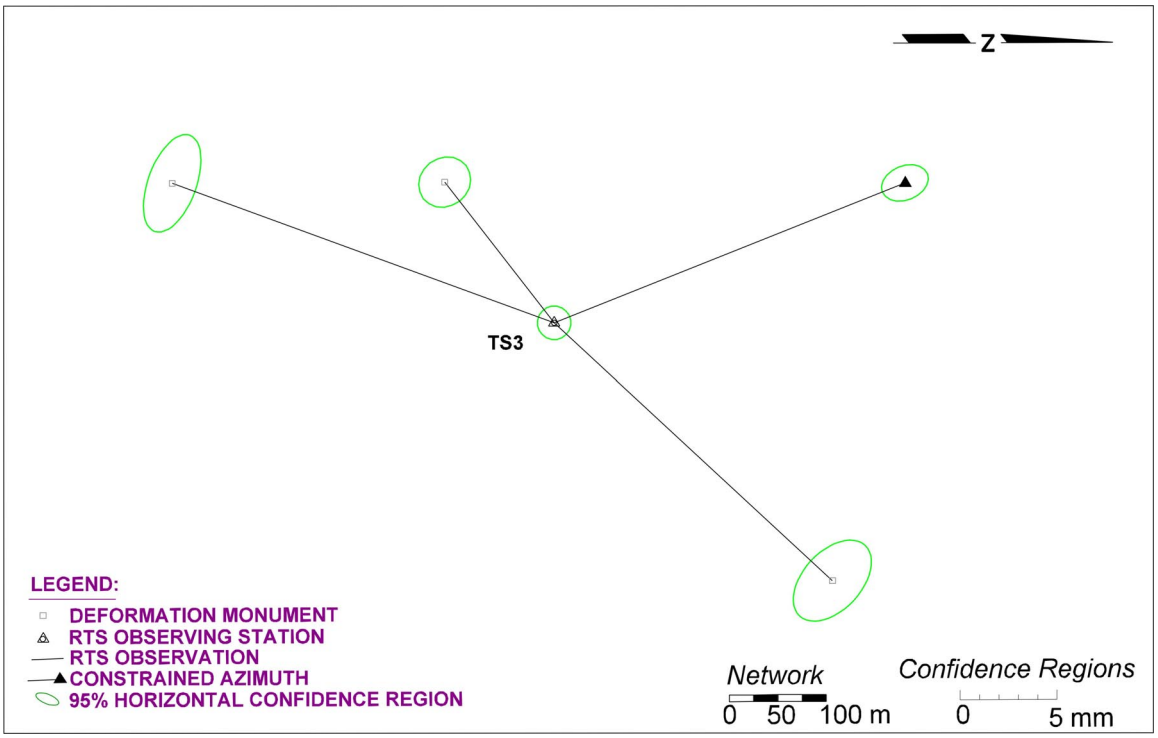

Figure 3-11. Pattern of confidence regions for reference points

Figure 3-11 demonstrates that uncertainty in the direction measurements is a major contributor to the point confidence regions for the longer lines of sight, as seen by their orientation perpendicular to the line of sight. For the constrained azimuth, however, distance uncertainty is the key factor. If the covariance matrix for these reference points is used in the determination of similarity transformation parameters, the reference point that was used in the azimuth constraint dominates the solution for the orientation parameter due to its higher weight. As a result, the corrected coordinates still tend to exhibit the same residual orientation errors as were observed for the minimum constraints technique.

Fortunately, there is a simple way to solve this problem. In the previous stage of data processing, the stability of the reference points was verified. Therefore, instead

of using the estimated covariance matrix for these points, all of the reference point coordinate values from the base cycle are assigned equal variances and the off-diagonal covariance matrix elements are ignored. The variances are chosen to be small (for example, 0.01 mm^2) so that the coordinates are effectively held fixed in the adjustment.

Because all of the stable reference points are given equal weight in the adjustment, the azimuth-defining points will not have undue influence on the estimated orientation parameter. This approach is not mathematically rigorous, because we know that not all of the reference point positions are determined with exactly the same precision. However, it is a practical approach and it works quite well in reducing residual orientation effects, especially when the reference stations are all at a similar distance from the observing point.

3. Weighted Constraints

The final method considered for computing point coordinates is weighted constraints. In this method, the reduced observations are readjusted, using the stable reference point coordinates from the base cycle as weighted constraints. The weighted constraints method has the same weakness in defining orientation as the Helmert transformation described in the previous section, so the base cycle coordinates of the reference points are reweighted in the same manner.

From an error propagation standpoint, this technique has some advantages over the Helmert transformation approach. Instead of using the stable points to determine transformation parameters and then using these parameters to correct the minimum

constraints coordinates, the stable point information is used without introducing the additional unknown transformation parameters. With the small amount of redundancy expected at DVL, this results in a considerable improvement in the point confidence regions as depicted in Figure 3-12.

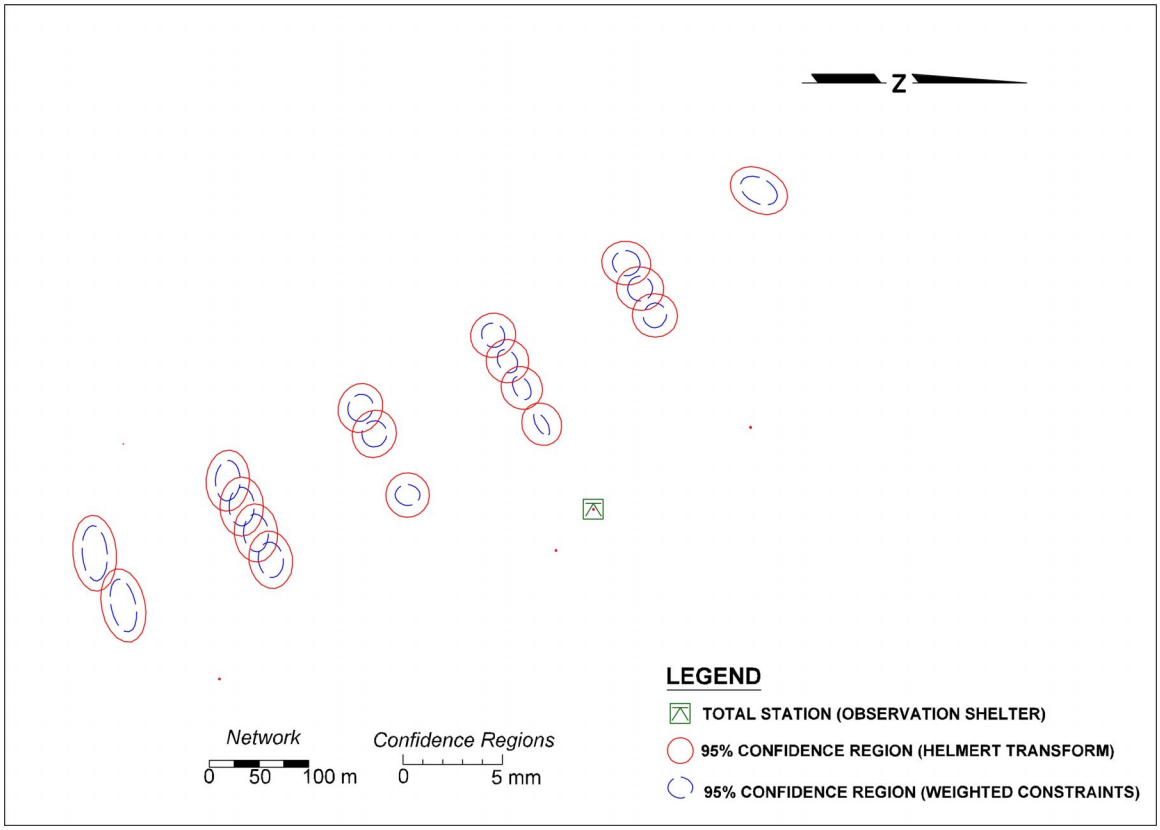

Figure 3-12. Precision improvement in weighted constraints solution

3.3.4.2 Algorithm used in DIMONS

Of the three main alternatives considered, the weighted constraints solution proved to be the best. It uses information from all of the stable reference stations to maintain a consistent datum definition from cycle to cycle, and it does not introduce unnecessary extra parameters in the solution of station coordinates. Because of these features, the

weighted constraints solution is used in DIMONS for the final calculation of station coordinates.

The weighted constraints coordinate solution is the final stage in data processing. At this point, the station coordinates are stored in the DIMONS database and are ready for interpretation by the system operator. Data interpretation is discussed in Chapter 5, in the form of an accuracy evaluation of the DVL monitoring system. Before this is done, however, Chapter 4 describes the Diamond Valley Lake monitoring system implementation.

CHAPTER 4
MONITORING SYSTEM IMPLEMENTATION

Construction of the DDM system at Diamond Valley Lake was carried out during most of the year 2000. Metropolitan performed the construction of survey monuments and instrument shelters, while installation of the power and communications systems was subcontracted to Spectria, a technology consulting firm based in Long Beach, California. While the monitoring hardware was being installed, the UNB development team created the DIMONS software to perform the data collection and processing. The monitoring system was largely completed by October 2000, with a final site visit made in December 2000 to perform final adjustments and train Metropolitan survey personnel in use of the monitoring software. This chapter describes the different components of the DDM system that was implemented at Diamond Valley Lake: instrumentation, power and communications systems, monumentation, the observation shelters, and software.

4.1 Instrument Selection and Calibration

The automated portion of the DVL monitoring system consists of two major types of instrumentation: the robotic total stations that collect survey measurements and the meteorological sensors that are required to correct the RTS measurements for atmospheric effects. The instrumentation used for this purpose at DVL is described in the following sections.

4.1.1 Meteorological Sensors

Under the terms of the software development contract, UNB was responsible for choosing the type of meteorological sensor to use for monitoring. The RFP specified that the chosen sensors must provide readings of atmospheric pressure to an accuracy of 2 millibars and temperature to an accuracy of 0.5 degrees Celsius. In addition to being used for meteorological correction of measured distances, the temperature measurements would be used to ensure that the RTS was not activated in extreme heat or cold.

After investigation of several possible suppliers, the Envirolink ENV-50-HUM sensor module was selected. This instrument is manufactured by SensorMetrics, a Massachusetts firm. Figure 4-1 shows the ENV-50-HUM connected to a notebook computer. This sensor module includes a humidity sensor with a precision of ±5%, a barometric pressure sensor with a precision of ±2.3 millibars, and a temperature sensor with a precision of ±0.5º C. A second temperature sensor was purchased for each sensor module so that it would be possible to monitor temperatures both inside and outside the observing shelters.

While the barometric pressure sensor of the ENV-50-HUM falls slightly outside the accuracy specification (its reading precision alone exceeds the accuracy requirement), it was the most attractive of the several models considered. Besides its low cost (approximately $500 US), the ENV-50-HUM was selected because it is rugged, requires little power, is easily programmable, and can be calibrated in the field. The user can

correct for both offset and scale biases by sending commands to the sensor module through a serial connection.

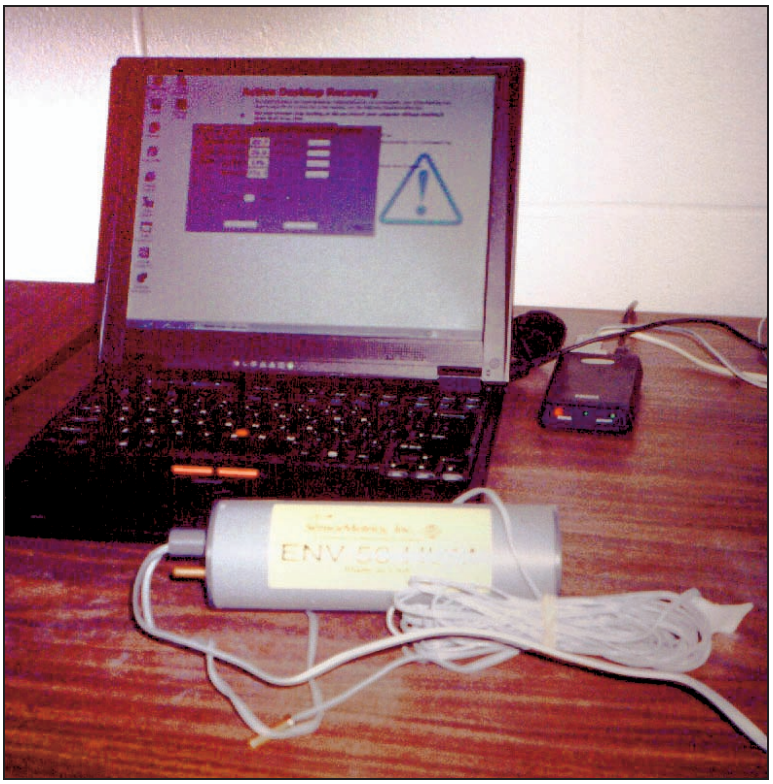

Figure 4-1. SensorMetrics ENV-50-HUM meteorological sensor module

The accuracy of the ENV-50-HUM sensor modules was confirmed at UNB before delivery to Metropolitan. Initially, one module was purchased and calibrated to match a Thommen model 2A aneroid barometer, which gives atmospheric pressure readings with a standard deviation of ±1.1 millibar [Revue Thommen AG, 2001]. Two mercury thermometers, with a temperature reading precision of ±0.2º C, were used for temperature calibration. No reference humidity sensor was available for comparison.

Over a period of several months, the readings were compared to the more precise instruments. Based on these comparisons, the standard deviation of atmospheric pressure

measurements was found to be approximately ±2.7 millibars and the standard deviation of temperature measurements was found to be approximately ±0.2º C.

When the sensor modules were taken to the site for installation, the Thommen barometer was used for field calibration. The Thommen barometer itself was calibrated before being taken to the field by comparing it to a mercury barometer installed at Metropolitan's Weymouth filtration plant in LaVerne, California. This was a Princo Instruments Nova type mercury barometer with a reading resolution of 0.1 millibars [Princo Instruments Inc., 2001]. For temperature measurements, a simple mercury thermometer with a reading resolution of 1ºC was the only instrument available for use as a calibration reference. This was not considered a problem, as the temperature sensors had already been observed to exhibit stability over long periods of time. A small temperature bias would remain constant between observing cycles, and thus would not significantly affect the computed point displacements.

At the request of Metropolitan, the sensor modules were installed inside the observation shelters, with one temperature sensor extended outside just under the roof overhang on the northern side of the shelter. From an accuracy standpoint, it would have been preferable to install the modules outside the shelter, leaving just one temperature sensor inside, but this would leave them more vulnerable to environmental effects.

4.1.2 Robotic Total Stations

Metropolitan selected Leica's model TCA1800S robotic total stations for use in the DDM system. The model TCA1800S is the same instrument as the model TCA1800

total station, which has a nominal distance standard deviation of ±2 mm ±2 ppm (for a single measurement) and a direction standard deviation of ±1 arcsecond (for the mean of measurements in both telescope faces) [Leica AG, 1996]. The 'S' designation applies to those units that have exhibited standard deviations of at most ±1 mm ±2 ppm for distances and ±0.8 arcseconds for directions in factory calibration tests.

Because the total stations had been calibrated at the factory, no field calibration was necessary. However, there were a number of configurable settings to check on each RTS. The communication parameters (baud rate, for example) were set to common values for all instruments. Each instrument was checked to ensure that its measurements were displayed in metres for distances and degrees for directions. The instrument scale factors were set to exactly one and the stored prism offsets were set to zero. DIMONS performs scale factor and prism offset corrections, so it was important to ensure that conflicting corrections were not applied by the instrument.

The final step in RTS setup at each observing station was the collection of initial readings to all visible targets These initial readings are stored in the DIMONS database and are used to approximately locate each target during a measurement cycle. Approximately 30 targets were visible from each RTS; the operator was required to guide the instrument to each target in turn so that a reading could be collected. After this training stage, DIMONS could collect all further observations in automatic mode.

4.2 Power Supplies

Because of the hot and sunny weather conditions at DVL, a combination of solar cells and heavy-duty batteries was chosen to supply electricity for the DDM equipment. Each observing station was equipped with a number of solar panels, as shown in Figure 4-2; these solar panels continuously charge the batteries. The RTS, meteorological sensor, communications equipment, and computer were connected to the batteries via a voltage regulator (and a 12VDC to 5VDC voltage converter, in the case of the communications hardware). Figure 4-3 shows the battery pack at observing station TS4, with the computer connected to the wall in the background. The computers were equipped with special DC power supplies to eliminate the need for DC-to-AC conversion hardware.

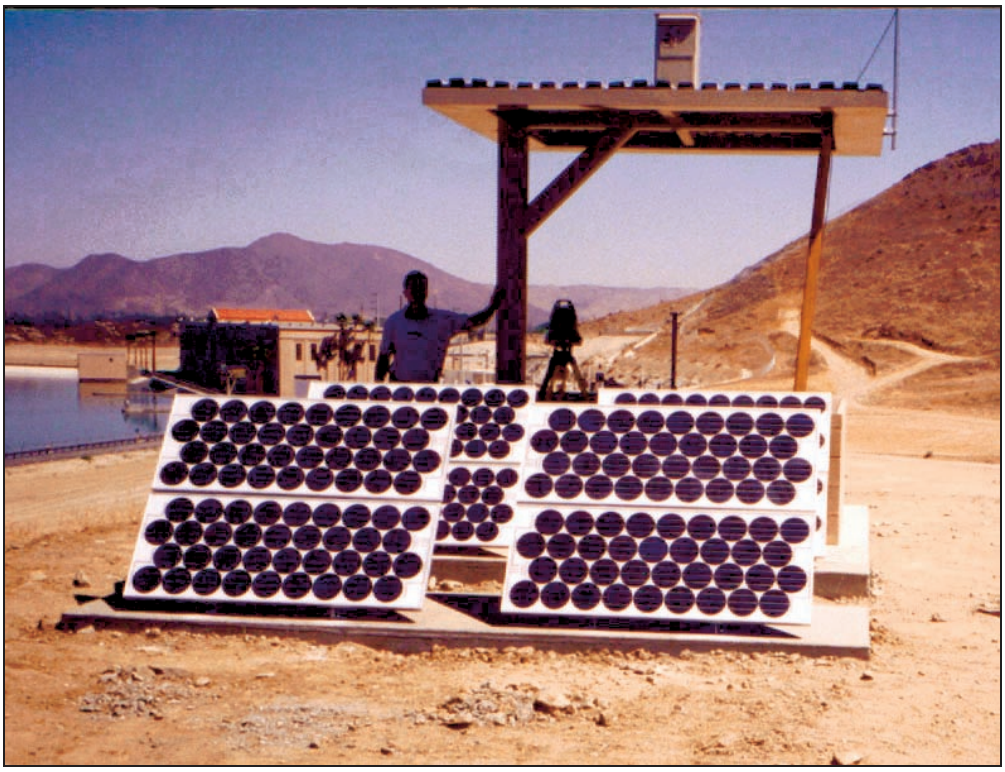

Figure 4-2. Solar panels at observing station TS4

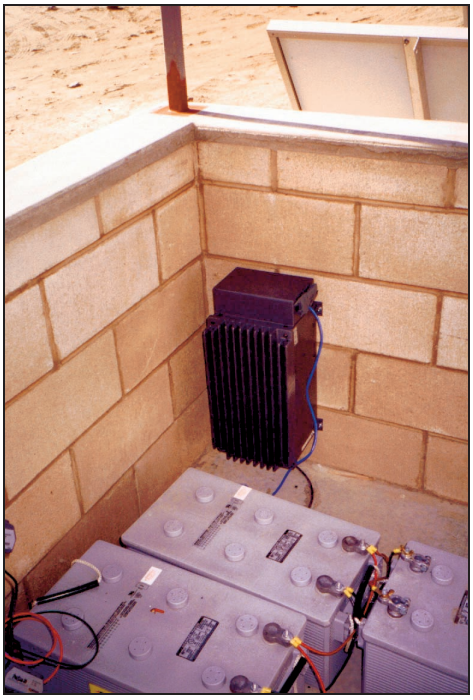

Figure 4-3. Batteries and computer at observing station TS4

When fully charged, the battery pack at each observing station stores enough energy to run the instrumentation for five full days of measurement without recharging [Dent, 2000]. Because of the sunny climate at DVL, however, the batteries were expected to be fully recharged by the solar panels nearly every day, making the monitoring system capable of continuous measurement if needed.

4.3 Communication System

Installation of the DVL communication system was covered under the same contract as the power system, and was thus carried out by the same company. Their communication system was built entirely from off-the-shelf, commercially available hardware, making maintenance and upgrades very simple. From a software development

standpoint, the communication system is ideal; the DIMONS host at each observing shelter was equipped with a wireless Ethernet hub and antenna. The host computer was connected to the hub using a standard 10Base-T Ethernet connector and operated exactly as if it were connected to a wired network.

Because the DVL wireless network offers the same functionality as a wired network, implementing remote access capability in DIMONS was straightforward. Software written and tested in the office could be used directly at DVL, with no modifications. Furthermore, any Windows software capable of operating over a TCP/IP connection would work at DVL. This enabled Metropolitan to use commercially-available remote-access utilities to monitor and configure the DIMONS field computers.

4.4 Monumentation

One of the most important aspects of any geodetic deformation monitoring network is the quality of monumentation. Improperly installed or unstable survey monuments can render an entire monitoring program useless, because they do not exhibit the same displacement pattern as the object or structure they are intended to monitor. Years of monitoring data and countless hours of labour are then lost because the engineers in charge of monitoring cannot determine what the movement patterns indicate.

At DVL, Metropolitan was very careful to avoid problems resulting from improper monumentation. During the design phase, there was some concern that it would be difficult to attach the survey monuments to the large but loose rocks at the face of the dam. Therefore, the survey monuments installed at the base and on the face of each dam

are of a very heavy-duty design, as shown in Figure 4-4(a). The survey pillar is made of concrete and is 30 centimetres in diameter, with a 5 centimetre steel pipe at its centre and a PVC casing on the outside [Whitaker, 1996]. It is mounted in a concrete base which extends at least 1.5 metres below the surface. The target (a Leica survey prism) is threaded onto a 1 centimetre (3/8") diameter stainless steel rod protruding from the top of the pillar and then permanently affixed to the pillar using epoxy. The stainless steel rod is welded onto a 3-centimetre thick steel plate, which is in turn welded onto the 5 centimetre diameter steel rod and embedded in the concrete at the top of the pillar.

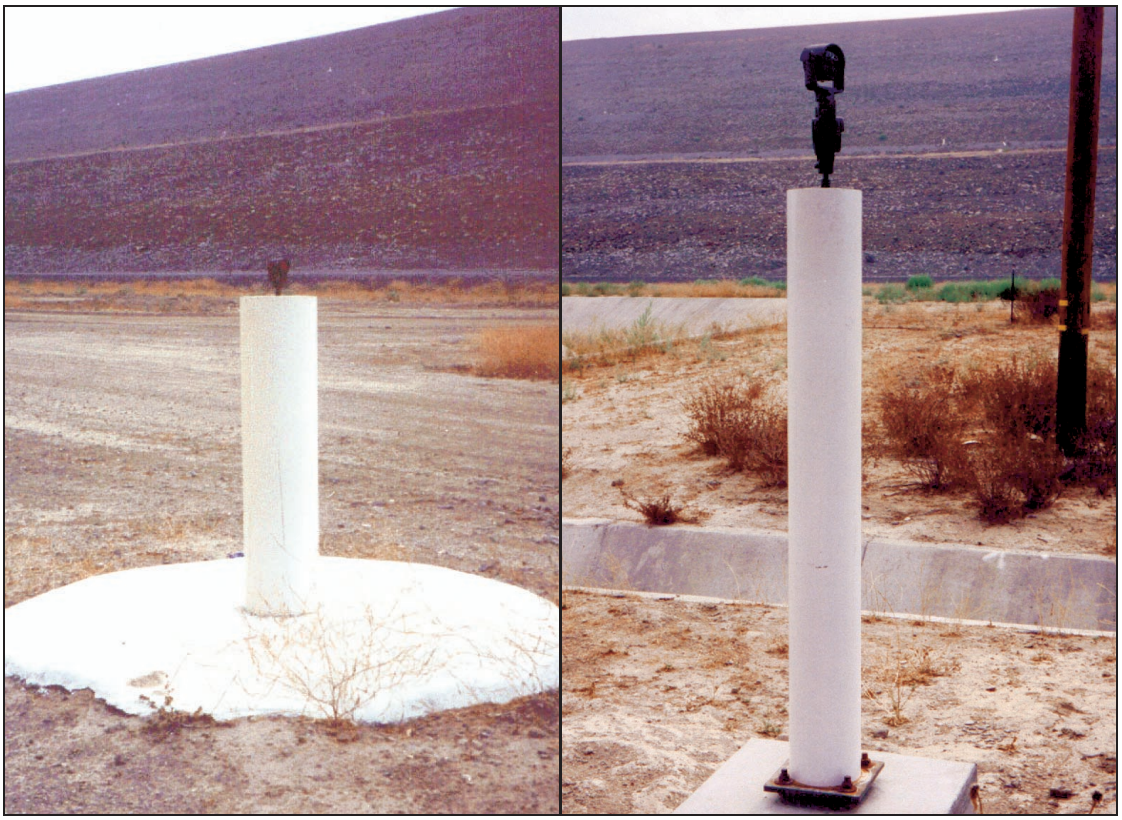

(a) **(b)**

Figure 4-4. (a) monument for dam face and (b) monument for bedrock

For survey monuments that can be directly affixed to bedrock, the design was somewhat less elaborate. As shown in Figure 4-4(b), these monuments have a smaller base that is attached to the bedrock. The pillar consists of a 5 centimetre diameter steel pipe that is embedded in the concrete base and extends to a height of approximately 1.5 metres above the ground. The steel pipe is encased with a 15-centimetre diameter PVC pipe, protecting it from direct solar radiation while allowing air circulation between the PVC and the metal. As with the more heavy-duty monuments, the survey targets are Leica survey prisms which are threaded and then epoxied onto the steel pipe.

4.5 Instrument Shelters

Each of the DVL observing stations was housed in a shelter, designed to protect the equipment from the elements as well as from vandalism or theft. The observing shelter design was conceived by Metropolitan and consists of an approximately 2.5 metre by 2.5 metre cinderblock structure, 2.7 metres tall, with large glass windows. Figure 4-5 shows instrument shelter TS4, located on the West Dam.

Because of the requirement to keep sight lengths below 500 metres, it was not possible to place all of the observing shelters on solid bedrock. Two of the East Dam observing stations were located on alluvial soil, while two of the West Dam stations were actually located on a berm of the dam itself. To provide maximum stability with respect to the ground, each observing shelter therefore rests on a heavy concrete pad, 3 metres by 3 metres square and 0.7 metres thick. The RTS was mounted to a survey pillar attached to this concrete pad, as shown in Figure 4-6.

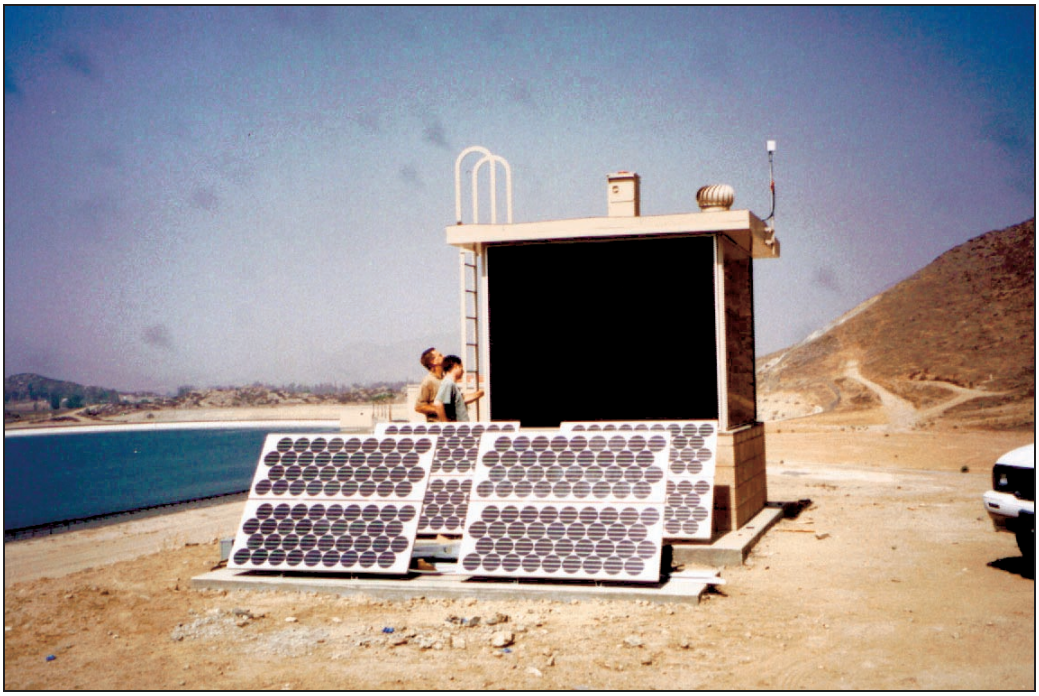

Figure 4-5. West Dam observing station TS4

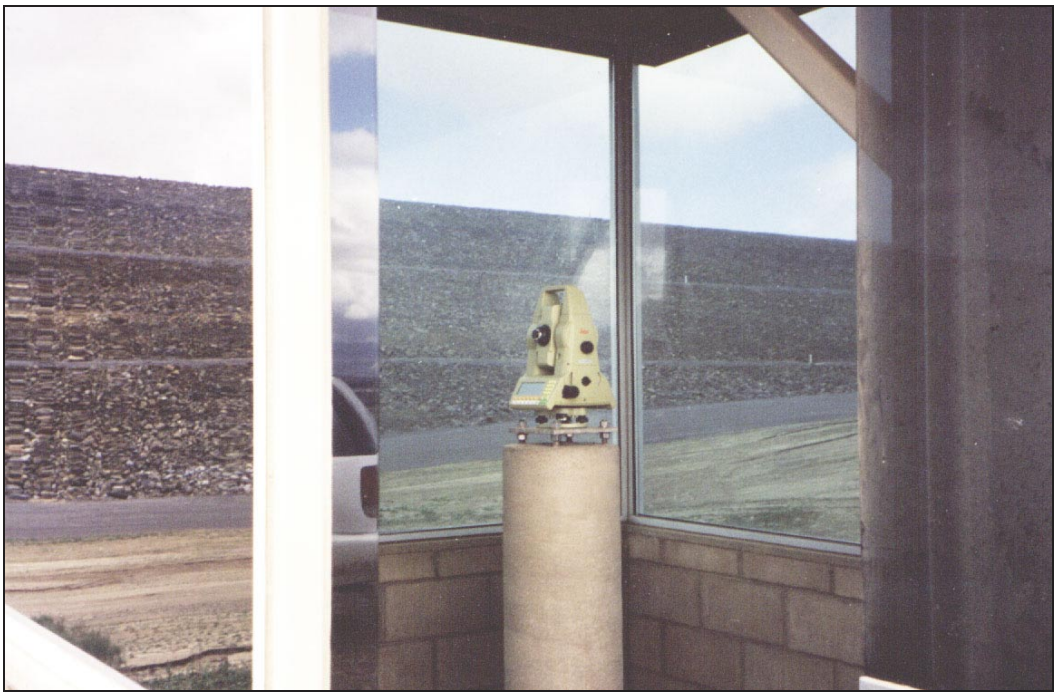

Figure 4-6. RTS mounted on observing pillar

Part of the normal operation of the automated monitoring system was to be the verification of the stability of the observing point, using measurements collected by the RTS. To provide external checks on observing station stability, provision was also made for both levelling and GPS measurements. The concrete base of each observing shelter contains three levelling benchmarks so that uneven settlement can be detected, while the roof was equipped with a tripod head to allow a GPS antenna to be centred over the survey pillar. Figure 4-7 shows the tripod head attachment at observing shelter TS7.

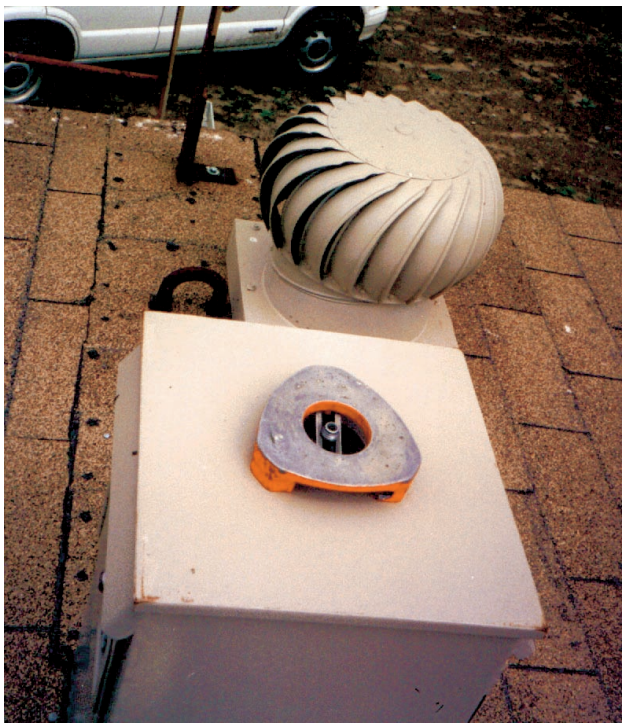

Figure 4-7. GPS antenna attachment on shelter roof

Construction of the observing shelters was performed throughout most of the year 2000, with final installation of the doors and shelter glass in October. The glass itself is dual-pane, 12.25 millimetres thick in total, and tinted to minimize heat buildup inside the shelters. Figure 4-5 above shows the glass at a finished structure. The tint looks very

dark from the outside, but it allows sufficient light to pass so that the RTS can collect measurements. Figure 4-6 shows the view from inside one of the observing shelters.

In Chapter 3 of this thesis, it was mentioned several times that RTS measurements through the shelter glass would be affected by refraction. This consideration was used as the basis for choosing a data processing methodology, but the magnitude of the refraction effect has not been discussed. In fact, for displacement monitoring purposes, the refraction effect caused by the glass itself is almost completely cancelled out when the displacement is computed from coordinate solutions at two different epochs. Appendix II presents sample calculations illustrating the error introduced in the computed coordinate differences; a point 100 metres from the RTS that moves by 1 metre would exhibit an error of less than 0.2 mm in the measured displacement. This is well below the precision of the measurements.

A much more serious refraction effect, one that was not considered at the design stage, occurs when there is a change in atmospheric conditions between the inside and the outside of the observing shelter. This causes a difference in the refractive index, which in turn causes a change in the ray path direction. Snell's Law, shown as equation (4.1), can be used to compute the change in direction:

$$n_i \sin\theta_i = n_o \sin\theta_o, \qquad \textbf{(4-1)}$$

where

θ_i is the angle between the RTS beam and the inside of the shelter glass, as shown in Figure 4-8,

θ_o is the angle between the RTS beam and the outside of the shelter glass,

n_i is the refractive index inside the shelter, and

n_o is the refractive index outside the shelter.

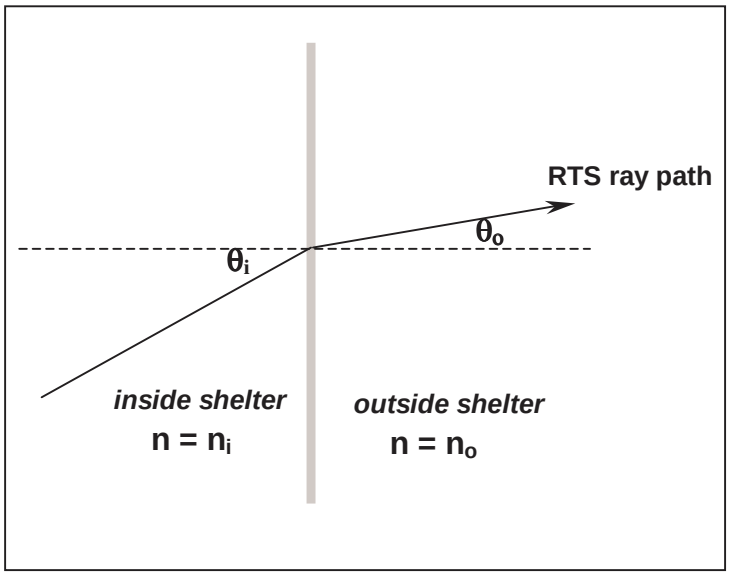

Figure 4-8. Ray path refraction caused by change in atmospheric conditions

Figure 4-9 shows the magnitude of ray path bending as a function of the temperature difference between the inside and outside of the shelter. In terms of the tolerance for detection of displacements in this project (10 mm at the 95% confidence level), this effect can be very significant. A temperature difference of 10 degrees Celsius causes a deflection of over 1 arcsecond for angles of incidence larger than 30 degrees. The maximum angle of incidence for lines of sight at DVL is approximately 40 degrees; depending on the magnitude and variability of the temperature difference, ray path bending could seriously impact the accuracy of measurement to these targets.

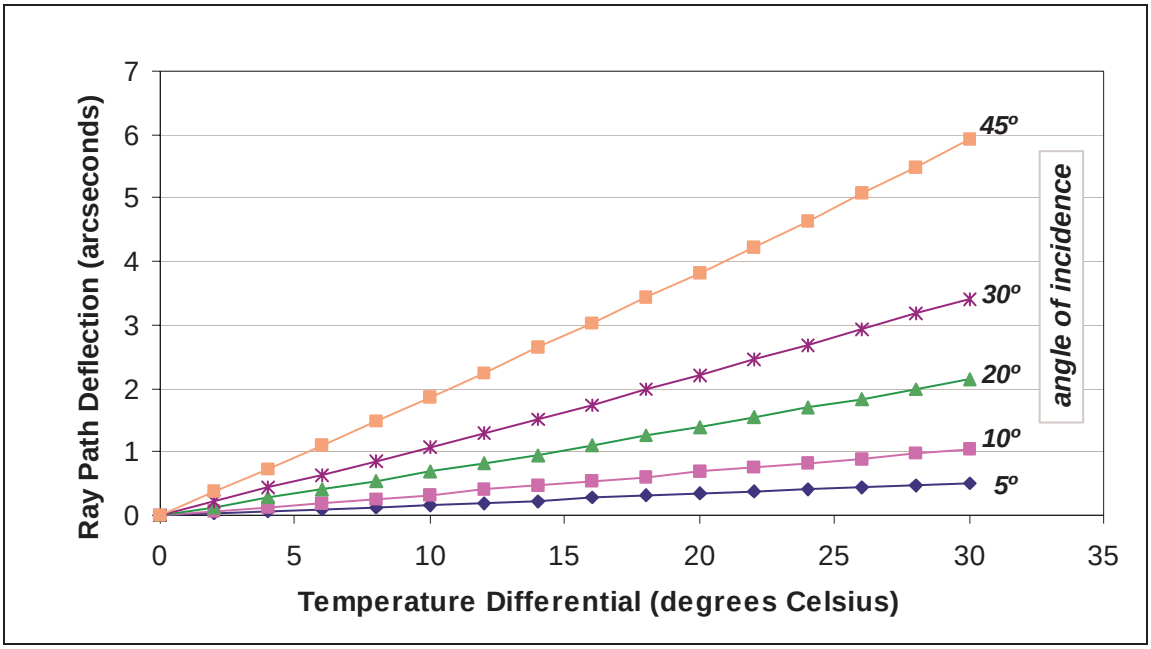

Figure 4-9. Ray path deflection as a function of temperature differential

Because the observing shelters are equipped with louvers near the base and a wind turbine on the roof, temperature buildup was not expected to be severe. However, this could only be verified by actual measurement. Chapter 5 presents a further discussion of this refraction effect in light of observed temperature differences during the first few months of system operation.

4.6 Software Configuration

Installation of glass at the observing shelters was the final stage of construction of the DDM system. Once this had been completed, the only remaining step was to configure DIMONS for data collection and processing. This software configuration was carried out in October 2000, as the shelter glass was being installed.

Software configuration at the observing sites was performed in tandem with installation of the total stations. As each RTS was installed on its observing pillar, the instrument height was measured and recorded in the DIMONS database. Intervisibility between the instruments and their targets were verified (initial readings had been collected during an earlier site visit), and targets that were no longer visible due to blockage by the window and door frames were removed from the list of points to be measured. Finally, a data collection task was defined, as described in section 3.2.1.3, and scheduled for automatic execution. In order to enable an assessment of system performance and to choose an optimal time of day for the observations, each observing station was scheduled for measurements four times per day: at 4a.m., noon, 8p.m., and midnight.

Because the observing sites were connected via an outdoor radio link, they could not be integrated directly into Metropolitan's computer network due to security concerns. Instead, a server computer was installed in an onsite structure (known as the Radial Gate structure) and connected to both the wireless network and Metropolitan's network. A secure firewall separates these connections, allowing Metropolitan to access the observing sites without introducing potential security holes in their enterprise network.

The Radial Gate computer was configured as the main data transfer and processing hub for the monitoring system. It was scheduled to download raw observations from the observing sites every day, and then to process these observations to determine the updated point positions. After the data is processed, it is copied to the Glendora survey

office, where another DIMONS host computer can be used for data browsing and generation of displacement plots.

When system changes are required, the system operator in Glendora can directly access the Radial Gate computer through Metropolitan's enterprise network. By using the Radial Gate computer as a gateway, direct access to the observing sites is also possible. When more advanced remote access is required, a commercial package called pcAnywhere is used to carry out any necessary operations.

Figure 4-10 illustrates the operations typically performed at the different DIMONS host computers.

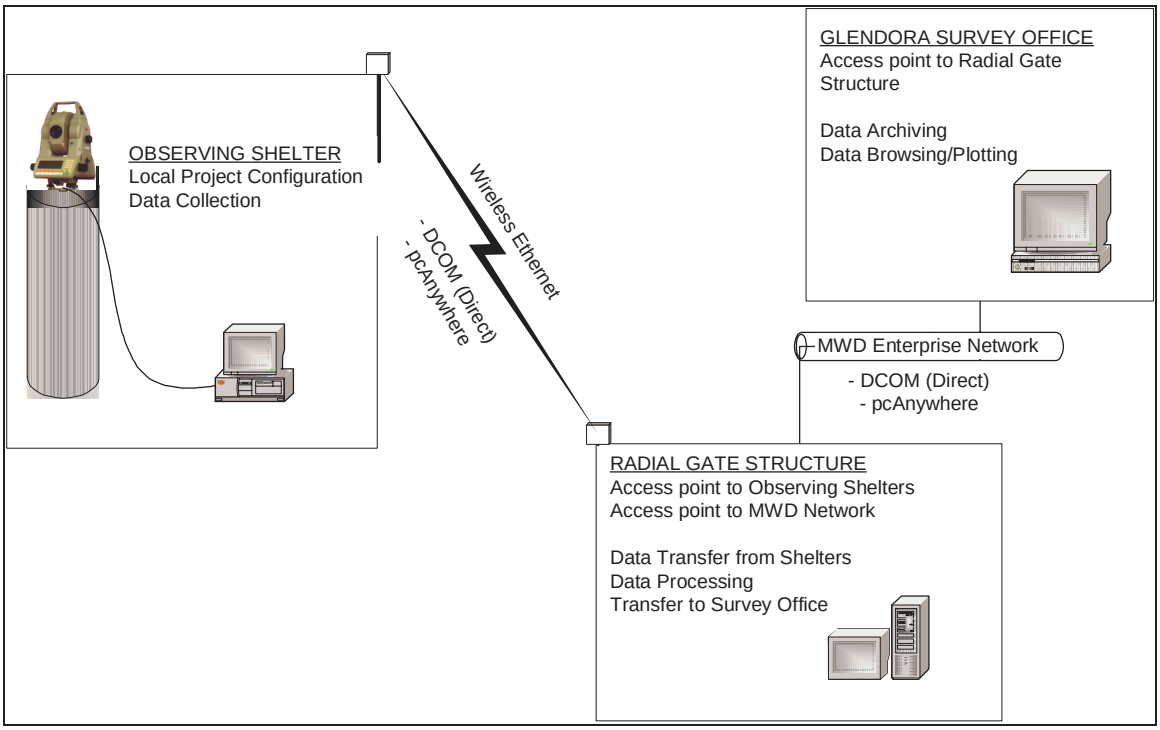

Figure 4-10. Relationships among DIMONS hosts at DVL

Using this configuration, the monitoring system was brought online in October 2000. A final site visit was made in December 2000 to perform some minor software upgrades

and to redefine the data collection schedule. The data collection schedule was relaxed in order to lessen the amount of data coming in; after only two months, it could be seen that data storage would be an issue if four cycles were collected daily at each site. Currently, the DDM system performs automated collection of ten observation cycles per week; at 4a.m., noon, and 8p.m. on Monday, Tuesday, Wednesday, and Thursday morning. This provides a good balance between having enough data for meaningful analysis and avoiding data storage problems.

CHAPTER 5
PRELIMINARY EVALUATION OF SYSTEM PERFORMANCE

Activation of the geodetic DDM system at DVL in October 2000 began the collection of what is hoped to be a continuous dataset covering a span of several years. Combined with the geotechnical instrumentation installed onsite, the scale and frequency of coverage offered by this system will give Metropolitan's engineers unprecedented detail in monitoring the behaviour of large dams, and will be a great benefit in planning future projects.

Although development and implementation of the monitoring system was successful, the system as a whole cannot be proclaimed a success without first evaluating the quality of collected data. This chapter, therefore, discusses the initial quality assessment that was performed after the first four months of system operation.

Thanks to the frequent monitoring interval and the measurement of several points from two adjacent observing stations, several forms of evaluation were possible. The first evaluation, presented in section 5.1, considers only the internal consistency achieved by the instrument over the course of a single observation cycle This is followed in section 5.2 by an analysis of the repeatability of point coordinates on different days, and at different times of day. The accuracy improvement to be gained by averaging the measurement results over several days is then discussed in section 5.3, followed in section 5.4 by the comparison of displacements at points measured by adjacent observing stations. Finally, the overall results of the evaluation are summarized in section 5.5.

5.1 Internal Precision of Individual Measurement Cycles

The first stage in system evaluation was determining what level of consistency was being achieved by each RTS over the course of one measurement cycle. This gives a good indication of the instrument performance in real-world conditions, as opposed to the factory-certified instrument ratings [Zeiske, 2001] that do not reflect the changing atmospheric effects often encountered in practice. At DVL, each measurement cycle can take from 15 to 45 minutes, depending on the number of targets and sets measured by the RTS. Atmospheric conditions can change considerably over this period of time, decreasing the agreement between different pointings to the same target.

To evaluate the internal precision of the measurement cycles, observation residuals from the least squares set reduction were examined. The variances of directions, zenith angles, and distances were estimated using equations (5-1) to (5-3), respectively:

$$\sigma_\delta^2 = \frac{1}{n_{obs} - n_s - n_T} \cdot \sum_{k=1}^{n_{obs}} \hat{r}_{\delta_k}{}^2 \qquad \textbf{(5-1)}$$

$$\sigma_z^2 = \frac{1}{n_{obs} - n_T} \cdot \sum_{k=1}^{n_{obs}} \hat{r}_{z_k}{}^2 \qquad \textbf{(5-2)}$$

$$\sigma_d^2 = \frac{1}{n_{obs} - n_T} \cdot \sum_{k=1}^{n_{obs}} \hat{r}_{d_k}{}^2 \qquad \textbf{(5-3)}$$

where

n_{obs} is the total number of measurements used in the least squares solution (e.g. if 10 targets were measured in 3 sets, with one outlying observation omitted from the solution, this number would be 29),

n_s is the number of sets,

n_T is the number of different targets observed,

$\hat{r}_{\delta_k}$, $\hat{r}_{z_k}$, and $\hat{r}_{d_k}$ are the estimated direction, zenith angle, and distance residuals for observation *k*, respectively, and

σ_δ^2, σ_z^2, and σ_d^2 are the estimated variances.

Observation variances were computed for each cycle measured at each observing point, and then the per-cycle estimates were averaged for each observing point to yield an overall value. Finally, the square roots of these averaged variances were computed to give the standard deviations listed in Table 5-1. The listed values represent the standard deviation of a pointing in a single set, averaged from both telescope positions.

Table 5-1. Empirical standard deviations of RTS measurements

Observing point	Average σ_δ (arcseconds)	Average σ_z (arcseconds)	Average σ_d (mm)
1720	1.4	1.6	0.3
1740	1.7	1.7	0.2
1760	1.4	1.7	0.2
2720	1.1	1.6	0.2
3720	1.5	1.7	0.2
3740	1.3	1.5	0.2
3760	1.8	1.8	0.4
3780	1.7	1.8	0.2

As the table indicates, the empirical standard deviations of direction and zenith angle measurements are somewhat higher than the factory value of ±0.8 arcseconds, while the distance standard deviations are lower than the ±1 mm ±2 ppm factory value. Experience with field surveys of this nature would suggest that the refractive index of air is reasonably constant during the measurement cycle (giving a good agreement among measured distances), while the precision of direction and zenith angle measurements is degraded by atmospheric scintillation.

Averaging values from all the observing points, an overall standard deviation of ±1.5 arcseconds for directions and ±1.7 arcseconds for zenith angles is obtained. Over a sight length of 500 metres, the ±1.5 arcsecond direction standard deviation will result in a 3.6 mm major semi-axis length of the horizontal point standard confidence region. This is larger than the required value of 2.9 mm, but it must be borne in mind that the values listed in Table 5-1 refer to measurements in a single set. Measurement cycles at DVL typically consist of between 3 and 5 sets, so the standard deviation of the least squares estimate will be smaller by a factor of at least $\sqrt{3}$. This means that, for the reduced observations used in computing point positions, standard deviations will be on the order of ±0.9 arcseconds for directions and ±1.0 arcseconds for zenith angles. These values translate into major semi-axis lengths of 2.2 mm and 2.4 mm for the horizontal and vertical components, respectively, well below the tolerance values of 2.9 mm and 3.6 mm.

5.2 Comparison of Different Cycles

Based upon the analysis of individual observation cycles presented in the previous section, it could be argued that the RTS measurements are meeting Metropolitan's accuracy requirements. In fact, for traditional monitoring systems based on repeated surveys, this conclusion would almost certainly be reached; measurements could be made on a monthly basis at best, so small differences in computed point positions would likely be attributed to point movement. The only useful information on measurement accuracy would be obtained from the type of analysis performed in section 5.1, or from any redundant measurements that were collected.

With an automated data collection system, however, a more detailed evaluation of the system accuracy is possible. Since the automated system can collect and process an entire cycle of survey measurements in less than an hour (as compared to weeks for a traditional system), the repeatability of measurements can be examined under different conditions while keeping the time interval short enough to ignore the effects of point movement. The following sections discuss the evaluation of DVL monitoring results in this light.

5.2.1 Cycles at Same Time of Day

In this section, the repeatability of point coordinates derived from measurement cycles collected at the same time on different days is examined. Because the weather at DVL is quite consistent (generally hot and sunny), meteorological conditions vary more

over the course of the day than they do from one day to the next. Therefore, this comparison shows the repeatability of the measurements at different times but under similar conditions, a much more useful indicator of system performance than the single-cycle evaluation discussed in section 5.1.

The comparison was performed by generating time series plots of the change in coordinate solutions for selected survey points. In this way, both the repeatability and any possible trends in the data could be examined simultaneously. Because the quantity of interest in this case is system performance and not point movement, the coordinate changes have been transformed from Easting, Northing, and Height into a coordinate system more suited for interpretation in terms of the variation in RTS measurements. This rotated coordinate system is depicted in Figure 5-1.

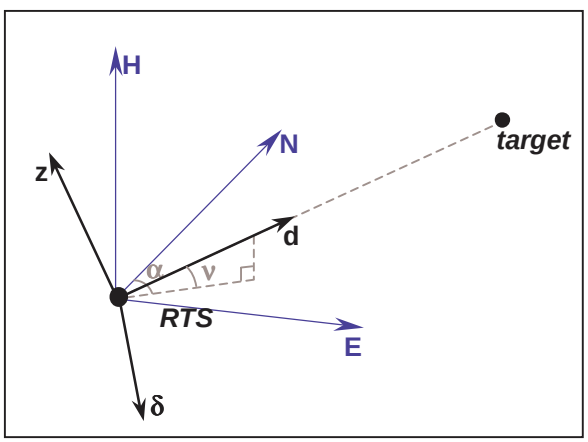

Figure 5-1. Coordinate system used to show variation in target positions

The coordinate transformation is carried out using equation (5-4):

$$\begin{bmatrix} \delta \\ d \\ z \end{bmatrix} = \begin{bmatrix} 1 & 0 & 0 \\ 0 & \cos\nu & \sin\nu \\ 0 & -\sin\nu & \cos\nu \end{bmatrix} \cdot \begin{bmatrix} \cos\alpha & -\sin\alpha & 0 \\ \sin\alpha & \cos\alpha & 0 \\ 0 & 0 & 1 \end{bmatrix} \cdot \begin{bmatrix} E \\ N \\ H \end{bmatrix}, \qquad \textbf{(5-4)}$$

where α is the azimuth from the RTS to the target (as obtained from approximate coordinates) and ν is the elevation angle. This coordinate system is convenient for evaluation of system performance because changes in δ, d, and z represent relative lateral displacement, a change in slope distance, and relative vertical displacement, respectively. Over the distance to the target, these correspond directly to changes in horizontal direction, slope distance, and zenith angle. Therefore, the different components of the RTS measurements can be analysed in terms of their relative effect on repeatability of the computed point coordinates.

Figure 5-2 shows a time series plot for a typical survey point, derived from measurements collected during the daily 12 p.m. measurement cycle (shown as displacements computed with respect to the mean coordinate values). The sight length from the RTS to this target is approximately 214 metres.

The general pattern shown in the figure is common to nearly all the survey points; first, it can be seen that little or no actual point movement has occurred over the nearly four-month period under consideration. Second, the repeatability of d is excellent, δ is somewhat more variable, and z has the highest standard deviation; in the author's experience, this is normal for survey measurements with precise total stations. Table 5-2 lists the computed standard deviations in δ, d, and z for a random sample of 15 survey points. For an average sight length of 343 metres, the mean δ standard deviation is ±2.7 mm, d is ±1.2 mm, and z ±3.2 mm.

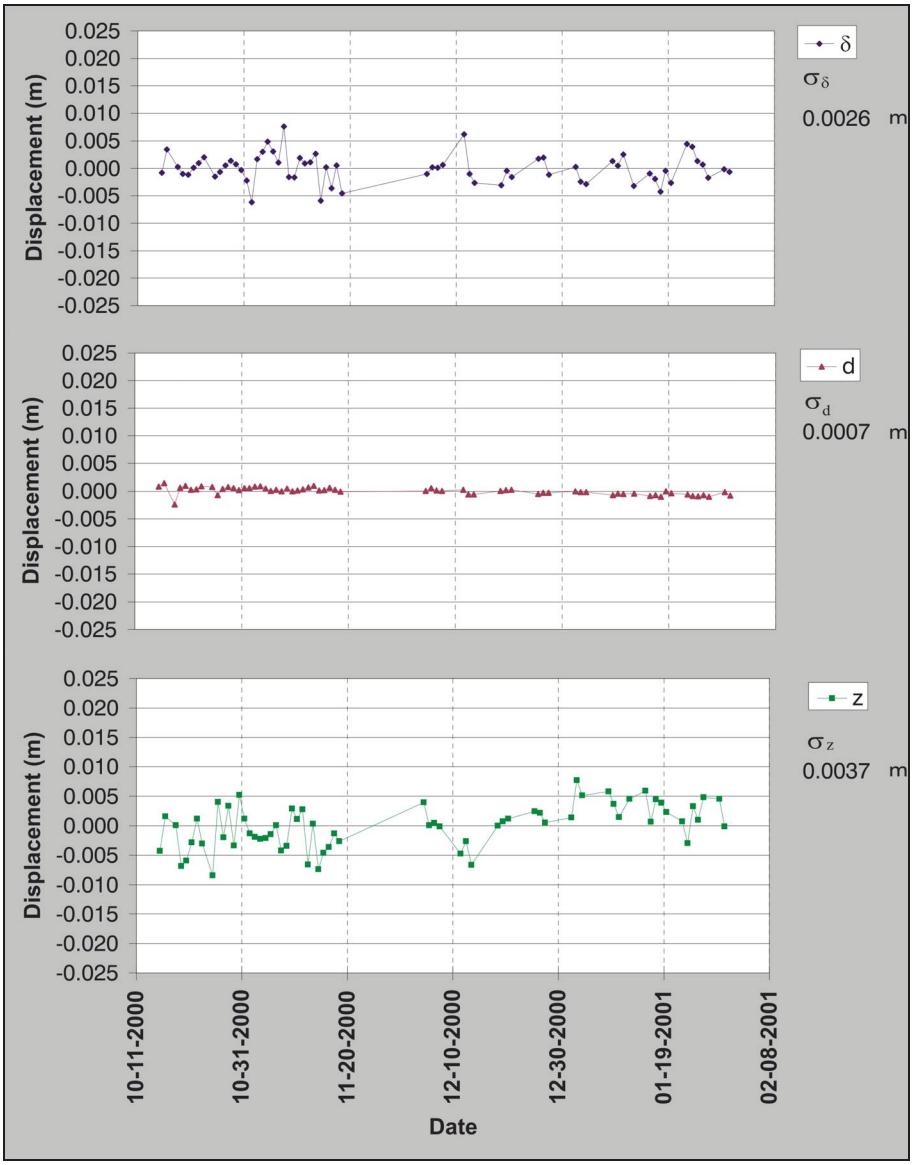

Figure 5-2. Point 1088 coordinate changes derived from 12 p.m. measurement cycles

Table 5-2. Standard deviations of coordinates derived from 12 p.m. measurements

Point	Distance from RTS (m)	σ_δ (mm)	σ_d (mm)	σ_z (mm)
1001	485	2.7	0.9	4.6
1051	156	1.4	0.3	1.3
1078	378	3.6	1.0	4.1
1109	256	1.5	0.7	2.7
1129	553	5.1	1.2	5.8
1405	374	2.4	0.9	2.9
2011	403	2.8	2.9	3.8
2024	219	1.4	1.3	1.5
2048	84	0.5	0.8	1.0
3001	519	4.5	1.5	5.2
3027	215	1.6	0.9	3.7
3040	413	3.5	1.4	3.1
3082	331	3.2	0.3	2.5
3115	505	3.3	2.9	3.7
3133	258	2.7	1.5	2.8

Because the survey point coordinates are derived from observations made at a single RTS, the δ–, d-, and z-axis directions coincide with the axis directions of the point confidence regions. Therefore, σ_δ or σ_d (whichever is larger) can be compared with the value of 2.9 mm that was presented in section 2.2.2 as necessary to detect horizontal movements of 10 mm at the 95% confidence level. This comparison is approximate because the d-axis is not in general horizontal; however, the elevation angle of all lines of sight at DVL is within ±22º, so it is close enough for a general evaluation. Using the same approximation, σ_z can be compared with the required value of ±3.6 mm for detecting vertical movements.

A quick look at Table 5-2 reveals that the required positioning accuracy is not being met in many cases, particularly for the longer lines of sight. However, part of the reason

for collecting several measurement cycles each day was to determine the best time for measurements; therefore, results from the 4 a.m. measurement cycles were examined next.

Surprisingly, it was found that the 4 a.m. measurement cycles generally exhibited a higher degree of variation than those at noontime. The 4 a.m. measurement cycle had been included specifically because an investigation by Chrzanowski [1989] had shown that vertical temperature gradients (and, thus, systematic refraction errors) are smallest at this time. However, Table 5-3 shows that the same points examined earlier averaged ±3.6 mm for σ_δ, ±1.1 mm for σ_d, and ±4.9 mm for σ_z when 4 a.m. results were considered.

Table 5-3. Standard deviations of coordinates derived from 4 a.m. measurements

Point	Distance from RTS (m)	σ_δ (mm)	σ_d (mm)	σ_z (mm)
1001	485	4.4	1.4	8.0
1051	156	1.2	0.6	2.4
1078	378	4.2	0.5	6.2
1109	256	1.5	1.3	3.8
1129	553	3.3	1.6	9.7
1405	374	2.8	1.0	4.6
2011	403	3.2	1.4	4.5
2024	219	1.4	0.9	1.7
2048	84	0.4	0.6	0.9
3001	519	7.8	1.4	8.3
3027	215	1.6	1.6	3.8
3040	413	8.3	1.5	5.8
3082	331	2.0	0.4	3.9
3115	505	7.5	2.2	7.5
3133	258	4.4	0.9	2.2

At first, it was thought that the higher variability of nighttime measurements was due to increased variability of the temperature differential between the inside and outside of the observing shelters. If the RTS shelters retained heat at night due to the computer equipment inside, this would cause an increased deflection of the RTS beam as discussed in section 4.5. However, an examination of the temperature records quickly ruled out this hypothesis. Figure 5-3 shows the record of temperature differentials at observing station 1740 as an example. The temperature differential during the 12 p.m. measurement cycles is both higher (in general) and more variable than that during the 4 a.m. cycles; therefore, if ray path deflection due to temperature buildup was a problem, it would cause a higher variation in the noontime cycles than the nighttime ones.

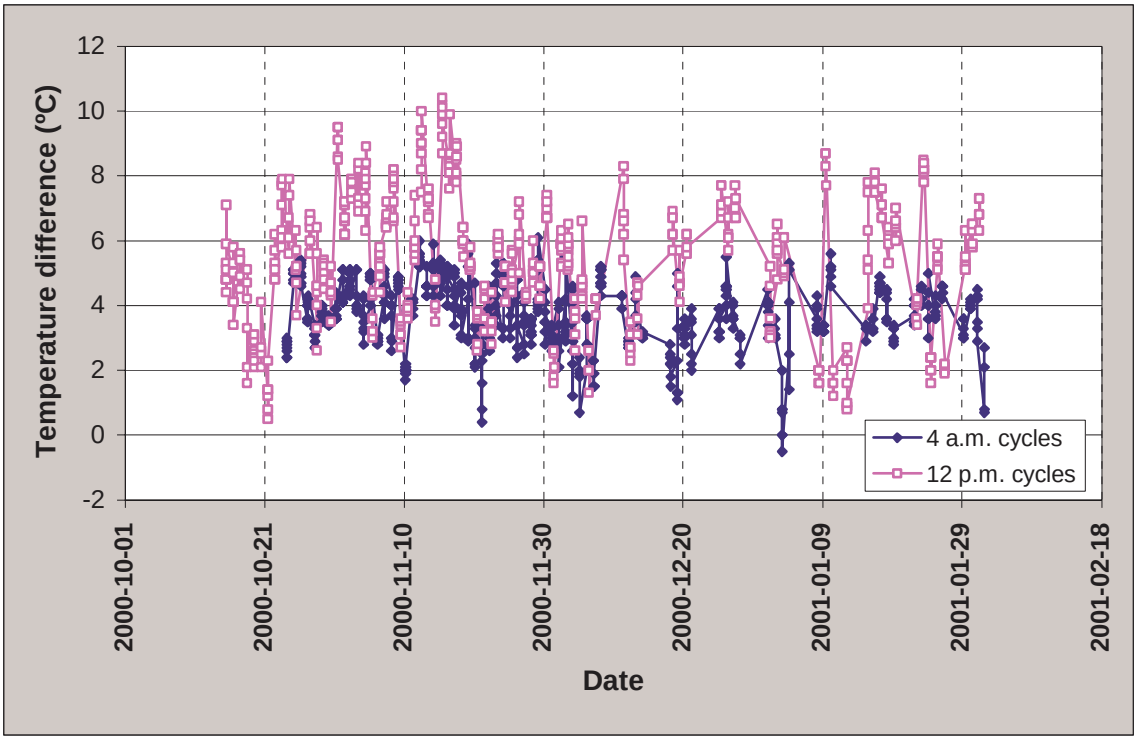

Figure 5-3. Temperature increase inside observing shelter, station 1740

Examination of the measurement cycle results showed that the 4 a.m. cycles often required more sets of observations before the required tolerance was met. The 4 a.m. cycles also contained a higher percentage of missed targets, i.e., targets that the RTS was sometimes unable to measure during the measurement cycle. One possible explanation for the higher variation of nighttime measurements, therefore, is that this type of RTS simply performs better in daylight. Further investigation will be required to determine whether or not this is the case.

5.2.2 Cycles at Different Times of Day

Although refraction could not be identified as a factor affecting the repeatability of nighttime measurements, it can be seen to play a role when these measurements are compared with the 12 p.m. observing cycles. In particular, a bias in the height (z) coordinate is seen for those survey points whose line of sight runs close to the ground. As an example, Figure 5-4 shows the coordinate variations derived from all collected measurement cycles of survey point 1088, the point for which noontime results were given in Figure 5-2. This survey point lies on a wide berm of the West Dam, and is very nearly at the same elevation as its observing station. The line of sight passes over hard-packed soil.

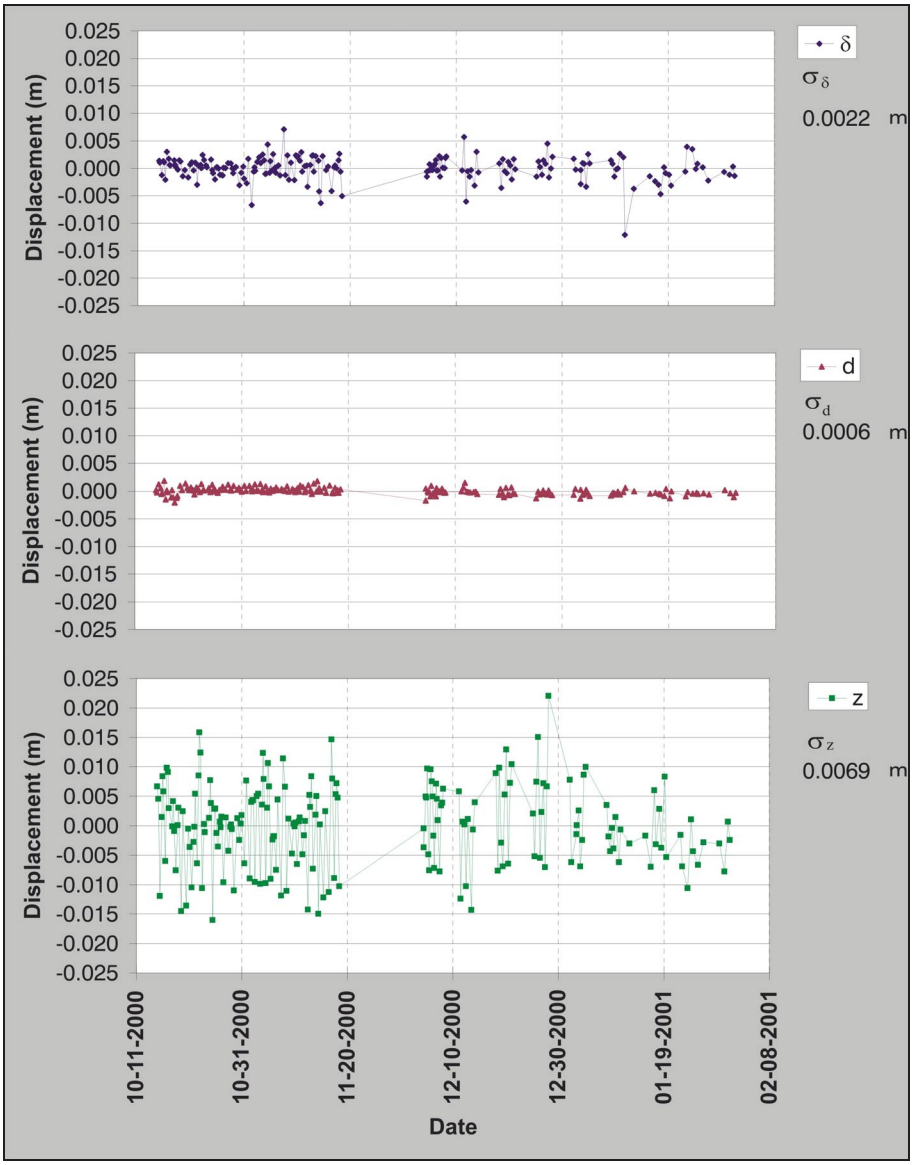

Figure 5-4. Point 1088 coordinate changes derived from all measurement cycles

While the δ and d coordinates show a slightly smaller standard deviation than for the 12 p.m. measurement cycles alone, the z coordinate is considerably worse. Moreover, the variation in the z coordinate over the course of a single day is much greater than can be explained by instrumental effects alone. Examination of the time series plot shows

that over the course of a day, the z values tend to cluster into two categories: a 'high' value and a 'low' value, with 10 to 15 mm difference between the two. Examination of the timetags associated with the coordinate solutions showed that the lower category invariably corresponded with the 12 p.m. measurements. The higher category corresponds with the 4 a.m. cycles as well as those collected at 8 pm and midnight.

Survey point 1079, which is also located on the wide berm of the West Dam at a distance of 340 metres from its observing point, shows an even larger difference between daytime and nighttime measurements. Figure 5-5 shows the 12 p.m. and 4 a.m. z coordinate changes for this point, plotted with respect to the combined mean of all values. The weekly averages are also plotted to give a picture of overall trend.

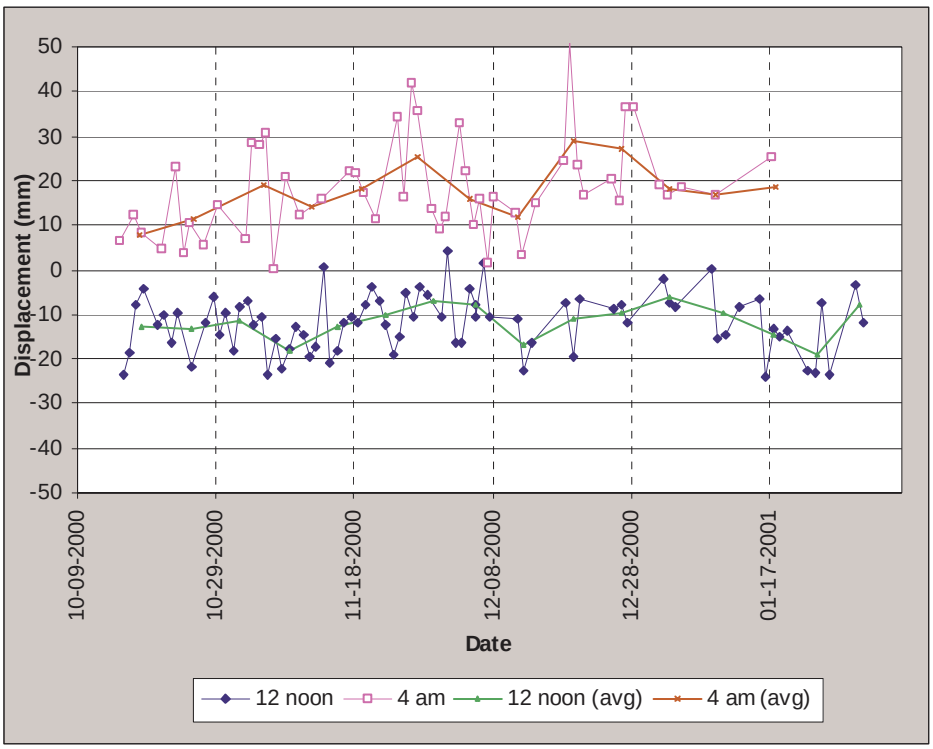

Figure 5-5. Time-of-day height bias, point 1079

On average, the 4 a.m. measurement cycles give a height solution that is 29 mm higher than the 12 p.m. measurement cycles. When the computed heights were compared with the external temperature observed during each measurement cycle, a correlation coefficient of –0.6 was found to exist. This fact, combined with the observation that only points with lines of sight close to the ground exhibit this bias, indicates strongly that refraction is the cause of these biases.

Assuming that the 12 p.m. to 4 a.m. difference in refraction is the cause of the observed height bias, there is a way to calculate the associated difference in temperature gradient. Equation (5-5), adapted from Blachut et al. [1979], is used to express the relationship between the two:

$$dz = \frac{8''}{\rho} \cdot \frac{PS^2}{T^2} \cdot \frac{dT}{dZ}, \qquad \textbf{(5-5)}$$

where

P is the average atmospheric pressure, expressed in millibars,

T is the average temperature, expressed in Kelvins,

S is the distance, expressed in metres,

ρ is the conversion factor from radians to arcseconds (206264.8"/rad),

dz is the observed height bias in metres, and

$\frac{dT}{dZ}$ is the difference in vertical temperature gradients, expressed in ºC/m.

Rearranging for $\frac{dT}{dZ}$, equation (5-6) is obtained:

$$\frac{dT}{dZ} = \frac{\rho \cdot dz \cdot T^2}{8 \cdot P \cdot S^2}. \qquad \textbf{(5-6)}$$

For the time series shown in Figure 5-5, the average temperature is 14ºC, the average pressure is 970 mb, and the distance is 340 metres. Since the 12 p.m. measurements are biased by –29 mm with respect to the 4 a.m. measurements, the average difference in temperature gradient must therefore be –0.55 ºC/m. This corresponds well with results presented by Chrzanowski [1989]; in that investigation, the reported difference in temperature gradient for these two times of day was –0.4 ºC/m over gravel. Therefore, refraction is the likely cause of the observed height biases.

5.3 Cycles Averaged Over Time

The discussion in the previous section has demonstrated that individual measurement cycles collected at DVL are not capable of achieving the precision required of the monitoring system. Refraction almost certainly plays a part in this, although refraction alone cannot explain why the 4 a.m. measurement cycles have poorer repeatability than the noontime ones. Further research is required to determine the cause of this phenomenon.

In order to improve the results, a decision was made to work with averaged cycles rather than individual cycles. Discussions with Metropolitan indicated that an averaging period of one week would be convenient; as the DVL dams are large structures, they were not expected to undergo rapid movement, and in any case the individual cycle results would still be available if needed for more detailed analysis. Therefore, during the

final site visit in December 2000, the DIMONS observing schedule was changed to so that only ten cycles per week were collected, as discussed in section 4.6. Computed coordinates from all measurement cycles collected in a given week are then averaged, and these averaged coordinates are used as the basis for comparison and interpretation.

To provide continuity with earlier discussions, Figure 5-6 shows the weekly averaged coordinate changes for point 1088. The improved repeatability when compared to individual cycles (Figure 5-2 and Figure 5-4) can immediately be seen; σ_δ, σ_d, and σ_z are now only ±0.9 mm, ±0.3 mm, and ±2.5 mm, respectively. For the 15 test points, the standard deviations of weekly averages are given in Table 5-4. The average standard deviations for these points are ±1.6 mm for σ_δ, ±0.6 mm for σ_d, and ±2.4 mm for σ_z. A couple of the points with longer sight lengths still show some variability (4-5 mm for σ_δ), but overall, the results are more than adequate to detect displacements of 10 mm at the 95% confidence level.

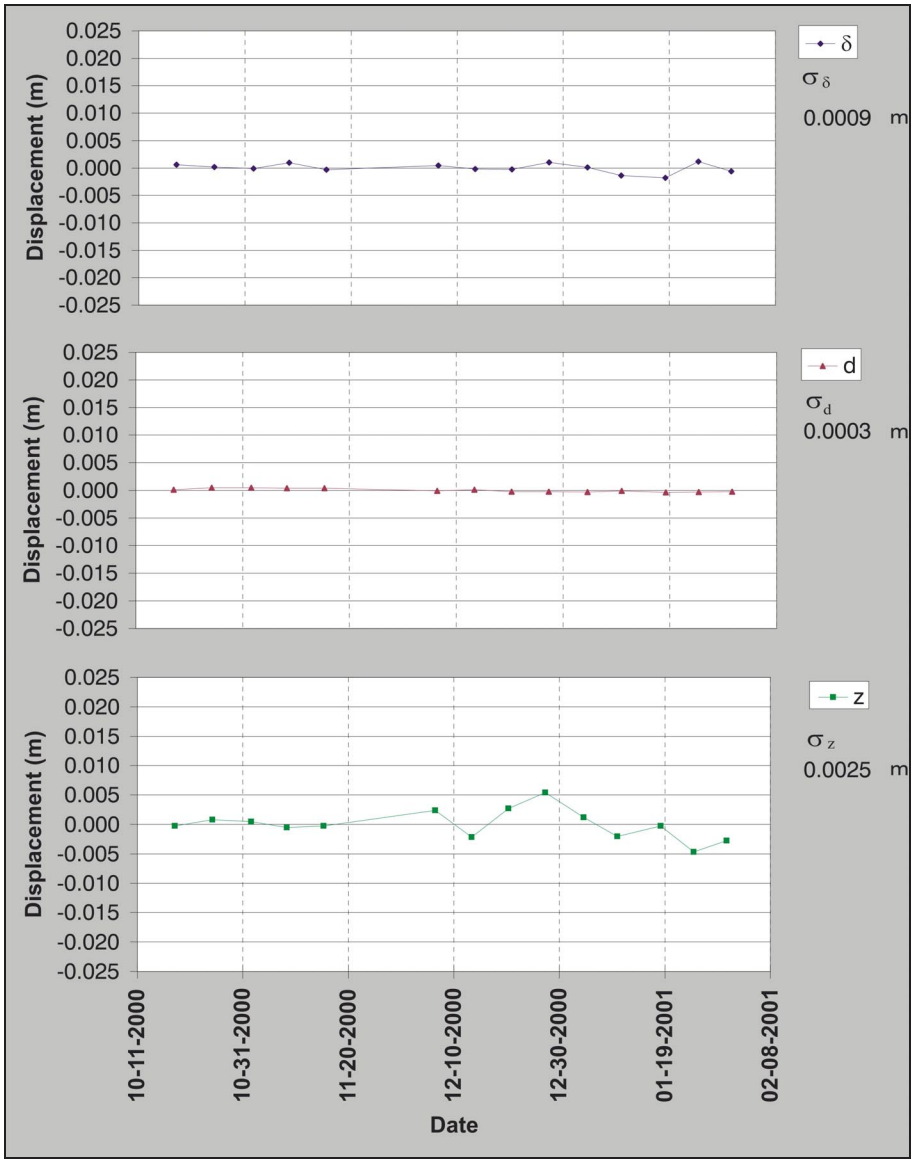

Figure 5-6. Point 1088 coordinate changes derived from weekly averages

Table 5-4. Standard deviations of coordinates derived from weekly averages

Point	Distance from RTS (m)	σ_δ (mm)	σ_d (mm)	σ_z (mm)
1001	485	1.3	0.5	2.4
1051	156	0.6	0.2	0.7
1078	378	1.7	0.3	4.1
1109	256	0.9	0.8	2.4
1129	553	1.8	0.7	3.9
1405	374	0.7	0.5	2.5
2011	403	2.2	1.1	2.6
2024	219	0.7	0.5	0.7
2048	84	0.3	0.7	0.9
3001	519	4.1	1.0	3.9
3027	215	1.3	0.6	3.1
3040	413	4.8	0.8	3.4
3082	331	0.9	0.3	1.7
3115	505	1.8	1.2	2.7
3133	258	1.6	0.5	1.2

5.4 Comparison of Displacements at Double Prisms

In the description of the geodetic DDM system design presented in section 2.2.2, it was mentioned that several of the survey points would be equipped with double prisms to allow a check of the measurements from adjacent observing stations. This section describes the evaluation of results from these double prisms, using the weekly coordinate averages as the basis for comparison.

Because the two prisms in a double-prism set are measured from different observing stations (Figure 4-4(b) shows a double prism, with the two prisms pointed in different directions), it is not valid to directly compare their coordinates. They are biased differently by refraction through the glass of the two observing shelters. This bias,

however, cancels out in the determination of displacements; therefore, the accuracy evaluation is based on comparison of computed displacements of the two prisms with respect to a common base cycle. The difference of these two displacements is a measurement of the error inherent in the monitoring system, including the effects of instrument pointing error, refraction, unstable reference points, and all other factors.

Using December 04, 2000 as a base cycle, weekly averaged displacements were computed for 11 double prism sets. Seven to eight weeks of data were available for each of these points, giving a total of 84 displacement differences for comparison (the displacement differences are listed in Appendix III). Given the requirement of detecting displacements 10 mm or larger, 95% of the computed displacement differences should be smaller than $\sqrt{2} \cdot 10\,\text{mm} =$ 14 mm in both the horizontal and vertical planes. Of the 84 displacement differences available, only one value exceeded this tolerance in the horizontal plane and four values exceeded the tolerance in the vertical plane. Therefore, the required accuracy level is being met by the monitoring system.

Finally, the standard deviations of the displacement components are computed based on the displacement differences. Because the two prisms are observed from different stations, the displacement differences are computed in Easting, Northing, and Height instead of the local δ, d, z coordinate system used earlier. A sample dataset for computation of the standard deviation of displacement components is shown in Figure 5-7, for the double prism set 3115/9115. Note that the listed standard deviations refer to the point displacements, not the displacement differences; they are smaller than the standard deviations of the displacement differences by a factor of $\sqrt{2}$.

	Point 3115			Point 9115			Differences 9115-3115		
Date	**dN (mm)**	**dE (mm)**	**dH (mm)**	**dN (mm)**	**dE (mm)**	**dH (mm)**	**ΔdN (mm)**	**ΔdE (mm)**	**ΔdH (mm)**
2000-12-11	0.0	-0.5	-2.8	-0.2	-0.7	-0.9	-0.3	-0.2	1.9
2000-12-18	0.4	-3.2	-2.1	0.1	1.2	-0.4	-0.3	4.5	1.7
2000-12-25	0.5	-1.8	-3.1	-1.3	0.1	-0.4	-1.8	1.9	2.6
2001-01-01	1.1	-3.8	-1.3	-1.1	0.2	-4.5	-2.2	4.0	-3.1
2001-01-08	1.0	6.0	-6.7	0.4	0.2	-5.9	-0.6	-5.7	0.9
2001-01-15	1.4	-2.0	-6.2	0.3	-0.1	-6.6	-1.1	1.8	-0.4
2001-01-22	1.6	1.2	-3.2	-1.8	-1.9	-6.4	-3.3	-3.1	-3.2
2001-01-29	0.3	-0.9	-6.6	0.7	0.4	-3.3	0.4	1.3	3.3
						std devs:	**0.9**	**2.5**	**1.8**

Figure 5-7. Computation of check point accuracy

Using this procedure, the standard deviations of displacement components have been computed for all points with double prisms; the computations are presented in Appendix III. Table 5-5 summarizes the results.

Table 5-5. Computed standard deviations of displacement components

Points	**σ_{dN} (mm)**	**σ_{dE} (mm)**	**σ_{dH} (mm)**
1034/7034	0.7	2.1	6.6
1079/7079	0.8	2.2	2.1
1082/7082	1.4	2.0	3.9
1723/1742	0.3	0.3	1.3
1743/1765	1.1	3.0	0.6
3038/9038	3.2	4.4	8.4
3041/9041	1.4	3.6	3.0
3082/9082	2.0	3.7	4.4
3083/9083	1.1	1.9	2.6
3115/9115	0.9	2.5	1.8
3744/3723	0.4	0.8	1.2

Averaging these values to get an overall picture of the displacement repeatability, values of ±1.2 mm, ±2.4 mm, and ±3.3 mm are obtained for σ_{dN}, σ_{dE}, and σ_{dH}, respectively. This is an excellent result, considering that the survey points with double prisms are located midway between observing stations and thus represent some of the longest lines of sight observed at DVL. The computed standard deviations compare favourably to the required standard deviations of $\frac{10\text{ mm}}{2.45}$ = 4.1 mm and $\frac{10\text{ mm}}{1.96}$ = 5.1 mm for horizontal and vertical displacements, respectively.

5.5 Summary of System Evaluation

In order to get a clear picture of the performance of the automated monitoring system, measurements and derived point coordinates from four months of data collection have been analysed. Initially, the analysis considered only the repeatability of measurements within each observing cycle; based on these results, the monitoring system appeared to easily meet its accuracy requirements. However, comparison of cycles measured at different times showed that atmospheric refraction is degrading the system accuracy; one line of sight running close to the ground exhibits an average difference of -29 mm in measured height when noontime measurements are compared with those taken at night. These refraction effects are reduced by working with weekly averages rather than individual cycles. When weekly averages are used, comparison of displacements determined at points with double prisms shows that movements of 10 mm can easily be detected by the monitoring system at the 95% confidence level.

CHAPTER 6
CONCLUSIONS AND RECOMMENDATIONS

This thesis has described the development of an automated data collection and processing system for structural displacement monitoring at Diamond Valley Lake in California. As the largest earthwork construction in North America, the three dams surrounding Diamond Valley Lake required a robust, reliable and cost-effective system to carry out displacement measurements during the two-to-five year filling period. To meet these requirements, a system was created that uses robotic total stations to perform periodic measurements of over two hundred survey points, with fully automated data processing and remote operation capability. At the time of this writing, the monitoring system has been implemented and has operated successfully for nearly a year.

While the work described in this thesis has been largely practical rather than theoretical in nature, it has led to a number of findings that may be of interest to future researchers. These findings, along with recommendations for further work, are presented in the following paragraphs.

When compared with alternative methods, the use of robotic total stations has been found to be a very cost-effective method for dam displacement monitoring. The ability to measure a large number of points from each station, combined with the capacity for fully automatic data collection, give RTS measurements a significant advantage over other monitoring techniques.

During the initial monitoring system design phase, a need was identified for development of custom data collection and processing software. Based upon the

software functionality requirements set out by Metropolitan, a component-based architecture was chosen as the most flexible design. Individual software components were developed as Distributed Component Object Model (DCOM) objects, greatly simplifying cross-network communications and mixed-language program development. Due to its power and ease of implementation, I highly recommend that this programming model be continued for future developments and additions to the DIMONS software.

Because DIMONS was developed for a single project, the software currently supports only one model of RTS and one model of meteorological sensor module. However, the system architecture implements a plug-in model for instrument controllers, so newly developed controller software can be included merely by registering the plug-in with the system. In order to support future hardware upgrades and to possibly use the monitoring software on other projects, controllers should be developed to support a wider variety of equipment manufacturers.

The reduction and processing of RTS data from the monitoring system, ordinarily a straightforward task, was complicated by the fact that each RTS must perform measurements through the glass windows of its observation shelter. While this has virtually no effect in the determination of point displacements, the bias caused by refraction through the shelter glass made it necessary to process data from each RTS separately from the others. This has led to difficulty in maintaining a consistent orientation for the coordinate solutions from different measurement cycles, because the pointing error of the instrument results in a small but noticeable bias from one cycle to the next. To reduce this problem, the coordinates of all stable reference points are

introduced as fixed in the calculation of object point coordinates. Of the alternatives considered, this technique was observed to yield the fewest orientation artefacts in the coordinate solutions.

During installation of the monitoring instrumentation and computer equipment at DVL, it was noted that the interior of the observation shelters is somewhat warmer than the exterior. While this temperature differential could theoretically cause a significant deflection of the RTS beam (depending on the angle of incidence with the shelter glass and on the temperature differential), evaluation of initial monitoring results indicates that this has not been a significant problem at DVL.

The frequent data collection interval (several times daily) employed during the first two months of system operation has yielded an excellent dataset for evaluation of the performance of the monitoring system. The initial system evaluation, which focused on the internal consistency of individual measurement cycles, suggested that Metropolitan's accuracy requirements were being met. However, comparison of measurement results collected under different atmospheric conditions indicate strongly that refraction is degrading the system accuracy; lines of sight running close to the ground exhibit up to two centimetres of height bias when daytime results are compared to those collected at night. This is far above the acceptable limit; therefore, it was necessary to perform averaging of measurement cycles collected over a period of one week. The weekly averages fall within Metropolitan's tolerances for repeatability, and comparison of results from dual-prism monitoring stations shows that when weekly averages are used, the system is capable of detecting displacements of 10 mm at the 95% confidence level.

Finally, the robotic total stations used for this project (Leica model TCA1800S) have been observed to perform somewhat better at midday than they do at night, a surprising result considering that refraction effects are expected to be higher in the daytime. Further study is needed to determine whether this result is caused by instrumental characteristics, by environmental conditions or by the particular equipment configuration employed at DVL.

The automated monitoring system at DVL has operated reliably since its inception in late 2000. In the year since its implementation, the system has measured the positions of its approximately 200 survey monuments more than five hundred times, delivering a high-quality dataset with a minimum of required maintenance on behalf of the system operators. In summary, the Diamond Valley Lake monitoring system has shown that, with due consideration paid to geodetic concerns and systematic effects, robotic total stations can be used to create a reliable, cost-effective and highly accurate system for dam displacement monitoring.

REFERENCES

Blachut, T., A. Chrzanowski, and J.H. Saastamoinen (1979). *Urban Surveying and Mapping*. Springer-Verlag, New York.

Burkhard, B. (2001). "Jurisdictional dam size." Retrieved 17 May 2001 from the World Wide Web. http://damsafety.water.ca.gov/juris-chart.htm

Chen, Y.Q. (1983). "Analysis of deformation surveys – a generalized method." Department of Geodesy and Geomatics Engineering Technical Report No. 94, University of New Brunswick, Fredericton, New Brunswick, Canada.

Chen, Y.Q., A. Chrzanowski and J.M. Secord (1990). "A strategy for the analysis of the stability of reference points in deformation surveys." *CISM Journal ACSGC*, Vol. 44 No. 2, pp.141-149.

Chrzanowski, A. (1986). "Geotechnical and other non-geodetic methods in deformation measurements." *Proceedings of the Deformation Measurements Workshop*, Massachusetts Institute of Technology, Cambrige, Massachusetts, 31 October – 01 November, pp. 99-139.

Chrzanowski, A. (1989). "Implementation of trigonometric height traversing in geodetic levelling of high precision." Department of Geodesy and Geomatics Engineering Technical Report No. 142, University of New Brunswick, Fredericton, New Brunswick, Canada.

Chrzanowski, A. (1996). "Evaluation of the proposed deformation monitoring plan at MWD Eastside Reservoir Project." Final contract report prepared by Dr. Adam Chrzanowski for the Metropolitan Water District of Southern California, Los Angeles, California, U.S.A., September, 13 pp.

Chrzanowski, A. (2001). Personal communication. Professor Emeritus, University of New Brunswick, Fredericton, New Brunswick, Canada, October.

Dent, A. (2000). Personal communication. Systems Consultant, Spectria, Long Beach, California, July.

Duffy, M. and C. Whitaker (1998). "Design of a Robotic Monitoring System for the Eastside Reservoir in California." *Proceedings of the ACSM Conference*, Vol. 1, pp. 34-44. Baltimore, Maryland, March 2-4, 1998.

Duffy, M., C. Hill, C. Whitaker, A. Chrzanowski, J. Lutes, and G. Bastin (2001). "An automated and integrated monitoring scheme for Diamond Valley Lake in

California." *Proceedings of the 10th FIG International Symposium on Deformation Measurements*, Orange, California, March 19-22, pp. K1-K23.

Grimes, R. (1997). *Professional DCOM Programming*. Wrox Press Ltd., Birmingham, UK.

Hudnut, K. (2001). "Southern California Integrated GPS Network (SCIGN) Home Page." Retrieved on 10 October 2001 from the World Wide Web. http://www.scign.org/

Leica AG (1996). "Producer inspection certificate." Facsimile communication between H Baertlein (Leica AG) and C. Whitaker (Metropolitan Water District of Southern California), 09 July 1996, 1 pp.

Leica Geosystems (2001). *Leica Geosystems – APSWin Software for Automated Polar Measurements*. Product brochure, retrieved 13 October 2001 from the World Wide Web. http://www.leica-geosystems.com/surveying/product/software/apswin.htm

Marks, C. (2001). *About MWD*. Retrieved 14 October 2001 from the World Wide Web. http://www.mwd.dst.ca.us/mwdh2o/pages/about/about01.html

Metropolitan Water District of Southern California (1999). "Request for Proposals to provide data collection software and displacement and stability analysis software for ESRP Deformation Monitoring System." Request for Proposals No. 418S of the Metropolitan Water District of Southern California, Los Angeles, California, U.S.A.

Metropolitan Water District of Southern California Public Affairs Division (1997). "Eastside Reservoir Project at a Glance." Public relations brochure, Metropolitan Water District of Southern California, Los Angeles, California, U.S.A.

Microsoft Corporation (1995). *The Component Object Model Specification*. Retrieved 08 February 2001 from the World Wide Web. http://www.microsoft.com/com/resources/comdocs.asp

Princo Instruments, Inc. (2001). "Instruction booklet for use with Princo Fortin type mercurial barometers." Retrieved 03 August 2001 from the World Wide Web. http://www.princoinstruments.com/booklet.pdf

Revue Thommen AG (2001). "Industrial instruments – our products." Retrieved 03 August 2001 from the World Wide Web. http://www.thommenag.ch/deutsch/indu2.htm#produkt9

Rüeger, J.M., F.K. Brunner and K. Becek (1989). "EDM monitoring surveys using a local scale parameter model." *Proceedings of the Symposium on Surveillance and*

Monitoring Surveys. Department of Surveying and Land Information, University of Melbourne, Australia, 9-10 November, pp. 183-194.

Rüeger, J.M. (1994). "Monitoring with surveying robots." *International Journal for Surveying, Mapping and Applied GIS*, Vol. 8, No. 2, pp. 58-63.

Rüeger, J.M., G. Alanko and T.J. Snow (1994). "Monitoring of an open cut mine with a surveying robot." *The Australian Surveyor*, December, pp. 252-266.

Rüeger, J.M. (1990). *Electronic Distance Measurement*, third edition. Springer-Verlag, Berlin.

Smith, D.W. (1989). "Surveillance measurements within California's Dam Safety Program." Technical report of the California Department of Water Resources Division of Safety of Dams. Retrieved 25 January 2001 from the World Wide Web. http://damsafety.water.ca.gov/tech-ref/dws-paper.pdf

Scripps Orbit and Permanent Array Center (SOPAC) (2001). "SCIGN array information." Retrieved 28 May 2001 from the World Wide Web. http://sopac.ucsd.edu/cgi-bin/dbShowArraySitesMap.cgi?array=SCIGN

Trimble Navigation Limited (2001). *Trimble 5600 Total Station Series.* Equipment brochure, retrieved 11 October 2001 from the World Wide Web. http://trl.trimble.com/dscgi/ds.py/Get/File-8889/5600datasheet.pdf

Wells, D. and E.J. Krakiwsky (1971). "The method of least squares." Department of Geodesy and Geomatics Engineering Technical Report No. 18, University of New Brunswick, Fredericton, New Brunswick, Canada.

Whitaker, C. (1996). "Eastside Reservoir Project Deformation Monitoring Plan." Unpublished internal report of the Metropolitan Water District of Southern California, Los Angeles, California, U.S.A.

Zeiske, K. (2001). "Current status of the ISO standardization of accuracy determination procedures for surveying instruments." Paper presented at the FIG Working Week 2001, Seoul, Korea, 06-11 May. Retrieved 06 September 2001 from the World Wide Web. http://www.ddl.org/figtree/pub/proceedings/korea/full-papers/pdf/ws_com5_3/zeiske.pdf

Appendix I. DIMONS Database Tables

This appendix lists the database tables used in the initial version of DIMONS, delivered to Metropolitan in December 2000. The description of each table below includes a list of the fields, their types, and descriptive comments where appropriate. Where fields in one table are used as an index to records in another table, the table and field to which they refer are indicated.

SurveyPoints
Information describing a survey point: its text name and numeric identifier, as well as some descriptive fields describing its location and what type of ground it is installed on.

Field	*Size/Type*	*Links to*	*Comments*
Id	Int		
Name	Char[32]		
FacilityName	Char[64]		
FoundationType	Char[64]		
Description	Char[80]		
LastModified	Date/Time		

RTS
Information describing an RTS: what type of instrument it is, its serial number, and what software controller is needed to operate it.

Field	*Size/Type*	*Links to*	*Comments*
Id	Int		
Name	Char[32]		
ControllerType	Char[32]		
SerialNumber	Char[16]		
Manufacturer	Char[32]		
Model	Char[32]		
Description	Char[80]		
LastModified	Date/Time		

RTSParameters Calibration parameters of the RTS that can be expected to change with time.			
Field	*Size/Type*	*Links to*	*Comments*
Id	Int	RTS:Id	
AdditiveConstant	Double		
ScaleFactor	Double		
Tstart	Date/Time		
Tend	Date/Time		
LastModified	Date/Time		

MetModules Information describing a meteorological sensor module: make, model and serial number, as well as a set of Boolean flags indicating what sensors are installed in the module.			
Field	*Size/Type*	*Links to*	*Comments*
Id	Int		
Name	Char[32]		
ControllerType	Char[32]		
SerialNumber	Char[16]		
Manufacturer	Char[32]		
Model	Char[32]		
Tdry	Int		
Tdry2	Int		
Twet	Int		
P	Int		
Rh	Int		
Description	Char[80]		
LastModified	Date/Time		

RemoteHosts Other DIMONS hosts that are accessible from the local computer.			
Field	*Size/Type*	*Links to*	*Comments*
HostName	Char[32]		
ConnectionType	Int		0 = direct (DCOM connection); 1 = connection via proxy
LastModified	Date/Time		

RemoteHostProxyInfo Describes what proxy host to use to connect to a given DIMONS host computer.			
Field	*Size/Type*	*Links to*	*Comments*
HostName	Char[32]	RemoteHosts:HostName	
ProxyHostName	Char[32]	RemoteHosts:HostName	
LastModified	Date/Time		

RemoteHostDcomInfo DCOM configuration parameters for remote connections.			
Field	*Size/Type*	*Links to*	*Comments*
HostName	Char[32]	RemoteHosts:HostName	
NetworkId	Char[64]		
UserId	Char[20]		
Passwd	Char[14]		
HostDomain	Char[64]		
LastModified	Date/Time		

Targets Information describing a target (i.e., retroreflector).			
Field	*Size/Type*	*Links to*	*Comments*
Id	Int		
SerialNumber	Char[16]		
Manufacturer	Char[32]		
Model	Char[32]		
AdditiveConstant	Double		
LastModified	Date/Time		

RtsHostConnection Serial communication parameters for connecting an RTS to a host computer.			
Field	*Size/Type*	*Links to*	*Comments*
RtsId	Int	RTS:Id	
HostName	Char[32]	RemoteHosts:HostName	
PortNum	Int		
Baudrate	Int		
Parity	Int		
Databits	Int		
Stopbits	Int		
Terminator	Int		
ReadInterval	Int		
ReadConstant	Int		
ReadMultiplier	Int		
WriteConstant	Int		
WriteMultiplier	Int		
LastModified	Date/Time		

MetModuleHostConnection
Serial communication parameters for connecting a meteorological sensor module to a host computer.

Field	*Size/Type*	*Links to*	*Comments*
ModuleId	Int	MetModules:Id	
HostName	Char[32]	RemoteHosts:HostName	
PortNum	Int		
Baudrate	Int		
Parity	Int		
Databits	Int		
Stopbits	Int		
Terminator	Int		
ReadInterval	Int		
ReadConstant	Int		
ReadMultiplier	Int		
WriteConstant	Int		
WriteMultiplier	Int		
LastModified	Date/Time		

TargetSurveyPointSetup
Parameters describing which targets are installed on which points at different times.

Field	*Size/Type*	*Links to*	*Comments*
TargId	Int	Targets:Id	
PtId	Int	SurveyPoints:Id	
Ht	Double		
Tstart	Date/Time		
Tend	Date/Time		
LastModified	Date/Time		

MetModuleSurveyPointSetup
Parameters describing which meteorological sensor modules are collecting data for which points at different times.

Field	*Size/Type*	*Links to*	*Comments*
ModuleId	Int	MetModules:Id	
PtId	Int	SurveyPoints:Id	
Tstart	Date/Time		
Tend	Date/Time		
LastModified	Date/Time		

RtsSurveyPointSetup Parameters describing which RTSs are installed on which points at different times.			
Field	*Size/Type*	*Links to*	*Comments*
RtsId	Int	RTS:Id	
PtId	Int	SurveyPoints:Id	
Hi	Double		
Tstart	Date/Time		
Tend	Date/Time		
LastModified	Date/Time		

RawObsTolerances Parameters describing the minimum/maximum number of sets for the RTS to collect, and the maximum allowable residuals from the least squares station adjustment.			
Field	*Size/Type*	*Links to*	*Comments*
ToleranceName	Char[32]		
MinSets	Int		
MaxSets	Int		
MaxHResid	Double		
MaxVResid	Double		
MaxDResid	Double		
Tstart	Date/Time		
Tend	Date/Time		
LastModified	Date/Time		

Pointsets Parameters describing point groupings for observation cycles.			
Field	*Size/Type*	*Links to*	*Comments*
PointsetName	Char[32]		
RtsPtId	Int	SurveyPoints:Id	
TargPtId	Int	SurveyPoints:Id	
TargSequence	Int		Sequence of observations.
Tstart	Date/Time		
Tend	Date/Time		
LastModified	Date/Time		

TargetSeek
Initial readings to which to turn RTS for target search, the search range, and timeout parameters.

Field	*Size/Type*	*Links to*	*Comments*
RtsPtId	Int	SurveyPoints:Id	
TargPtId	Int	SurveyPoints:Id	
Hcr	Double		
Vcr	Double		
Dist	Double		
MaxRetries	Int		
Timeout	Int		
Hsearch	Double		
VSearch	Double		
LastModified	Date/Time		

RawRtsCycles
Header information describing what instruments and settings were used to collect a given cycle of measurements.

Field	*Size/Type*	*Links to*	*Comments*
PtId	Int	SurveyPoints:Id	
RtsId	Int	RTS:Id	
ModuleId	Int	MetModules:Id	
Tstart	Date/Time		
Tend	Date/Time		
PointsetName	Char[32]	Pointsets:PointsetName	
ToleranceName	Char[32]	RawObsTolerances:ToleranceName	
Alias	Char[80]		
TerminationCode	Int		
LastModified	Date/Time		

RawRtsObs A single raw RTS observation.			
Field	*Size/Type*	*Links to*	*Comments*
ObsTime	Date/Time		
RtsPtId	Int	SurveyPoints:Id	
CycleStart	Date/Time	RawRtsCycles:Tstart	
SetNum	Int		
Face	Int		
TargPtId	Int	SurveyPoints:Id	
Sequence	Int	Pointsets:TargSequence	
Hcr	Double		
Vcr	Double		
Distance	Double		
CrossInc	Double		Axis tilt in cross-telescope direction
LengthInc	Double		Axis tilt in along-telescope direction
LastModified	Date/Time		

RawMetObs A single raw meteorological observation.			
Field	*Size/Type*	*Links to*	*Comments*
ObsTime	Date/Time		
ModulePtId	Int	SurveyPoints:Id	
Tdry	Double		
Tdry2	Double		
Twet	Double		
P	Double		
Rh	Double		
ObsPresent	Int		Bitmask describing which of the five available measurements were collected.
LastModified	Date/Time		

ScreenedRawRtsObs Used to single out individual RTS observations to be ignored in data processing.			
Field	*Size/Type*	*Links to*	*Comments*
RtsPtId	Int	SurveyPoints:Id	
ObsTime	Date/Time	RawRtsObs:ObsTime	
LastModified	Date/Time		

ScreenedRawMetObs
Used to single out individual meteorological observations to be ignored in data processing.

Field	*Size/Type*	*Links to*	*Comments*
ModulePtId	Int	SurveyPoints:Id	
ObsTime	Date/Time	RawMetObs:ObsTime	
LastModified	Date/Time		

ScreenedRawRtsCycles
Used to single out individual RTS observation cycles to be ignored in data processing.

Field	*Size/Type*	*Links to*	*Comments*
PtId	Int	RawRtsCycles:PtId	
ObsTime	Date/Time	RawRtsCycles:Tstart	
LastModified	Date/Time		

ObsReductionSettings
Normally, each cycle is reduced using the observation tolerances with which it was collected. Records in this table indicate that a given cycle is to be reduced using a different set of reduction tolerances.

Field	*Size/Type*	*Links to*	*Comments*
RtsPtId	Int	SurveyPoints:Id	
CycleStart	Int	RawRtsCycles:Tstart	
ObsTolerances	Char[32]	RawObsTolerances:ToleranceName	
LastModified	Date/Time		

ReducedRtsObs
Observations output from the field data reduction stage, ready to be used in calculation of coordinates.

Field	*Size/Type*	*Links to*	*Comments*
RtsPtId	Int	SurveyPoints:Id	
CycleStart	Date/Time	RawRtsCycles:Tstart	
TargPtId	Int	SurveyPoints:Id	
Sequence	Int	Pointsets:TargSequence	
Hcr	Double		
Vcr	Double		
Distance	Double		
LastModified	Date/Time		

ReducedRtsCycles
Header information describing what instruments and settings were used to reduce a set of observations, and the empirically-derived observation standard deviations resulting form the least squares set reduction.

Field	*Size/Type*	*Links to*	*Comments*
PtId	Int	SurveyPoints:Id	
RtsId	Int	RTS:Id	
ModuleId	Int	MetModules:Id	
Tstart	Date/Time	RawRtsCycles:Tstart	
Tend	Date/Time	RawRtsCycles:Tend	
PointsetName	Char[32]	Pointsets:PointsetName	
ToleranceName	Char[32]	RawObsTolerances:ToleranceName	
Alias	Char[32]		
SdDir	Double		
SdZen	Double		
SdDis	Double		
Description	Char[80]		
LastModified	Date/Time		

BaseCycles
The base cycle to use for coordinate comparisons when point coordinates are to be checked for stability.

Field	*Size/Type*	*Links to*	*Comments*
RtsPtId	Int	SurveyPoints:Id	Observing point
BaseCycle	Date/Time	RawRtsCycles:Tstart	
LastModified	Date/Time		

CoordCalcSettings
Parameters to use for computation of point coordinates by minimum constratints.

Field	*Size/Type*	*Links to*	*Comments*
RtsPtId	Int	SurveyPoints:Id	
FixedPtId	Int	SurveyPoints:Id	
Easting	Double		
Northing	Double		
Height	Double		
AzFromPtId	Int	SurveyPoints:Id	‘From’ point of specified azimuth
AzToPtId	Int	SurveyPoints:Id	‘To’ point of specified azimuth
Azimuth	Double		
SdDir	Double		Standard deviations to use for variance
SdZen	Double		propagation
SdDis	Double		
LastModified	Date/Time		

IWSTSettings Parameters to use for point stability check.			
Field	*Size/Type*	*Links to*	*Comments*
RtsPtId	Int	SurveyPoints:Id	
RefPointset	Char[32]	NonObsPointsets:PointsetName	This can be left blank, in which case all points define the datum in stability checking.
ConvergenceCriterion	Double		
MaxIterations	Int		
ConfidenceLevel	Double		
LastModified	Date/Time		

ModelSettings Parameters to use for final calculation of coordinates.			
Field	*Size/Type*	*Links to*	*Comments*
RtsPtId	Int	SurveyPoints:Id	
RefPointset	Char[32]	NonObsPointsets:PointsetName	This can be left blank, in which case the software uses the IWST-indicated stable points.
ConvergenceCriterion	Double		
MaxIterations	Int		
ConfidenceLevel	Double		
LastModified	Date/Time		

NonObsPointsets Point groupings that are used for computation rather than data collection (i.e., no target sequence field is needed).			
Field	*Size/Type*	*Links to*	*Comments*
PointsetName	Char[32]		
PtId	Int	SurveyPoints:Id	
RtsPtId	Int	SurveyPoints:Id	
LastModified	Date/Time		

ApproxCoordinates
Approximate point coordinates, suitable for plotting purposes or for initial approximations in least squares adjustment.

Field	*Size/Type*	*Links to*	*Comments*
PtId	Int	SurveyPoints:Id	
Easting	Double		
Northing	Double		
Height	Double		
LastModified	Date/Time		

PreliminaryCoordsHeader
Header information associated with a set of minimally constrained point coordinates computed using the reduced RTS observations and coordinate calculation settings.

Field	*Size/Type*	*Links to*	*Comments*
RtsPtId	Int	SurveyPoints:Id	
CycleStart	Date/Time	RawRtsCycles:Tstart	
Defects	Int		
Alias	Char[32]		
Dof	Double		
VarianceFactor	Double		
CovarianceFile	Char[255]		
Description	Char[80]		
LastModified	Date/Time		

PreliminaryCoordinates
Initial (minimally-constrained) point coordinates that have not been subjected to stability analysis or datum bias correction

Field	*Size/Type*	*Links to*	*Comments*
PtId	Int	SurveyPoints:Id	
RtsPtId	Int	SurveyPoints:Id	
CycleStart	Date/Time	RawRtsCycles:Tstart	
Easting	Double		
Northing	Double		
Height	Double		
Covariance	Char[255]		
LastModified	Date/Time		

CoordsHeader Header information associated with a cycle of final point coordinates, that have been screened for unstable reference points and subjected to datum bias correction.			
Field	*Size/Type*	*Links to*	*Comments*
RtsPtId	Int	SurveyPoints:Id	
CycleStart	Date/Time	RawRtsCycles:Tstart	
Defects	Int		
Alias	Char[32]		
Dof	Double		
VarianceFactor	Double		
CovarianceFile	Char[255]		
Description	Char[80]		
LastModified	Date/Time		

Coordinates Final point coordinates.			
Field	*Size/Type*	*Links to*	*Comments*
PtId	Int	SurveyPoints:Id	
RtsPtId	Int	SurveyPoints:Id	
CycleStart	Date/Time	RawRtsCycles:Id	
Easting	Double		
Northing	Double		
Height	Double		
Covariance	Char[255]		
LastModified	Date/Time		

The presence of start and end times in many of the database tables causes difficulty in ensuring consistency among database records. By accessing the database only through the DIMONS database manager, a number of rules can be enforced to maintain consistency. Some of the rules enforced by the DIMONS database manager are listed below.

1. Each RTS can be connected to only one host computer at a given time.
2. Each host computer can be connected to any number of RTSs at a given time.
3. Each RTS can be set up on only one survey point at a given time.
4. Each meteorological sensor module can be connected to only one host computer at a given time.

5. Each host computer can be connected to any number of meteorological sensor modules at a given time.
6. Each meteorological sensor module can be associated (collecting data for) one survey point at a given time.
7. Each target can be set up on only one survey point at a given time.
8. No two RTSs can have the same ID or name.
9. No two meteorological sensor modules can have the same ID or name.
10. No two targets can have the same ID.
11. No two pointsets associated with a given observing point (i.e., with the same RtsPtId field) can have the same name.
12. No two raw observation tolerance records valid at a given time can have the same name.
13. No two non-observation pointsets associated with a given survey point (i.e., with the same RtsPtId field) can have the same name.
14. No two RawRtsCycles records for a given observing point can have temporal overlap (start and end times).
15. No two ReducedRtsCycles records for a given observing point can have temporal overlap.
16. No two PrelimCoordsHeader records for a given observing point can have temporal overlap.
17. No two CoordsHeader records for a given observing point can have temporal overlap.

Appendix II. Refraction Effects on Displacement Accuracy

The calculations in this appendix illustrate the effect of refraction caused by the glass windows of the RTS observing shelters on the computed displacements of the observed targets. The calculations are performed under five assumptions: (1) the glass is perfectly flat on both sides, (2) the inside and outside surfaces of the glass are parallel, (3) the refractive index of the glass is uniform, (4) the refractive index of air is uniform, and (5) the refractive index of air inside the shelter is identical to that outside the shelter.

For ease of visualization, a coordinate system has been chosen such that the RTS is located at position (0,0), with the surface of the glass oriented in the North-South direction. This choice of coordinate system in no way affects the validity or generality of the results.

Figure II-1 illustrates the effect of refraction on the RTS measurements as they pass through a glass window of the observation shelter. The RTS beam strikes the glass at an angle of incidence α with respect to the surface normal. It is refracted according to Snell's Law and passes through the glass at an angle α_g with respect to the surface normal. Because the refractive index of glass is greater than that of air, the RTS beam is also slowed as it passes through the glass. Upon emerging from the glass, the RTS beam is refracted once more so that its angle with respect to the surface normal is again α, resuming its original speed as well.

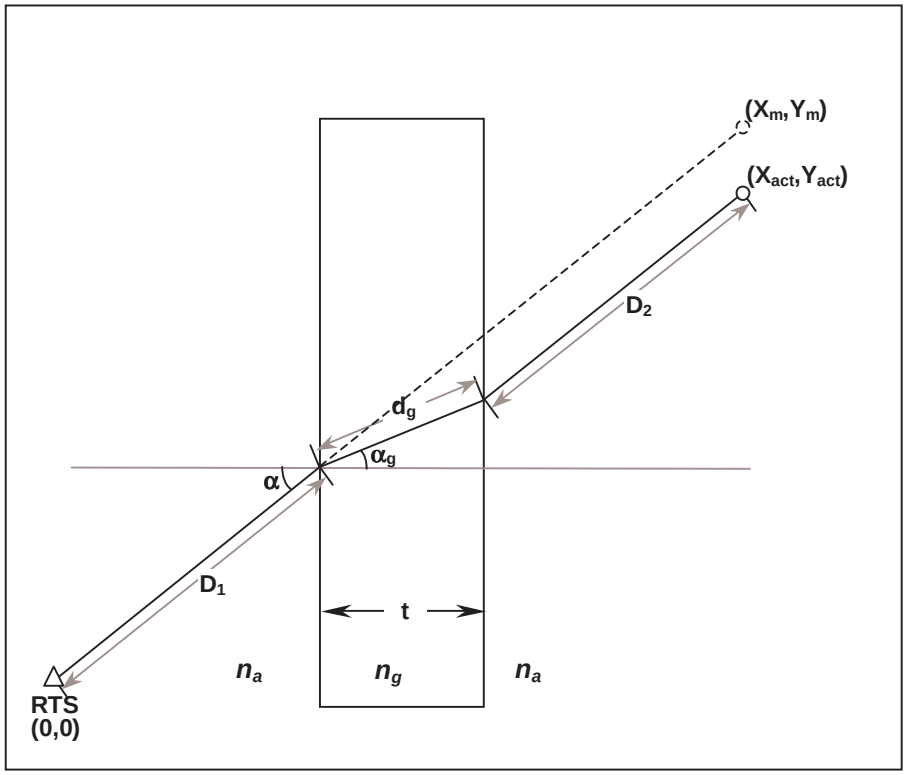

Figure II-1. Quantities involved in determining refraction effects on RTS displacement measurements

In the chosen coordinate system, the surface normal of the glass is oriented in the East-West direction. The actual coordinates (X_{act}, Y_{act}) of the observed point are therefore computed using equation (II-1):

$$\begin{aligned} X_{act} &= (D_1 + D_2) \cdot \cos(\alpha) + d_g \cdot \cos(\alpha_g) \\ Y_{act} &= (D_1 + D_2) \cdot \cos(\alpha) + d_g \cdot \sin(\alpha_g) \end{aligned} \qquad \textbf{(II-1)}$$

where

D_1 is the distance from the RTS to the inner surface of the glass,

D_2 is the distance from the outer surface of the glass to the target,

α is the angle of incidence of the RTS beam with respect to the surface normal of the glass,

$d_g = \dfrac{t}{\cos(\alpha_g)}$ is the distance travelled by the RTS beam through the glass,

$\alpha_g = \sin^{-1}\left(\sin(\alpha)\cdot\dfrac{n_a}{n_g}\right)$ is the angle of refraction within the glass,

t is the thickness of the glass,

n_a is the refractive index of air, and

n_g is the refractive index of glass.

However, all of these quantities are not generally taken into account (nor are their values known) when computing positions from RTS measurements. The RTS merely measures a direction and a distance, and the point coordinates are computed from these quantities. Therefore, the position of the observed point will be computed from the observed values as:

$$\begin{aligned} X_m &= (D_1 + D_2 + d_{gm})\cdot\cos(\alpha) \\ Y_m &= (D_1 + D_2 + d_{gm})\cdot\sin(\alpha) \end{aligned} \qquad \textbf{(II-2)}$$

where

$d_{gm} = d_g \cdot \dfrac{n_g}{n_a}$ is the distance that would be measured by the RTS through the glass if the refractive index n_a were assumed instead of the correct value n_g.

To test the resultant effect of refraction on the RTS displacement measurements, a series of Mathcad calculations are shown below. A point located at a distance of approximately 100 metres from the RTS is located such that the angle of incidence of the RTS beam with the shelter glass is 50 degrees. The position of this point is changed by approximately 1 metre perpendicular to the line of sight, and the effect of this movement on the observed displacement is computed.

Computation of Refraction Effects on RTS Displacement Measurements

Epoch 1: Before Displacement

$D_1 := 2 \cdot m$	Distance of RTS from shelter glass inner surface
$D_2 := 98 \cdot m$	Distance of target from shelter glass outer surface
$t := 0.012 \cdot m$	Thickness of shelter glass
$n_a := 1.00028$	Refractive index of air
$n_g := 1.52$	Refractive index of shelter glass
$\alpha := 50 \cdot deg$	Angle of incidence of RTS beam with shelter glass

1. Angle of refraction of the RTS beam

$$\alpha_g := \operatorname{asin}\left(\sin(\alpha) \cdot \frac{n_a}{n_g}\right) \qquad \alpha_g = 30.273 \cdot deg$$

2. Distance the RTS beam passes through glass

$$d_g := \frac{t}{\cos(\alpha_g)} \qquad d_g = 13.895 \cdot mm$$

3. Measured distance through the RTS glass

$$d_{gm} := d_g \cdot \frac{n_g}{n_a} \qquad d_{gm} = 21.114 \cdot mm$$

4. Actual target position with respect to the RTS

$$X_{act1} := (D_1 + D_2) \cdot \cos(\alpha) + d_g \cdot \cos(\alpha_g) \qquad X_{act1} = 64.2908 \cdot m$$

$$Y_{act1} := (D_1 + D_2) \cdot \sin(\alpha) + d_g \cdot \sin(\alpha_g) \qquad Y_{act1} = 76.6114 \cdot m$$

5. Position that would be determined based on the RTS measurements

$$X_{m1} := (D_1 + D_2 + d_{gm}) \cdot \cos(\alpha) \qquad X_{m1} = 64.2923 \cdot m$$

$$Y_{m1} := (D_1 + D_2 + d_{gm}) \cdot \sin(\alpha) \qquad Y_{m1} = 76.6206 \cdot m$$

Epoch 2: After Displacement

$\alpha := 49.4 \cdot deg$ Angle of incidence of RTS beam with shelter glass

1. Angle of refraction of the RTS beam

$$\alpha_g := asin\left(sin(\alpha) \cdot \frac{n_a}{n_g}\right) \qquad \alpha_g = 29.978 \cdot deg$$

2. Distance the RTS beam passes through glass

$$d_g := \frac{t}{cos(\alpha_g)} \qquad d_g = 13.853 \cdot mm$$

3. Measured distance through the RTS glass

$$d_{gm} := d_g \cdot \frac{n_g}{n_a} \qquad d_{gm} = 21.051 \cdot mm$$

4. Actual target position with respect to the RTS

$$X_{act2} := (D_1 + D_2) \cdot cos(\alpha) + d_g \cdot cos(\alpha_g) \qquad X_{act2} = 65.0894 \cdot m$$

$$Y_{act2} := (D_1 + D_2) \cdot sin(\alpha) + d_g \cdot sin(\alpha_g) \qquad Y_{act2} = 75.9341 \cdot m$$

5. Position that would be determined based on the RTS measurements

$$X_{m2} := (D_1 + D_2 + d_{gm}) \cdot cos(\alpha) \qquad X_{m2} = 65.0911 \cdot m$$

$$Y_{m2} := (D_1 + D_2 + d_{gm}) \cdot sin(\alpha) \qquad Y_{m2} = 75.9431 \cdot m$$

Point Displacements

Actual

$dX_{act} := X_{act2} - X_{act1}$ $\quad dX_{act} = 0.79866 \cdot m$

$dY_{act} := Y_{act2} - Y_{act1}$ $\quad dY_{act} = -0.6774 \cdot m$

Measured

$dX_{m} := X_{m2} - X_{m1}$ $\quad dX_{m} = 0.79879 \cdot m$

$dY_{m} := Y_{m2} - Y_{m1}$ $\quad dY_{m} = -0.6775 \cdot m$

Difference

$dX_{diff} := dX_{m} - dX_{act}$ $\quad dX_{diff} = 0.13 \cdot mm$

$dY_{diff} := dY_{m} - dY_{act}$ $\quad dY_{diff} = -0.11 \cdot mm$

Displacement Magnitudes

Actual

$Displ_{m} := \sqrt{dX_{m}^{2} + dY_{m}^{2}}$ $\quad Displ_{m} = 1.04741 \cdot m$

Measured

$Displ_{act} := \sqrt{dX_{act}^{2} + dY_{act}^{2}}$ $\quad Displ_{act} = 1.04725 \cdot m$

Difference

$Displ_{diff} := \sqrt{dX_{diff}^{2} + dY_{diff}^{2}}$ $\quad Displ_{diff} = 0.17 \cdot mm$

The computed displacement of this point is incorrect by less than 0.2 mm. The location chosen for this point (100 metres distant with an angle of incidence of 50 degrees) represents the worst scenario that would be possible at DVL, given the layout of RTS and monitoring points. Therefore, refraction caused by the shelter glass will not adversely affect the monitoring results if the assumptions set forth at the beginning of this appendix are reasonable.

Appendix III. Displacement Differences Observed At Double Prisms

The following tables list differences of weekly averaged coordinates for all double-prism survey points with respect to their averaged coordinates for the week of December 04-10, 2000. The displacements of the two prisms in each set are then differenced, and standard deviations of the displacements are computed based on these displacement differences.

	Point 1034			Point 7034			Differences 7034-1034		
Date	**dN (mm)**	**dE (mm)**	**dH (mm)**	**dN (mm)**	**dE (mm)**	**dH (mm)**	**ΔdN (mm)**	**ΔdE (mm)**	**ΔdH (mm)**
2000-12-11	-1.4	-1.1	-10.9	0.6	-2.7	-15.4	1.9	-1.5	-4.6
2000-12-18	0.1	1.1	0.4	-0.7	1.0	2.9	-0.9	-0.1	2.5
2000-12-25	0.5	4.0	-6.4	0.2	-3.8	2.0	-0.3	-7.9	8.4
2001-01-01	0.3	-1.6	-2.8	0.9	-3.0	6.9	0.6	-1.4	9.7
2001-01-08	0.7	2.2	-8.0	0.5	-1.2	-12.0	-0.3	-3.4	-4.0
2001-01-15	-0.3	-4.0	-8.1	1.3	-2.1	-13.2	1.6	1.9	-5.1
2001-01-22	0.3	-0.9	-9.9	1.7	-4.0	-27.3	1.4	-3.1	-17.4
2001-01-29	-0.1	-0.5	-6.8	1.1	-0.3	-18.7	1.2	0.2	-11.9
						std devs:	**0.7**	**2.1**	**6.6**

	Point 1079			Point 7079			Differences 7079-1079		
Date	**dN (mm)**	**dE (mm)**	**dH (mm)**	**dN (mm)**	**dE (mm)**	**dH (mm)**	**ΔdN (mm)**	**ΔdE (mm)**	**ΔdH (mm)**
2000-12-11	1.6	5.0	-11.7	-0.7	1.2	-11.2	-2.3	-3.8	0.5
2000-12-18	1.6	3.1	5.8	-0.3	-0.8	7.7	-1.9	-3.9	1.9
2000-12-25	2.0	4.2	-0.4	-0.1	-1.0	1.3	-2.1	-5.3	1.7
2001-01-01	2.9	5.9	-0.6	-1.1	2.0	-2.1	-4.0	-3.9	-1.5
2001-01-08	4.6	10.8	-5.3	-0.4	-0.7	-7.1	-5.0	-11.5	-1.8
2001-01-15	3.7	7.9	-13.5	-0.4	-1.6	-11.8	-4.1	-9.4	1.7
2001-01-22	2.6	5.2	-23.5	-1.4	2.2	-16.9	-4.0	-3.0	6.6
2001-01-29	2.0	5.9	-19.3	-0.5	0.1	-13.9	-2.4	-5.8	5.4
						std devs:	**0.8**	**2.2**	**2.1**

	Point 1082			Point 7082			Differences 7082-1082		
Date	**dN (mm)**	**dE (mm)**	**dH (mm)**	**dN (mm)**	**dE (mm)**	**dH (mm)**	**ΔdN (mm)**	**ΔdE (mm)**	**ΔdH (mm)**
2000-12-11	2.6	2.8	-0.6	2.1	-2.6	-0.6	-0.4	-5.4	0.0
2000-12-18	2.5	-0.3	2.1	0.3	-0.8	-1.7	-2.2	-0.5	-3.8
2000-12-25	5.0	3.5	-1.9	0.8	-3.0	2.4	-4.3	-6.6	4.3
2001-01-01	5.8	4.4	-2.4	-0.1	-1.2	0.5	-5.9	-5.6	2.8
2001-01-08	5.5	5.1	-3.6	1.9	-4.5	-3.3	-3.6	-9.6	0.3
2001-01-15	1.6	3.7	-14.1	1.1	-1.0	-3.5	-0.4	-4.7	10.6
2001-01-22	5.0	7.5	-11.3	0.2	-0.3	-3.0	-4.8	-7.8	8.3
2001-01-29	3.4	7.6	-15.6	0.8	-1.1	-4.1	-2.6	-8.7	11.6
						std devs:	**1.4**	**2.0**	**3.9**

	Point 1723			Point 1742			Differences 1742-1723		
Date	**dN (mm)**	**dE (mm)**	**dH (mm)**	**dN (mm)**	**dE (mm)**	**dH (mm)**	**ΔdN (mm)**	**ΔdE (mm)**	**ΔdH (mm)**
2000-12-11	0.2	-0.6	-2.2	-0.5	0.0	-2.8	-0.7	0.5	-0.6
2000-12-18	0.6	-1.0	2.0	-0.1	-0.1	0.7	-0.8	0.9	-1.3
2000-12-25	0.4	-0.5	1.8	-0.2	-0.1	0.2	-0.6	0.4	-1.6
2001-01-01	-0.2	-0.6	4.7	0.1	-0.9	0.9	0.3	-0.3	-3.8
2001-01-08	-0.5	-0.4	2.3	-0.1	-0.4	-2.7	0.3	-0.1	-5.0
2001-01-15	-0.1	-0.4	0.3	-0.3	-0.9	0.6	-0.2	-0.5	0.3
2001-01-22	-0.4	-1.0	0.6	-0.3	-0.7	-1.9	0.2	0.3	-2.5
2001-01-29	0.1	-1.2	4.0	-0.5	-1.1	0.4	-0.6	0.1	-3.6
						std devs:	**0.3**	**0.3**	**1.3**

	Point 1743			Point 1765			Differences 1765-1743		
Date	**dN (mm)**	**dE (mm)**	**dH (mm)**	**dN (mm)**	**dE (mm)**	**dH (mm)**	**ΔdN (mm)**	**ΔdE (mm)**	**ΔdH (mm)**
2000-12-11	0.7	-0.8	-2.4	-1.1	-0.9	-4.8	-1.8	-0.1	-2.4
2000-12-18	0.3	-0.5	1.7	-0.4	0.3	-2.5	-0.7	0.8	-4.2
2000-12-25	0.6	-0.9	0.2	-0.7	-0.5	-1.4	-1.3	0.3	-1.6
2001-01-01	-1.7	6.7	-1.3	0.0	0.2	-3.7	1.7	-6.5	-2.4
2001-01-08	-0.7	3.6	-2.1	-0.5	0.2	-5.1	0.2	-3.4	-3.0
2001-01-15	-1.9	8.3	-2.2	-0.1	0.6	-4.4	1.8	-7.7	-2.3
2001-01-22	-2.3	9.2	-3.6	-0.4	-0.4	-5.0	1.9	-9.6	-1.4
2001-01-29	-1.7	7.8	-2.7	-0.2	0.1	-4.7	1.5	-7.7	-2.0
						std devs:	**1.1**	**3.0**	**0.6**

	Point 3038			Point 9038			Differences 9038-3038		
Date	**dN (mm)**	**dE (mm)**	**dH (mm)**	**dN (mm)**	**dE (mm)**	**dH (mm)**	**ΔdN (mm)**	**ΔdE (mm)**	**ΔdH (mm)**
2000-12-11	-1.9	9.4	-32.4	2.7	3.4	-3.6	4.6	-6.1	28.8
2000-12-18	-1.3	13.3	-2.1	-0.5	0.7	6.2	0.7	-12.6	8.3
2000-12-25	-3.3	9.0	-29.7	3.3	3.2	0.6	6.6	-5.8	30.3
2001-01-01	-2.0	1.8	12.7	-1.7	-2.9	12.1	0.2	-4.8	-0.6
2001-01-08	-0.4	-2.5	-14.1	0.5	1.7	-8.2	0.9	4.2	5.9
2001-01-15	3.9	9.4	-31.1	-3.4	-3.4	-11.9	-7.4	-12.8	19.2
2001-01-29	-0.5	2.5	-12.0	-1.8	3.3	-3.2	-1.2	0.8	8.8
						std devs:	**3.2**	**4.4**	**8.4**

	Point 3041			Point 9041			Differences 9041-3041		
Date	**dN (mm)**	**dE (mm)**	**dH (mm)**	**dN (mm)**	**dE (mm)**	**dH (mm)**	**ΔdN (mm)**	**ΔdE (mm)**	**ΔdH (mm)**
2000-12-11	-1.5	-0.9	-5.1	2.4	-2.9	-0.4	4.0	-2.0	4.7
2000-12-18	-2.6	5.6	-4.7	-2.1	-0.7	-1.7	0.6	-6.3	3.0
2000-12-25	-0.8	-8.4	-9.2	-1.8	-7.0	-2.6	-1.0	1.4	6.6
2001-01-01	-2.3	2.9	1.8	-4.5	-3.8	-3.6	-2.2	-6.7	-5.5
2001-01-08	-2.5	2.9	-3.4	-1.0	-1.6	0.1	1.5	-4.5	3.5
2001-01-15	-1.8	0.0	-5.0	-0.6	3.5	-1.4	1.3	3.5	3.5
2001-01-29	-1.3	-4.7	-9.0	-2.2	1.9	-1.5	-0.8	6.6	7.5
						std devs:	**1.4**	**3.6**	**3.0**

	Point 3082			Point 9082			Differences 9082-3082		
Date	**dN (mm)**	**dE (mm)**	**dH (mm)**	**dN (mm)**	**dE (mm)**	**dH (mm)**	**ΔdN (mm)**	**ΔdE (mm)**	**ΔdH (mm)**
2000-12-11	0.4	0.2	-2.2	1.4	0.9	-7.5	1.0	0.8	-5.2
2000-12-18	0.3	0.4	-1.5	-0.8	-2.9	-4.8	-1.1	-3.3	-3.3
2000-12-25	0.1	-0.4	-0.6	-0.4	-7.6	-10.4	-0.4	-7.2	-9.8
2001-01-01	0.5	1.3	-0.9	-3.7	-7.5	8.4	-4.2	-8.8	9.3
2001-01-08	-0.5	0.9	-4.4	2.6	5.6	-6.4	3.0	4.6	-2.0
2001-01-15	0.3	2.4	-0.5	4.9	6.6	-9.2	4.5	4.2	-8.7
2001-01-29	0.0	1.8	-2.2	1.5	0.7	-6.3	1.5	-1.1	-4.0
						std devs:	**2.0**	**3.7**	**4.4**

	Point 3083			Point 9083			Differences 3083-9083		
Date	**dN (mm)**	**dE (mm)**	**dH (mm)**	**dN (mm)**	**dE (mm)**	**dH (mm)**	**ΔdN (mm)**	**ΔdE (mm)**	**ΔdH (mm)**
2000-12-11	0.6	0.2	-1.2	2.8	1.4	-10.2	2.2	1.2	-9.0
2000-12-18	0.5	0.8	1.3	-1.1	-3.0	-4.1	-1.6	-3.9	-5.5
2000-12-25	0.4	0.6	0.1	1.2	-3.4	-5.9	0.8	-4.0	-6.0
2001-01-01	0.6	2.3	-0.3	0.5	-0.2	2.3	-0.2	-2.5	2.6
2001-01-08	-0.4	1.3	-1.8	2.9	3.8	-6.1	3.2	2.6	-4.2
2001-01-15	0.1	-0.5	-0.4	0.9	-1.8	-2.3	0.8	-1.4	-1.9
2001-01-29	-0.2	0.8	-3.4	0.2	-3.6	-7.8	0.3	-4.3	-4.4
						std devs:	**1.1**	**1.9**	**2.6**

	Point 3115			Point 9115			Differences 9115-3115		
Date	**dN (mm)**	**dE (mm)**	**dH (mm)**	**dN (mm)**	**dE (mm)**	**dH (mm)**	**ΔdN (mm)**	**ΔdE (mm)**	**ΔdH (mm)**
2000-12-11	0.0	-0.5	-2.8	-0.2	-0.7	-0.9	-0.3	-0.2	1.9
2000-12-18	0.4	-3.2	-2.1	0.1	1.2	-0.4	-0.3	4.5	1.7
2000-12-25	0.5	-1.8	-3.1	-1.3	0.1	-0.4	-1.8	1.9	2.6
2001-01-01	1.1	-3.8	-1.3	-1.1	0.2	-4.5	-2.2	4.0	-3.1
2001-01-08	1.0	6.0	-6.7	0.4	0.2	-5.9	-0.6	-5.7	0.9
2001-01-15	1.4	-2.0	-6.2	0.3	-0.1	-6.6	-1.1	1.8	-0.4
2001-01-22	1.6	1.2	-3.2	-1.8	-1.9	-6.4	-3.3	-3.1	-3.2
2001-01-29	0.3	-0.9	-6.6	0.7	0.4	-3.3	0.4	1.3	3.3
						std devs:	**0.9**	**2.5**	**1.8**

	Point 3723			Point 3744			Differences 3744-3723		
Date	**dN (mm)**	**dE (mm)**	**dH (mm)**	**dN (mm)**	**dE (mm)**	**dH (mm)**	**ΔdN (mm)**	**ΔdE (mm)**	**ΔdH (mm)**
2000-12-11	1.8	2.3	-3.1	0.2	-0.3	-1.5	-1.7	-2.6	1.6
2000-12-18	0.5	1.4	1.9	0.3	1.1	2.9	-0.2	-0.3	1.0
2000-12-25	0.1	0.0	-0.7	-0.3	0.2	-2.4	-0.4	0.2	-1.7
2001-01-01	1.1	0.8	2.8	-0.5	0.6	-0.2	-1.6	-0.2	-3.0
2001-01-08	1.3	1.6	-5.2	-0.1	2.1	-5.8	-1.4	0.4	-0.7
2001-01-15	1.1	0.0	-1.5	0.0	0.2	0.0	-1.1	0.2	1.5
2001-01-22	0.9	-0.7	1.0	-0.2	0.2	-1.1	-1.2	0.9	-2.1
2001-01-29	1.0	0.0	0.6	0.0	0.3	-0.7	-1.0	0.3	-1.4

std devs:	**0.4**	**0.8**	**1.2**

VITA

Candidate's full name:	James Anthony Lutes
Place and date of birth:	Moncton, New Brunswick, Canada 1973-08-17
Permanent address:	3495 Route 112 Second North River, New Brunswick E4J 2T9 CANADA
Universities Attended:	University of New Brunswick, Fredericton, Canada, Department of Geodesy and Geomatics Engineering 1991 – 1996 **B.Sc.E.**
	University of New Brunswick, Fredericton, Canada, Department of Geodesy and Geomatics Engineering 1996 – 2001 **M.Sc.E. candidate**

Publications:

Duffy, M., C. Hill, C. Whitaker, A. Chrzanowski, J. Lutes, and G. Bastin (2001). "An automated and integrated monitoring program for Diamond Valley Lake in California." *Proceedings* (CDROM), 10th FIG International Symposium on Deformation Measurements, MWD, USGS and SOPAC, Orange, CA, March 19-23.

Lutes, J., A. Chrzanowski, G. Bastin and C. Whitaker (2001). "'DIMONS' software for automatic data collection and automatic deformation analysis." *Proceedings* (CDROM), 10th FIG International Symposium on Deformation Measurements, MWD, USGS and SOPAC, Orange, CA, March 19-23.

Chrzanowski, A., A. Szostak-Chrzanowski, G. Bastin and J. Lutes (2000). "Monitoring and modelling of ground subsidence in mining areas – case studies." *Geomatica*, Vol. 54, Number 4, pp. 405-413.

Chrzanowski, A., A. Szostak-Chrzanowski, G. Bastin and J.Lutes (1998). "Ground subsidence studies in potash mines." *Proceedings of the FIG XXI International Congress*, Brighton, UK, 19-25 July, pp. 202-216.

Chen, Y.Q. and J. Lutes (1998). "Development of the methodology for single epoch GPS deformation monitoring." *Journal of Wuhan Technical University of Surveying and Mapping*, Vol. 23, No.4, pp. 324-328 (in Mandarin).

Lutes, James (1996a). "Geometrical analysis of Earth deformation from VLBI data." *Proceedings of the 8th FIG International Symposium on Deformation Measurements*, Hong Kong, 25-28 June, pp.309-314.

Lutes, James (1996b). "Development of methodology for rapid and precise GPS positioning." Internal technical report of the Department of Land Surveying and Geo-Informatics, The Hong Kong Polytechnic University, Hong Kong.

Oliver, M., J. Secord, M.-H. Lavoie, J. Lutes, L. Thomas, J. Rickards, and E. Biden (1995). "Instrumentation calibration in a simulated forest machine cab for ergonomic studies." Paper presented at the 17th Annual International Conference of the IEEE Engineering in Medicine and Biology Society & 21st Canadian Medical and Biological Engineering Conference, Montréal, Canada, 20-23 September.

Conference Presentations:

Dial, G., J. Grodecki, J. Lutes and B. Morey (2001). "DEM Accuracy Evaluation." Poster presentation at *Measuring the Earth – Digital Elevation Technologies and Applications*, MAPP, ASPRS and NASA, St. Petersburg, Florida, U.S.A., 31 October – 02 November.

Major Contract Reports:

Chrzanowski, A., G. Bastin, and J. Lutes (2000). "2000 results of ground subsidence surveys in the mining area of Potash Corporation of Saskatchewan – N.B. Division near Sussex, New Brunswick." Final contract report prepared for Potash Corporation of Saskatchewan – New Brunswick Division, Penobsquis, New Brunswick, Canada, 125pp.

Chrzanowski, A., G. Bastin, and J. Lutes (1999). "1999 results of ground subsidence surveys in the mining area of Potash Corporation of Saskatchewan – N.B. Division near Sussex, New Brunswick." Final contract report prepared for Potash Corporation of Saskatchewan – New Brunswick Division, Penobsquis, New Brunswick, Canada, 83pp.

Lutes, J. and A. Chrzanowski (1999). "Displacement analysis of the Copper Basin Dam." Contract report prepared by A. Chrzanowski & Associates for the Metropolitan Water District of Southern California, Geometronics Division, Los Angeles, California, 36pp.

Chrzanowski, A., Lutes, J. and A. Szostak-Chrzanowski (1999). "Evaluation of surveying design schemes for monitoring structural deformations on large concrete gravity dams." Contract report prepared by A. Chrzanowski & Associates for the U.S. Army Corps of Engineers Topographic Engineering Center, Alexandria, Virginia, 90pp.